An Investigation into the Impacts of the Benguela Niño on Rainfall over southern Africa

Kabumbwe Hansingo

BSc (Zambia), MSc (Cape Town)

Department of Oceanography
University of Cape Town

Thesis

Presented to the Faculty of Science

for the Fulfillment of the Requirements for the Degree of

Doctor of Philosophy

November, 2008

Dedication

This thesis is dedicated to
the Almighty God
and
my family and friends.
A special dedication to my late parents Nicholas and Elizabeth, my young brother Mark and my family who endured the brunt of my academic pursuit.

Declaration

I declare that this thesis is my own work and has not been submitted in any form for another degree or diploma at any university or other institute of tertiary education. Information derived from the published and unpublished work of others has been acknowledged in the text and a list of references is given.

Kabumbwe Hansingo
November 20, 2008

Acknowledgments

I acknowledge the support, encouragement and guidence rendered by my supervisor Professor Chris Reason. I thank Doctor Mark Tadross, Department of the Climate Systems Analysis Group (**CSAG**) at the University of Cape Town, for the C source code (which I later converted to FORTRAN) for manipulating dates in the model dump and boudary data files. I thank Professor Frank Shillington, the Head of Department and Ms Rachmat Harris, the administrative assistant for their due administrative support. I am grateful to Mr. Nchimunya Mwiinga and Dr. Haabatwa Mweene of the Physics Department at the University of Zambia for giving me space to work from when I spent six months in Zambia. Members of staff and postgraduate students in the Department of Oceangraphy, University of Cape are acknowledged for providing a conducive and interactive research environment.

Many thanks to the global change **S**ys**T**em for **A**nalysis, **R**esearch, and **T**raining (**START**) and National Research Foundation (**NRF**) of the Republic of South Africa for funding this research and the Centre for High Performance Computing (**CHPC**), Cape Town, for their computing facilities.

I am appreciative of the hospitable environment rendered by the Mowbary Seventh-day Adventist Church and Mr. Fhatuwani L. Ramukosi during my stay in Cape Town. I thank the Almight God for his abound mercies during the research when this work seemed so impossible and useless.

Finally, I want to address my sincerest thanks to my wife who never failed to encourage me inspite of the fact that I had to be away from home. Without her understanding and her continuous support this thesis would never have been written.

Abstract

The impacts of the Benguela Niño on southern African rainfall and circulation are investigated using an atmospheric general circulation model. The model used is the United Kingdom Met Office Hadley Centre Atmospheric General Circulation Model version 3 and experiments using idealizations of observed regional and remote SST anomalies during various Benguela Niño events were performed. It is found that SST forcing in tropical South East Atlantic induces a regional baroclinic response and that a Benguela Niño is capable of forcing anomalous wet conditions over western Angola on its own, via changes to uplift and evaporation over the SST forcing. It is also capable of forcing anomalous rainfall much further inland when the intensity is increased.

An experiment with the tropical South East Atlantic SST anomaly shifted slightly further north produced a larger circulation and rainfall response in the model. Additional experiments with various SST anomalies in the South West Indian Ocean/central equatorial Pacific combined with those in the South East Atlantic were performed. These experiments are motivated by the fact that equatorial Pacific/South Indian Ocean SST anomalies of varying signs often occur at the same time as the Benguela Niño Events. The results suggest that depending on its sign, magnitude and location, SST forcing from the South West Indian Ocean may augment or oppose the southern African rainfall anomalies occurring during a Benguela Niño event to varying degree.

The experiment with cooling in the central equatorial Pacific combined with warming in the South East Atlantic produced similar rainfall anomalies over southern Africa with the experiment with the forcing only in the Pacific. Different near-surface circulation anomalies are produced over the South West Indian Ocean. These results suggest that the La Niña signal tends to dominate the Benguela Niño signal over southern Africa

and vice versa over the southwest subtropical Indian Ocean when these events occur simultaneously.

Contents

List of Tables

List of Figures

Chapter 1

Introduction

There is increasing interest in the sea surface temperature (SST) variability of the South Atlantic Ocean (e.g. Garzoli *et al.*, 1996, Florenchie *et al.*, 2003, Hickey and Weaver, 2004, Colberg *et al.*, 2004, Haarsma *et al.*, 2005, Colberg and Reason, 2006). These studies mainly focus on the dynamics associated with the observed variability rather than consider the climate impacts on the neighbouring landmasses. Thus, rather less research has been done on the possible links between variability of SST in the South Atlantic Ocean and the climate of neighbouring southern Africa and the possible mechanisms.

Although there is some evidence of links between SST variability in the South Atlantic Ocean and southern African rainfall (e.g. Hirst and Hastenrath, 1983, Reason *et al.*, 2002, Rouault *et al.*, 2003, Reason and Jagadheesha, 2005a), the associated mechanisms are not well understood. Motivated by the occurrence of extreme climatic events in the Angola region, about 25 years ago Hirst and Hastenrath (1983) sought to investigate the general causes of these events. They endeavoured to explain mechanisms of large scale atmosphere-hydrosphere interaction in the tropical Atlantic. With the exception of the work of Shannon *et al.* (1986), this topic was then rather neglected until recently.

The main region of interest in this study is the Angola Benguela Frontal (ABF) zone in the southeast Atlantic Ocean where anomalously warm SSTs have been observed to occur on occasion, and based on the work of Hirst and Hastenrath (1983), Shannon *et al.* (1986), and Rouault *et al.* (2003), are thought to influence rainfall over neighbouring Angola and Namibia. This frontal zone separates warm tropical Angola Current waters (SST exceeds

28°C in late summer) from the cool Benguela Current upwelled waters off Namibia (SST less than 20°C). Shannon *et al.* (1986) have termed large warm events 'Benguela Niños' because of their apparent similarities with El Niño events. To date, not much evidence has been shown of a link between Benguela Niños and ENSO (Enfield and Mayer, 1997, Latif and Barnett, 1995) and certainly these phenomena do not typically occur in unison (Florenchie *et al.*, 2003, Reason *et al.*, 2006). Moreover, Benguela Niños are less intense and less frequent than El Niños (Shannon *et al.*, 1986) and typically occur in late austral summer, February-April. Recent examples of Benguela Niños occurred in 1984, 1986 and 1995 and 2001 (Florenchie *et al.*, 2003, Rouault *et al.*, 2003). The composite anomaly plot for these events is shown in Figure 1.1. The centre and magnitude of maximum SST anomalies varies among these events, from about 15°S to about 17°S and from about 2°C to about 4°C respectively.

Hirst and Hastenrath (1983), Nicholson and Entekhabi (1987) and Rouault *et al.* (2003) have observed that anomalous atmospheric conditions occur over areas of anomalously warm SST in the southeast tropical Atlantic and may be linked with above average rainfall along the coast of Angola and Namibia and sometimes also inland areas of Southern Africa, e.g. Zambia. However, it is not clear as how influential a Benguela Niño is on the rainfall further inland.

During Benguela Niño events, for example 1995 and 2001, cooling or warming may also occur in the Indian and/or Pacific Oceans. It has long been recognised that ENSO and SST variability in the Indian Ocean influence rainfall variability in many parts of southern Africa (e.g. Mason and Jury, 1997, Reason and Mulenga, 1999, Reason *et al.*, 2000). Therefore much research on southern African Climate variability has concentrated on influence from ENSO and the Indian Ocean because it is believed that they exert more influence over southern Africa than the Atlantic Ocean. For example, Lindesay *et al.* (1986), Nicholson and Entekhabi (1986), Ropelewski and Halpert (1987, 1989) suggest that severe droughts (floods) over southern Africa are associated with El Niño (La Niña) events. Some wet summers over southeastern Africa are associated with locally forced warm sea surface temperature (SST) in the South Indian Ocean (Behera and Yamagata,

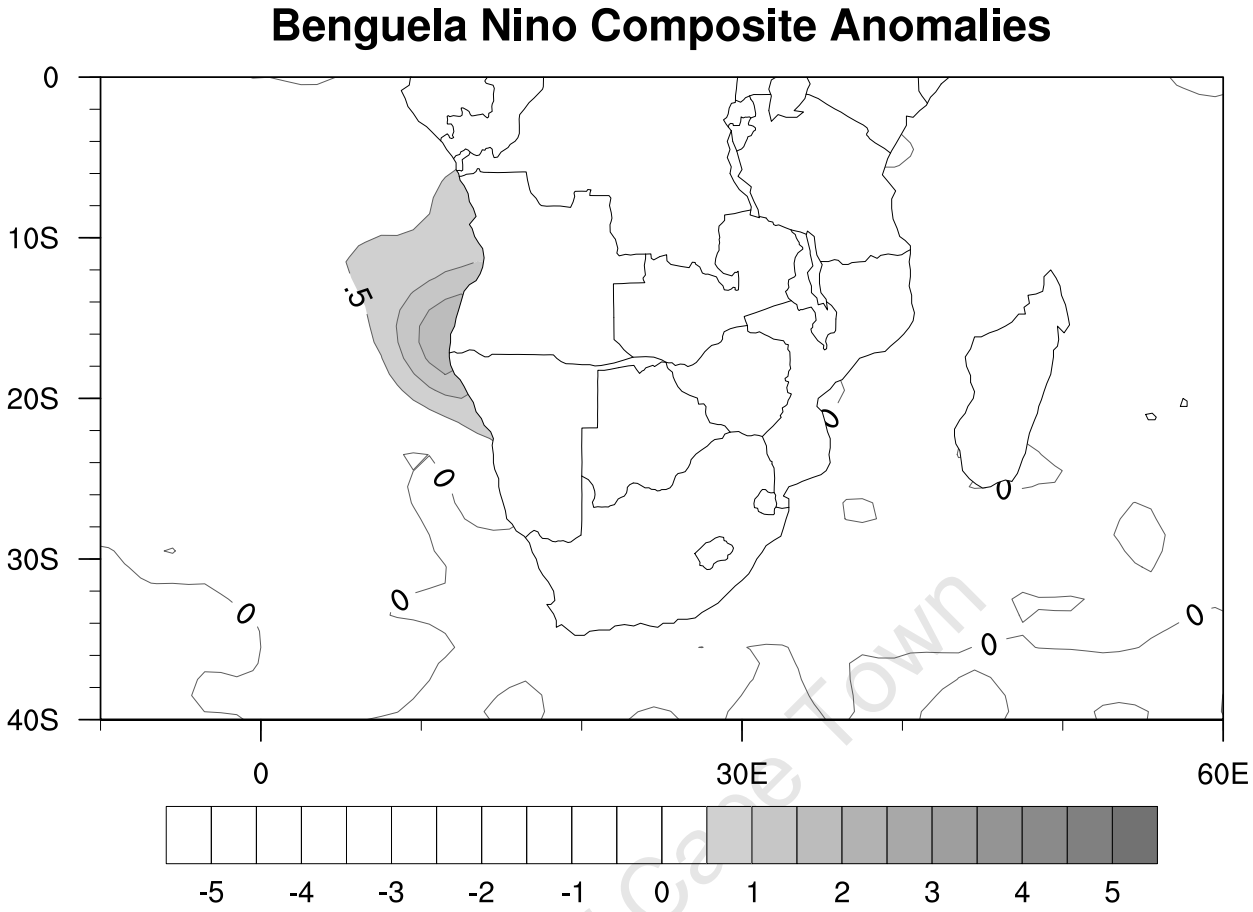

Figure 1.1: Composite SST anomaly of the 1984, 1986, 1995 and 2001 Benguala Niños. Anomalies greater than 0.5°C are shaded.

2001, Reason, 2001). However, little work has been done on the influence of the Atlantic Ocean on southern African climate. The Benguela Niño is the most prominent example of variability in the South East Atlantic Ocean and therefore, the objective in this thesis is to investigate the impacts of Benguela Niño on rainfall over southern Africa.

To help achieve the above objective, this research will try to address the following questions:

1. What is the effect of warm SST anomaly intensity in the southeast Atlantic Ocean, when there is neither warming nor cooling in the Indian Ocean?

2. What is the rainfall and circulation response over southern Africa when there are warm or cool SST anomalies in the southwest Indian Ocean in addition to a Benguela Niño event?

3. How does the location of anomalous warming of SST in the tropical southeast Atlantic influence the atmospheric response over southern Africa?

4. What is the rainfall and circulation response over southern Africa when there is a La Niña event in the Pacific occurring at the same time as a Benguela Niño?

The main tool used in this investigation is the United Kingdom Met Office (UKMO) Hadley Centre Atmospheric Model version 3 (HadAM3) general circulation model. Grid-point atmospheric general circulation models (AGCMs) numerically solve fundamental or primitive equations describing the conservation of mass, energy, momentum and moisture for each atmospheric gridbox while taking into account the transfer of those quantities between gridboxes. Like in many other grid-point AGCMs, the SST field is used to force HadAM3 at the surface. Thus one can prescribe desired SST patterns at the surface boundary. In this thesis, the model is forced with various prescribed idealised SST anomalies in the southeast tropical Atlantic, southwest subtropical Indian and central equatorial Pacific Oceans.

Having stated the objective, the overview of the structure of this thesis is as follows:

Chapter 2 gives a review of the existing literature on some of the rain-bearing systems over southern Africa and the possible influence of the Atlantic Ocean on southern African rainfall.

Chapter 3 provides a brief description of HadAM3's dynamics and parameterisation schemes. This chapter also a description of the data used in this thesis. A description of the design of a set of experiments with the model is also given in this chapter. These experiments help to address the questions above.

Chapter 4 presents results on the models ability in simulating the observed climate. The model is validated using NCEP/NCAR reanalyses.

It is important to understand the performance of climate models in the current climate where validation is possible. Any strengths and weaknesses of the models need to be understood before they are used on climate change scenarios runs, for example. Although this study may be important to climate change studies, it excludes anthropogenic impacts

on climate change. It focuses on atmospheric response to SST forcing in the Angola-Benguela-Front region and other SST forcing.

Chapter 5 presents results from experiments which involve forcing HadAM3 with idealised warm SST anomalies only in the southeast tropical Atlantic Ocean. Results in this chapter try to address the first and third questions.

Chapter 6 presents results from experiments in which the model is forced with idealised SST anomalies in the southeast tropical Atlantic Ocean and the southwest subtropical Indian Ocean (SWIO). This chapter addresses the second question.

Chapter 7 presents results from experiments in which the model is forced with idealised SST anomalies in the southeast tropical Atlantic and the central equatorial Pacific Oceans. Therefore this chapter addresses the fourth question.

Chapter 8 summaries the findings of this thesis and concludes the thesis.

Chapter 2

Literature Review

2.1 Introduction

Southern Africa is prone to pronounced flood and drought events and climate variability on a range of time scales. Some of the variability, floods and droughts is thought to be forced remotely via El Niño Southern Oscillation (ENSO) (e.g. Nicholson and Entekhabi, 1986, Lindesay, 1988, Nicholson and Kim, 1997, Reason *et al.*, 2000) and the surrounding Indian and Atlantic Oceans (e.g. Hirst and Hastenrath, 1983, Walker, 1990, Mason, 1995, Rocha and Simmonds, 1997a, Reason and Mulenga, 1999, Behera and Yamagata, 2001, Reason, 2001, 2002, Nicholson, 2003). However, much research on southern African climate variability has concentrated on influence from ENSO and the Indian Ocean, because it is believed that they exert more influence over southern Africa than the Atlantic Ocean. For example, Lindesay *et al.* (1986), Nicholson and Entekhabi (1986), Ropelewski and Halpert (1987, 1989) suggest that severe droughts over southern Africa are associated with ENSO and wet summers over southeastern Africa are associated with locally forced warm sea surface temperature (SST) in the Indian Ocean (Behera and Yamagata, 2001, Reason, 2001). However, little work has been done on the influence of the Atlantic Ocean on southern African climate. A review is given in Reason *et al.* (2006). The objective of this chapter is to review the existing literature on some rain-bearing systems over southen Africa and the possible influence of the Atlantic Ocean on southern African rainfall.

Although the ENSO phenomenon in the Pacific has profound impact on global weather patterns, not all anomalous patterns are linked to it and it has become increasingly clear that other modes of climate variation besides ENSO can have significant influence on regional climate (Chang *et al.*, 1998). Among them is a variation of SST in the tropical Atlantic Ocean. Following the pioneering work of Hirst and Hastenrath (1983) and Lough (1986), more recent research has indicated the importance of South Atlantic Ocean variability for southern African climate (e.g. Fauchereau *et al.*, 2003, Rouault *et al.*, 2003, Florenchie *et al.*, 2004, Hermes and Reason, 2005, Reason and Jagadheesha, 2005a). Sea surface temperature variations in the tropical Atlantic and atmospheric circulation variations over this region could influence atmospheric dynamics, moisture supply and hence rainfall over Africa. Fauchereau *et al.* (2003) suggest that atmospheric anomalies over southern Africa are related to SST variations in subtropical Atlantic in addition to Indian Ocean. For example, SST variations in the tropical Atlantic Ocean have been found to influence late summer (February-March-April) rainfall over coastal regions of southwest Africa and further inland (Hirst and Hastenrath, 1983, Rouault *et al.*, 2003, Florenchie *et al.*, 2004). Other regions influenced by SST variations in the tropical Atlantic include Northeast Brazil (Enfield, 1996, Harzallah *et al.*, 1996), the Sahel region (Folland *et al.*, 1986) and coastal West Africa (Reason and Rouault, 2006).

Variation in the surrounding and remote oceans alone is not sufficient to understand climate variability over southern Africa, the effect of local atmospheric and land processes may also contribute to observed climate variations over southern Africa. For example, meridional and zonal convergence of moist air over the subcontinent, within the Intertropical and South Indian convergence zones respectively may influence the spatial distribution and magnitude of rainfall anomalies over Southern Africa (Cook, 2000). Variations in synoptic features, such as heat or thermal troughs, have also been linked to rainfall variability over Southern Africa (Mulenga, 1998). Harrison (1986) suggests that year to year fluctuations in rainfall over Africa are determined by circulation regimes that alter the preferred location of tropical convection and the Intertropical convergence zone (ITCZ). These local continental processes and variations in the surrounding oceans may

interact with one another in a complex way and thus produce observed climate variations over southern Africa.

2.2 Heat-lows

Heat lows or troughs are shallow disturbances and are a prominent climatological feature of many arid land areas of the world in low latitudes (Rácz and Smith, 1999). These features tend to form during daytime in warmer months when insolation is at its peak, particularly during summer and may be thought of as low-level maxima in cyclonic relative vorticity, which are linked to horizontal gradients of diabatic heating. Heat lows have been observed over south-western and northern Africa (Ramage, 1971), West Pakistan and northern India (Joshi and Desai, 1985), Saudi Arabia (Bitan and Sa'aroni, 1992), Australia (Leighton and Deslandes, 1991), Spain (Portela and Castro, 1996) and southwestern USA and Mexico (Rowson and Colucci, 1992). These disturbances are usually confined below 700 hPa and are characterised by a convergent cyclonic circulation at low levels and a divergent anticyclonic circulation aloft. Their horizontal scale ranges from 500 to 2500 km. After studying heat lows over Saudi Arabia, Blake *et al.* (1983) suggested that ascending motion over heat lows occur below 800 hPa and during the morning. Contrary to this finding, Hart (1990), who investigated vertical-velocity profiles over heat lows over northern Australia, concluded that a deeper layer of ascending occurs in the evening. Recent studies on the dynamics of heat lows (e.g. Rácz and Smith, 1999, Reichmann and Smith, 2003) attribute this difference to orography. Reichmann and Smith (2003) suggest that orography may induce a broad-scale circulation, a circulation in which sea breezes and other flows such as anabatic and katabatic winds contribute. Anabatic winds reinforce low-level convergence, therefore one expects strengthened relative-vorticity over a plateau rather than a flat land. Also, low-level wind maxima tend to be weaker over flat land than over the plateau (Reichmann and Smith, 2003). The presence of orography leads to a deeper mixed layer and higher wind speeds and the top of the mixed layer is higher over the plateau than over the plain. Reichmann and Smith (2003) propose that heat lows may occur mostly over regions of elevated terrain. The behaviour of heat lows

or troughs may also be influenced by the presence of a large-scale flow and the persistence of this flow (Rácz and Smith, 1999).

A heat low observed over southern Angola and northern Namibia during about OctoberMarch is locally known as the Angola-low. Mulenga (1998) identified this heat-low as an inland low level pressure wind vortex at 850 hPa and associated it with high surface temperatures. Harrison (1986), Makarau (1995), Rocha and Simmonds (1997b) and Reason and Jagadheesha (2005a) suggest that variations in seasonal rainfall over southern Africa may be related to this inland low and may therefore contribute to interannual variability of summer rainfall. The position of the inland low is critical in determining wet areas as it modulates the convergence of moist air over the subcontinent. A well-developed surface low over Angola and western Zambia linked to mid-latitude westerly waves passing south of Africa, results in tropical extra-tropical cloud bands extending to the southeast and heavy rains over Zambia, Botswana and South Africa (Mulenga, 1998). Sometimes, the combination of the Angola-low and cyclones over Mozambique results in diffluent flow over Zambia, Zimbabwe, Botswana, and Malawi. This situation usually results in drought conditions. The Angola-low may influence the Benguela upwelling system and may therefore be related to the warm and cool events over the southeast Atlantic Ocean. Further south, heat lows may also form over southern Namibia and the western interior of South Africa.

2.3 Tropical-Temperate Troughs or Tropical-Extratropical Cloudbands

Most of southern Africa is affected by tropical and mid-latitude weather systems and their interactions. Interactions between tropical and mid-latitude (temperate) weather systems form an intriguing element of the general circulation (Washington and Todd, 1999). During most of the year, circulation over the southern region (south of 25°S) is dominated by extra tropical weather systems such as westerly waves, cut-off lows and cold fronts (Dyson and van Heerden, 2002). During summer, tropical weather systems,

in the form of tropical cyclones, tropical lows and easterly waves migrate southwards and interact with midlatitude weather systems. A linkage involving a tropical disturbance such as an easterly wave or a tropical low (e.g. Angola-low) and a subtropical low or temperate westerly wave results in a feature commonly referred to as the tropical-temperate trough (TTT, Harangozo and Harrison, 1983, Crimp *et al.*, 1997). Over southern Africa, a TTT is an elongated trough extending in a northwest-southeast direction across the subcontinent and the southwest Indian Ocean and is identified from satellite imagery as long cloud bands that extend over both continental southern Africa and the southwest Indian Ocean (Todd and Washington, 1999). Circulation within a TTT is characterised by surface convection and upper air divergence, which result in ideal conditions for strong vertical uplift and the formation of the cloud bands (Crimp *et al.*, 1997). The cloud bands form eastward of upper air, semi-stationary long waves, which may be orographically forced or thermally forced in the atmosphere. Crimp *et al.* (1997) reports that systems like cut-off lows, may occur simultaneously with TTTs, often enhancing convection and rainfall production. A combination of such two systems can produce heavy rainfall and flooding.

Variability in southern African rainfall during January to March is caused primarily by changes in the position, frequency and strength of TTTs and these systems have been identified as greater contributors of rainfall over the region than any other summer rainfall-producing systems (Crimp *et al.*, 1997). Tropical lows, subtropical troughs and westerly waves in the region have been found to be associated with wet conditions. This finding suggests a link between TTT frequency and higher rainfall. Crimp *et al.* (1997) have found that TTTs form most frequently over southern Africa during January when the Inter-Tropical Convergence Zone (ITCZ) is furthest south. This circulation allows for a more regular interaction between midlatitude westerly waves and the region of tropical convergence. The dissipation of cloud bands occurs with the eastward or westward movement of the TTT and/or the eastward or westward extension of the ridge of high pressure south of South Africa so that the link with the cold front to the south breaks down.

Jury and Lindesay (1991) have associated major flood events in the interior of southern Africa with TTTs. A westerly trough over the western subcontinent at the 500 and 700

hPa levels and a tropical low over northern Namibia/Botswana have been observed to occur during wet periods. During wet summers, tropical lows are found to be situated over the western-central interior and relatively far south (20°S) but over the eastern subcontinent and further north (15°S) during dry months (Crimp *et al.*, 1997).

Crimp *et al.* (1997) linked the formation, strength and position of the TTTs to global scale circulations like the Hadley and Walker circulations. They suggested that a strengthened Hadley circulation is associated with more frequent TTT formation and a wet summer over southern Africa. The shifting of the Walker circulation during an El Niño event and the associated eastward shift of the regions of convection is associated with the TTT forming more frequently to the east of the subcontinent (Crimp *et al.*, 1997).

Cloud bands facilitate the poleward distribution of mass, momentum and energy from the tropics to the mid-latitude (Crimp *et al.*, 1997, Todd *et al.*, 2004).Transport over southern Africa of latent heat, water vapour and kinetic energy occurs primarily with the TTTs situated along the leading edge of the upper trough. This location is important for the maintenance of the Hadley circulation over the subcontinent. Todd *et al.* (2004) indicates that TTT events facilitate a substantial water vapour flux from the tropics into the mid-latitudes and are major regions of moisture convergence. Crimp *et al.* (1998) has indicated that the strength of TTTs may be sensitive to SST south of South Africa. This work suggests that SST variability in the neighbouring Indian and Atlantic Oceans may influence TTT location and intensity.

2.4 Tropical Atlantic Ocean and Southern African Rainfall

Since southern Africa is a relatively narrow landmass that ends in the subtropics, its climate may be influenced by variations in atmosphere-ocean interaction in the neighbouring tropical Atlantic Ocean basin as well as that over the Indian Ocean. For example, Biasutti *et al.* (2004) suggested that the atmospheric response to changes in tropical and subtropical SST is advected inland and forces changes in sea-level pressure and low-level

convergence across a large part of tropical Africa. Observational (e.g. Hirst and Hastenrath, 1983, Nicholson and Entekhabi, 1987, Rouault *et al.*, 2003) and numerical model (e.g. Reason and Jagadheesha, 2005b) studies suggest that warm SST in the southeast Atlantic are associated with above average rainfall over southern Africa, the western half in particular (Jury, 1996). On the other hand, Rautenbach and Jury (1997) suggested that southeast tropical Atlantic cold events may also significantly enhance late summer rainfall over southern Africa.

Climatologically, SSTs in the southern tropical Atlantic are highest, over 28°C, during February and occur in the region between 10°S and 5°N (Figure 2.1**a**) and may therefore influence southern African rainfall, in particular, during this period – the Optimum Interpolated SST dataset (Reynolds *et al.*, 2002) is used in this literature review, for details see chapter 3. During this season, the equatorial winds are weakest and the thermocline is deepest in the east (Xie and Carton, 2004). While the peak rain season over southern Africa is from December to February (DJF) Figure 2.1**b** recent severe floods (e.g. Mozambique floods in 2001) and droughts (e.g. Zambia during 2005) have occurred during the FMA season. During this season, northern Angola, Zambia and Mozambique, southern Tanzania and Congo-Brazzaville, Madagascar, Gabon and Equatorial Guinea receive rainfall well over 5 mm/day (Figure 2.1**d**, Climate Prediction Centre (CPC) Merged Analysis Precipitation (CMAP) dataset (Xie and Arkin, 1996) is used in this literature review, see chapter 3 for details).

The various studies cited above highlight the modification of regional moisture fluxes and convergence, via temperature and pressure gradients, as a possible mechanism linking southeast Atlantic warm events and southern African rainfall. Rouault *et al.* (2003) suggested that rainfall over western Angola/Namibia is greatest for those SST events (Figure 2.2) for which the local circulation anomalies act to strengthen the climatological westwards flux of Indian Ocean sourced moisture. Note that the western Indian Ocean is the major source of moisture for austral summer rainfall over southern Africa (Figure 2.3). The above circulation accompanied with an anticyclonic flow over the warmest SST, which

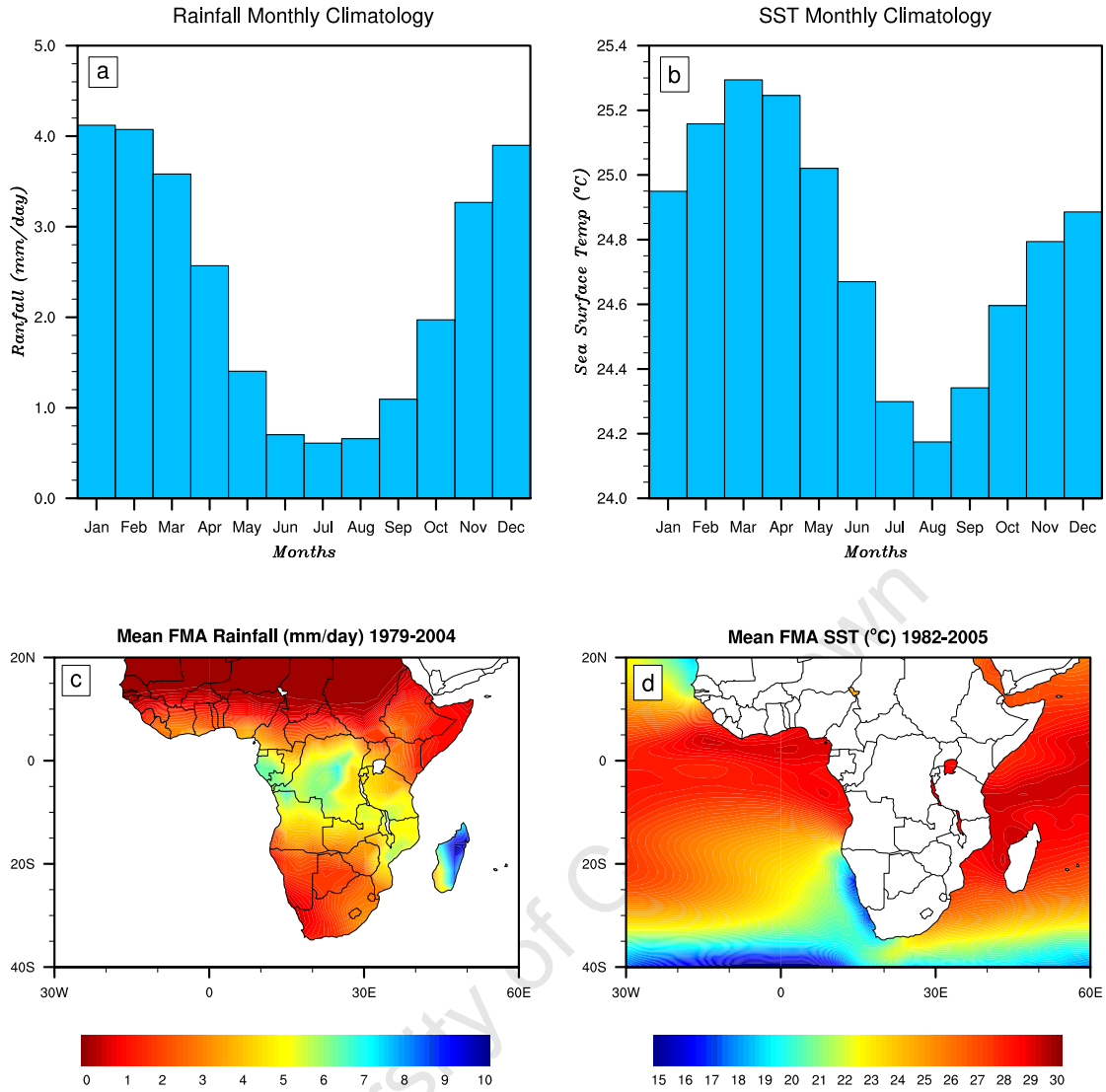

Figure 2.1: Precipitation (CMAP) and SST (OISST) climatology; (**a**) Precipitation annual cycle averaged over southern Africa (12°E-40°E; 35°S-0°), (**b**) SST annual cycle averaged over tropical Atlantic (60°W-15°E; 30°S-30°N), (**c**) FebruaryApril climatological precipitaiton over southern Africa, (**d**) February-April climatological SST over tropical Atlantic Ocean.

may weaken the mean southeasterly moisture flux away from Africa over the SE Atlantic may result in anomalous rainfall over western Angola/Namibia (Rouault *et al.*, 2003).

Figure 2.2 shows four observed warm events in the south east Atlantic Ocean (Benguela Niños) during late austral summer (left column) and their associated rainfall anomalies (right column). SST anomalies as high as 3°C off the Angola/Namibia coast are observed in the 1995 event. The expression of the SST anomalies of this event and that during 1984 is stronger than for the 1986 and 2001 events. However, the latter events show stronger rainfall anomalies over the northern (1986 event) and southern (2001 event)

regions of southern Africa and all events show substantially positive rainfall anomalies over the coastal northern Angolan border. Hirst and Hastenrath (1983) suggest that SST variations in the eastern tropical South Atlantic accounts for about 36% of the rainfall variability along the Angolan coast. During some events, above average rainfall is observed over inland regions of southern Africa (Rouault *et al.*, 2003).

Figure 2.4 shows 850 hPa moisture flux (vectors) and moisture convergence (shaded) anomalies for these events. Moisture flux and moisture convergence variables are derived from the U-, V-wind components and specific humidity of the National Centre for Environmental Prediction/National Centre for Atmospheric Research (NCEP/NCAR) Reanalysis dataset (Kalnay *et al.*, 1996), see chapter 3 for details. Plots in this figure are discussed together with Figure 2.3, which shows the February to April 850 hPa mean moisture flux and convergence. As mentioned above, the western Indian Ocean is the primary source of moisture for austral summer rainfall over the subcontinent. The South Atlantic Ocean is a secondary moisture source for subtropical southern Africa and mainly advects a relatively cool and dry air mass over western Namibia and South Africa from the Benguela current region. This South Atlantic air mass may converge in summer in the heat low and the TTT region with a warm moister air mass from the western Indian Ocean over the interior of southern Africa (Figure 2.3). From about 22°S to about 8°S on the west coast, moisture flux is offshore but somewhat alongshore north of 6°S. Warm and moist air from the primary western Indian and the secondary tropical Atlantic Ocean converge over Angola. Rouault *et al.* (2003) suggest that warm events in the southeast Atlantic Ocean can only act as a local perturbation to moisture flux from the tropical Atlantic Ocean.

Strengthened moisture flux over Angola, Zambia and southern Congo-DR and moisture convergence over the northern coast of Angola characterise the warm events of 1984 (Figure 2.4**a**) and 1986 (Figure 2.4**b**). These events are also characterised by a relatively weak moisture convergence southeast of the Angola-low region. However, the moisture flux is weaker (stronger) than average over the southwest Indian Ocean during the 1986 (1984) event and the moisture flux anomaly is onshore (offshore) over the Angola/Namibia

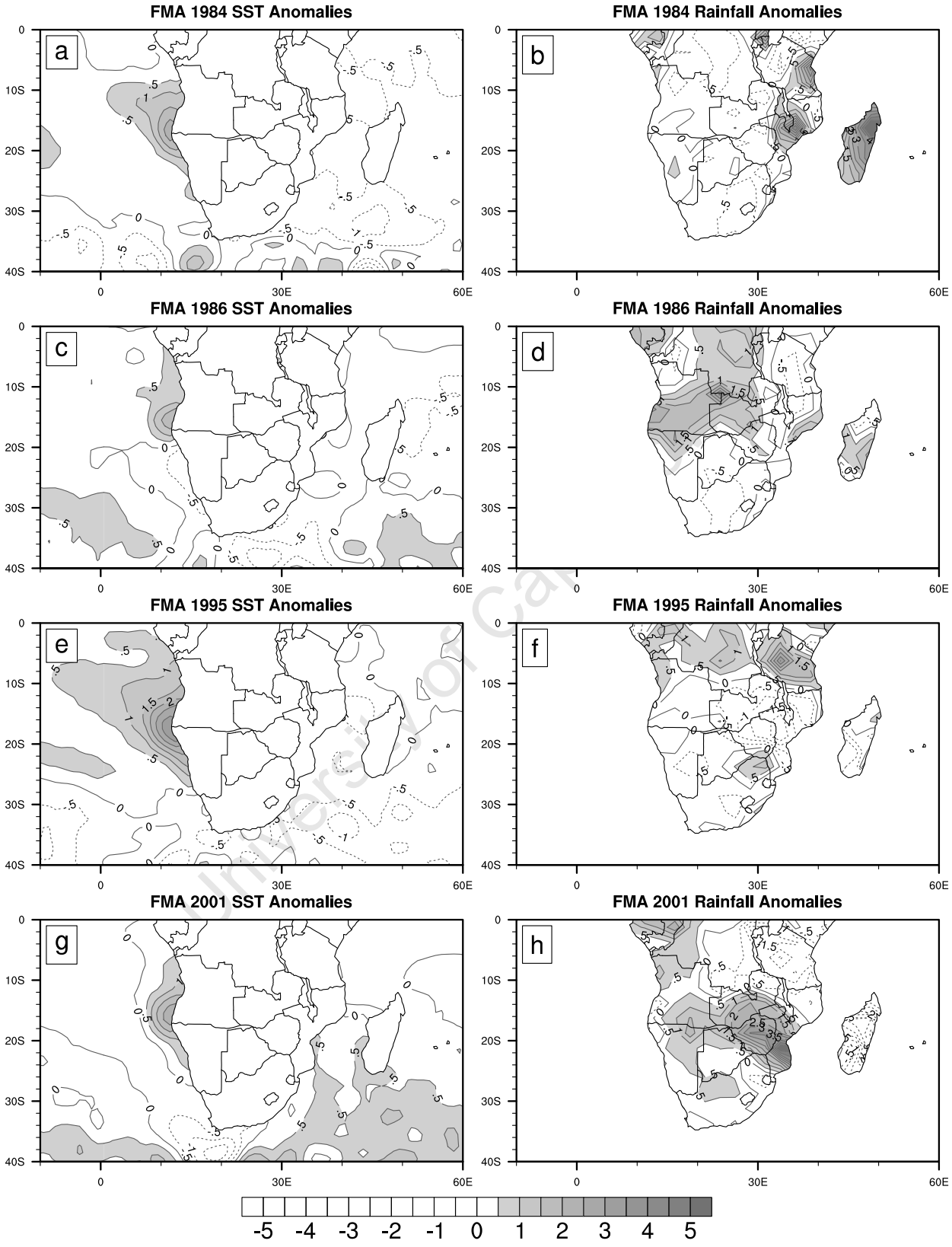

Figure 2.2: FMA sea surface temperature (left column, IOSST) and precipitation (right column, CMAP) anomalies during 1984, 1986, 1995 and 2001 southeast Atlantic warm events.

coast during 1986 (1984). These circulation anomalies suggest that the 1984 event was associated with more moisture over the eastern subcontinent than the 1986 event. However, Figure 2.2 indicates wet conditions over central Africa during the 1986 event and dry conditions during 1984. A cyclonic moisture flux anomaly and moisture convergence over Angola, Botswana, Namibia and Zambia, characterise the 1995 and 2001 events. However, the offshore anomaly over the Namibian coast is weaker in the 2001 event than in the 1995 and the former is characterised by a strong northwesterly anomaly extending from the equatorial region to the cyclonic anomaly over southern Angola. Also, the anomaly circulation pattern in the tropical southern Indian Ocean and southwest Indian was roughly opposite for the two events. Figures 2.4**c** and 2.4**d** indicate increased (reduced) moisture advection over southeastern Africa from the tropical southwest Indian during the 2001 (1995) event and reduced (increased) moisture advection over eastern Southern Africa from tropical southern Indian Ocean. The relatively wet (dry) conditions over eastern Southern Africa during 2001 (1995) may be because tropical air masses are moister than subtropical air masses. The cyclonic moisture flux anomaly over Angola, Botswana, Namibia and Zambia suggests a stronger thermal low or trough during these events. Of the four events, the 1986 event shows weak moisture flux anomalies over Angola and the 2001 event shows weak moisture flux from the southwest Indian Ocean. However, these two events show anomalously wet condition over southern Africa and warm SST anomalies in southwest Indian Ocean. This observation suggests that conditions in the Indian Ocean may modulate the effect of these warm events.

The influence of SST variability in the South Atlantic Ocean on southern African climate is not limited to the summer season. Reason and Jagadheesha (2005b) have identified a pattern of SST anomalies occurring in winter (May to September) in this region and associate it with winter rainfall anomalies over the southwestern region of South Africa. This pattern is characterised by warm SST anomalies in the southwest and southeast Atlantic and cool anomalies in the central South Atlantic Ocean during wet winters. Changes to subtropical jet position and strength, low-level relative vorticity, and convergence of moisture and latent heat flux are associated with this pattern. Robertson

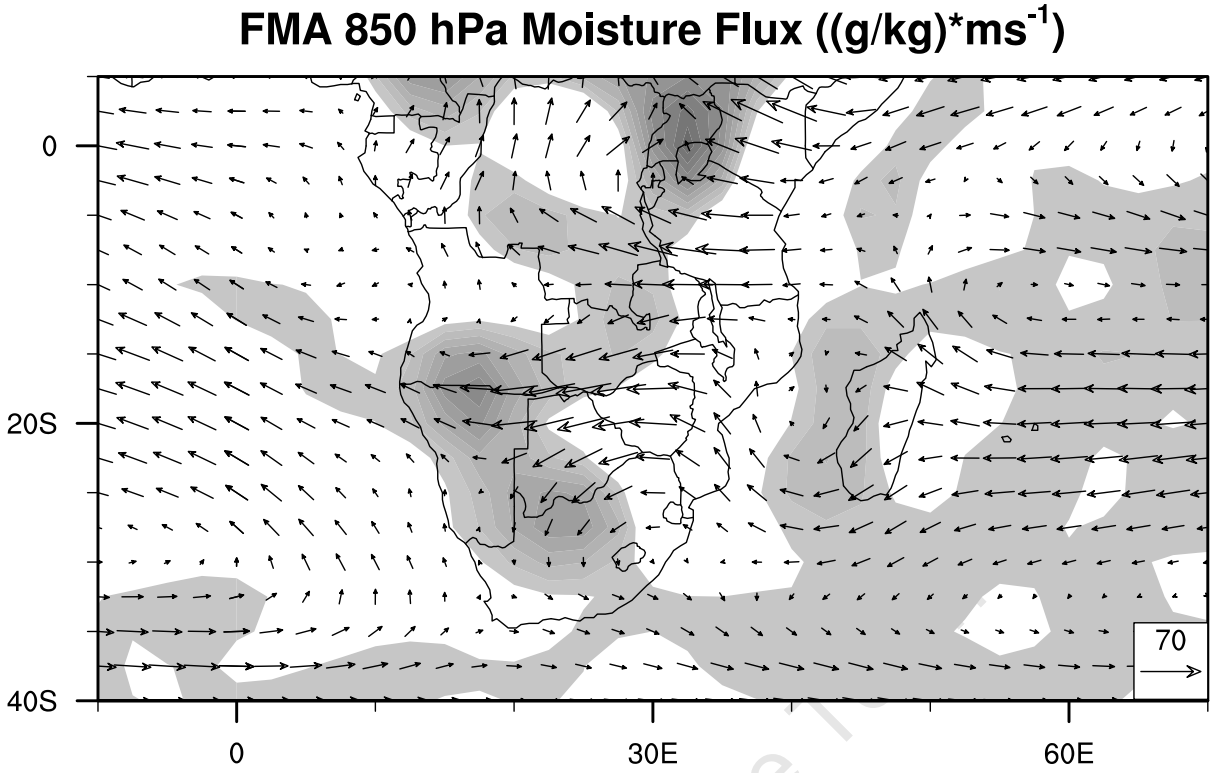

Figure 2.3: 850 hPa FMA moisture flux (vectors) and convergence (shaded) climatology (1974 - 2003).

et al. (2003) have done numerical model experiments in which their model was forced with the leading SST modes in the tropical Atlantic austral winter and spring. These experiments showed little or no precipitation changes over southern Africa. There was however more precipitation over the ocean than over the neighbouring continents in the model simulation.

Given the above evidence, it can be argued that the relationship between the size of the SST anomaly during warm events in the southeast Atlantic Ocean and the corresponding rainfall anomaly over southern Africa is nonlinear. This result suggests that rainfall anomalies during southeast Atlantic warm events may be modulated by other regional signals. An important regional pattern is the existence of a dipole like SST anomaly in the South Indian Ocean which is well known to influence southern African rainfall (Behera and Yamagata, 2001, Reason, 2001, 2002). Observations suggest that 1984 and 1995 were characterized by a negative phase SST dipole in the South Indian Ocean (unfavourable for southern African rainfall) and 1986 and 2001 by a positive phase SST dipole (favourable for southern African rainfall). These preliminary results therefore indicate that a better

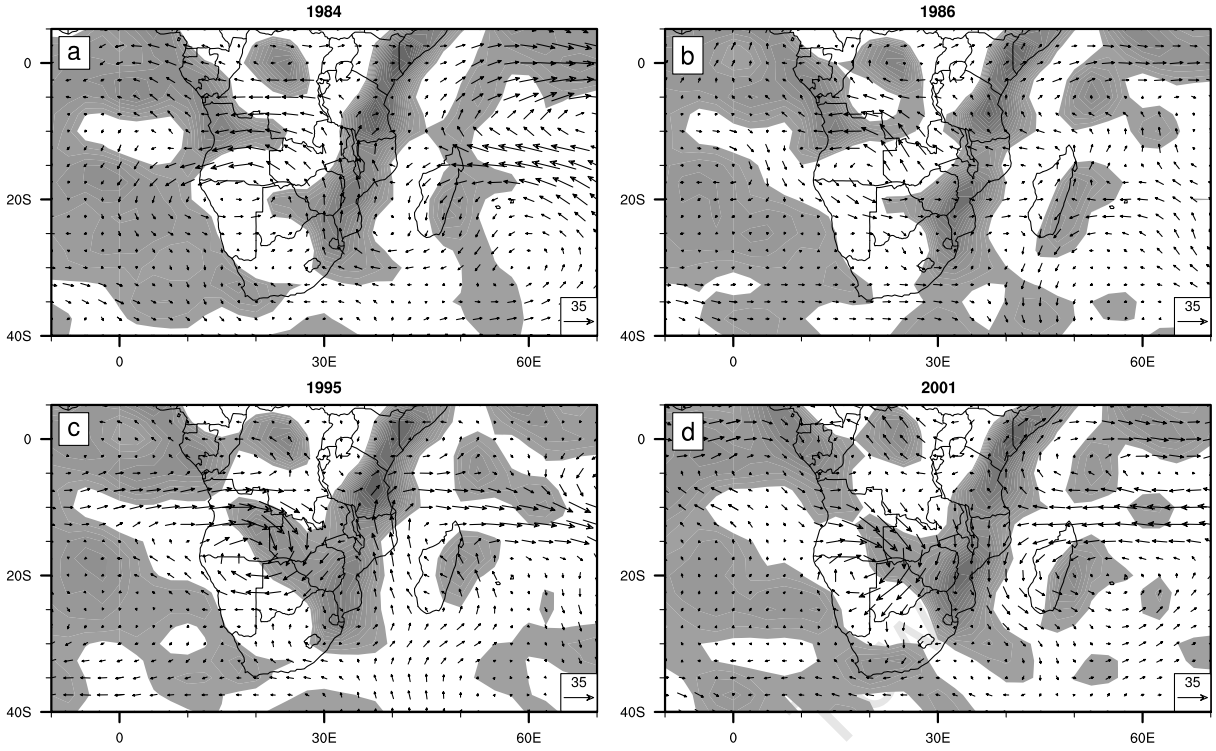

Figure 2.4: 850 hPa moisture flux anomalies (vectors) and moisture convergence (shaded) for 1984, 1986, 1995 and 2001 southeast Atlantic warm events (NCEP).

understanding of the impact of the southeast Atlantic warm events on southern African rainfall is required together with the potential modulation by South Indian Ocean SST and this is the focus of this thesis. Therefore, not all warm events in the southeast Atlantic produce above normal rainfall over southern Africa, but may modulate rainfall over coastal Angola by controlling regional atmospheric moisture and stability (Hirst and Hastenrath, 1983).

2.5 Modes of SST Variability in the Tropical Atlantic

Unlike the tropical Pacific which displays SST anomalies on a variety of time scales - the dominant ENSO timescale, quasi-biennial, near annual and decadal time scales (Wu and Kirtman, 2005) - low frequency variability in the tropical Atlantic is complex and hard to observe due to the weakness of this signal compared to the dominant seasonal one (Dommenget and Latif, 2000, Arnault *et al.*, 2004). The tropical Atlantic region is characterised by a fairly regular annual cycle around which there are climatically significant interannual

and decadal timescale variations (Servain *et al.*, 1998). Also, this region is not dominated by any single mode of climate variability, like the tropical Pacific Ocean; rather, this region is subject to multiple competing influences of comparable importance (Sutton *et al.*, 2000) and can experience significant anomalous perturbations. Two modes of variability have been found to be dominant over the tropical Atlantic Ocean; an equatorial Atlantic oscillation or zonal mode, which can be viewed as the Atlantic analogue of the equatorial Pacific, but much less vigorous (Latif and Grötzner, 2000) and a off-equatorial variability characterised by an anomalous cross-equatorial SST gradient (Haarsma *et al.*, 2005), the Atlantic meridional gradient mode (Servain, 1991, Huang and Shukla, 1997). Another mode of variability observed in the tropical Atlantic region is characterised by warmer than usual SST off the southwest coast of Africa, the Benguela Niño (Shannon *et al.*, 1986). This mode tends to merge with the zonal mode as the leading mode of variability in an EOF analysis of SST in the South Atlantic (Colberg and Reason, 2006). Studies (e.g. Tourre *et al.*, 1999, Sutton *et al.*, 2000, Colberg *et al.*, 2004, Huang, 2004) suggest that SST variability in the Atlantic Ocean is also affected by ENSO. The question whether the Benguela Niño, and the zonal and meridional modes are locally forced or remotely forced by ENSO, is still under debate. However, the general expectation is that external variability (i.e. strong ocean-atmosphere coupling) is important in the tropics. The frequency and amplitude of these deviations from the climatology have socio-economic ramifications and can be quite severe, particularly for countries that border the Atlantic at both ends of the basin (Busalacchi, 1998). The following sections discuss some of the modes of SST variability in the Atlantic Ocean.

2.5.1 Equatorial Atlantic Oscillation or Zonal Gradient Mode

The equatorial Atlantic is a region of strong SST variability (Latif and Grötzner, 2000). Houghton and Tourre (1992) performed a Principal Component Analysis (PCA) of monthly SST anomalies over the tropical region and two dominant modes account for about 70% of the variability. The first mode accounts for about 38.7% of the variability (Houghton and Tourre, 1992) and is tightly focused on the equator (Zebiak, 1993). The second mode

accounts for 31.2% of the variability (Houghton and Tourre, 1992). Detailed discussion of the second mode is deferred until the next section. The first mode is identified as the Equatorial Atlantic Oscillation or Zonal gradient mode and is characterised by SST anomalies of the same sign across the equatorial Atlantic region, similar to the ENSO mode in the Pacific (Lough, 1986). Houghton and Tourre (1992) and Zebiak (1993) have estimated its period to be about four years and Busalacchi (1998) suggest that this mode varies on seasonal to interannual time scales. However, using time series analysis of an equatorial Atlantic SST index (ATL-3), computed from an area average of anomalous SST over the region of strongest equatorial variability (3°N - 3°S and 20°W - 0°), Latif and Grötzner (2000) have shown that a quasi-biennial oscillation is the dominant interannual variability mode in the equatorial Atlantic SSTs. They further suggest that this mode is stable and consistent with observations and results obtained from statistical methods. It is however, debatable that this mode is the southern component of the second mode, the meridional gradient mode, which is dipolar in nature. The equatorial Atlantic oscillation pattern is correlated with rainfall variations in the Sahel region (Lamb 1978 cited in Zebiak, 1993) and Gulf of Guinea coastal region (Wagner and da Silva, 1994).

Dommenget and Latif (2000) suggested that the same physical mechanism that produces the ENSO mode in the Pacific can also produce an ENSO-like mode in the Atlantic except that it may be weaker in the Atlantic because of different basin geometry. During its warm phase, trade winds in the western equatorial Atlantic are weak and SST near the equator is unusually high, especially in the east. During its cold phase, trade winds in the western equatorial Atlantic are strong and SST near the equator is anomalously low. The onset of an equatorial cold or warm event can occur rapidly on time scales of weeks to months, involving the excitation and propagation of wind-forced equatorial Kelvin and Rossby waves. The climatic impacts of equatorial warm events include increased rainfall in the Gulf of Guinea and disruption of the marine ecosystem in the Benguela current region (Busalacchi, 1998). The eastern equatorial tongue or zonal gradient mode, as this mode of variability is often referred to, is open to the South Atlantic but isolated from the North Atlantic by West Africa and thus the subtropical anticyclone over the South

Atlantic directly influences this mode of variability through the southeast trade winds (Robertson *et al.*, 2003). However, the impact of this mode of variability on southern African climate is less well understood.

2.5.2 Meridional Gradient Mode

The Atlantic dipole or meridional gradient mode is characterised by a north-south inter-hemispheric gradient in SST anomalies, i.e., anomalies of opposite sign in each hemisphere evolving on decadal time scales. This mode of variability comes out as the second mode in the S-EOF (EOF in spatial domain) analysis of SST in the tropical Atlantic (Houghton and Tourre, 1992) and as the first mode in the T-EOF (EOF in temporal domain, Palastanga *et al.*, 2002). The occurrence of these antisymmetric SST anomalies is not always simultaneous and there is considerable debate regarding whether the northern and southern components are dynamically related in the form of a coupled mode (Busalacchi, 1998).

The northern hemisphere component of the dipole could be linked to the North Atlantic Oscillation (NAO) (Sutton *et al.*, 2000). Penland and Matrosova (1998) argue that such a dipole might dominate the anomalous tropical Atlantic SST signal if the tropical Atlantic SST anomalies were primarily associated with atmospheric conditions related to Pacific conditions. Although a dipole structure in SST anomalies in the tropical Atlantic does sometimes appear, along with its influence on precipitation, the question exists as to whether this pattern arises purely through chance or whether it has a dynamical origin. Studies (e.g. Kim and Schneider, 2003, Huang, 2004, Huang and Shukla, 2005, Haarsma *et al.*, 2005) have associated changes in trade winds in the tropical Atlantic with SST anomalies. Therefore this pattern may be related to tradewind change on either sides of the equator. In spite of the debate, changes in the meridional gradient in SST are highly correlated with the north-south translation of the ITCZ and its influence on continental precipitation over South America and Africa. Like the zonal gradient mode, the possible influence of the meridional gradient mode on southern Africa is less well understood.

2.5.3 Benguela Niños

The Southeast Atlantic Ocean near southern Africa is a unique and highly dynamic environment, comprising the subtropical cool Benguela current and the tropical warm Angola current (Hardman-Mountford *et al.*, 2003, Kim *et al.*, 2002). The Angola-Benguela front (ABF), the convergence between warm tropical and cool subtropical waters, is a prominent feature in this region (Kim *et al.*, 2002) and is located near 16°S - 19°S (Meeuwis and Lutjeharms, 1990, Shannon and Nelson, 1996, Colberg and Reason, 2006), i.e. the northern region of the Benguela upwelling system. Meeuwis and Lutjeharms (1990) suggested that the location of this front varies with the season.

Extreme warm SSTs have been observed in the area of the ABF and Shannon *et al.* (1986) have termed these warm events Benguela Niños because of their apparent similarities with El Niño events. To date, not much evidence has been shown of a link between Benguela Niños and ENSO (Enfield and Mayer, 1997, Latif and Barnett, 1995) and certainly these phenomena do not typically occur in unison (Florenchie *et al.*, 2003). Moreover, Benguela Niños are less intense and less frequent than El Niños (Shannon *et al.*, 1986). While Benguela Niños are less frequent, minor warm and cool events occur regularly along the coasts of Angola and Namibia (Florenchie *et al.*, 2004). As yet, no clear and completely objective classification for Benguela Niños has been identified. However, a strong warm event in the southeast Atlantic with a clear link through the thermocline to the equatorial Atlantic Ocean and with devastating environmental impacts and significant increase in rainfall over the adjacent land masses is generally classified as a Benguela Niño. Strong cold events are referred to as Benguela Niñas. Of the three dominant modes of variability in the tropical Atlantic Ocean, Benguela Niños and Niñas are the most important for southern Africa.

Benguela Niños and warm events in the southeast Atlantic are mainly limited to the ABF at the surface, but beneath the surface they extend northeast along the thermocline to the equator (Florenchie *et al.*, 2003) and across the equatorial Atlantic towards Brazil. Typically the southern extent of the SST anomaly varies between 20°S to as far as 25°S (Currie *et al.*, 2002). Nonetheless, the location of the SST anomalies associated with

these events is always apparent over 10°-20°S, 8°E to the coast of south-western Africa and can be as high as 4°C because this where the thermocline shoals towards the southwest Atlantic.

What causes these warm events? From year to year, there is a poleward intrusion of warm water from the Angolan current into the northern Benguela upwelling system (Boyer *et al.*, 2000, Florenchie *et al.*, 2003), but during a Benguela Niño, the ABF is displaced south, causing the advection of warm equatorial water as far as 25°S (Shannon *et al.*, 1986). This tends to happen during the late austral summer period (FMA) (Currie *et al.*, 2002, Rouault *et al.*, 2003). Blanke *et al.* (2002) suggest that changes in strength and direction of alongshore winds may result in anomalously warm or cold temperatures along the coast. Furthermore, Jury (1996) suggest that warm events in the southeast Atlantic may be as result of reduced local trade winds. On the other hand, studies with an ocean general circulation model (e.g. Florenchie *et al.*, 2003, 2004) suggest that temperature anomalies in the southeast are a result of a Kelvin wave-like disturbance propagating on the thermocline across the equatorial Atlantic Ocean, brought about by the modification of trade winds in this region. Other studies have suggested that these events could be linked to a relaxation of zonal wind stress in the western equatorial Atlantic (Delecluse *et al.*, 1994) and a change of between 25 to 50% in the average windstress for this region may be responsible for creating the required thermocline displacement (Florenchie *et al.*, 2003). Therefore, Benguela Niños and other warm events are thought to be a result of remote atmospheric anomalous conditions in the western tropical Atlantic (Boyer *et al.*, 2000).

As mentioned above, warm events tend to occur during the late austral summer period and a number of these events have occurred since the early 20^{th} century. They occurred in 1934, 1949 1963, 1984, 1986, 1995 and 2001 (Shannon *et al.*, 1986, Florenchie *et al.*, 2003, Rouault *et al.*, 2003) of which the 1984 and 1995 events were notable for their exceptional intensity and persistence at the sea surface and are recent examples of Benguela Niños. Observational studies (e.g Hirst and Hastenrath, 1983, Nicholson and Entekhabi, 1987, Rouault *et al.*, 2003) have shown that anomalous atmospheric conditions occur over

areas of anomalous SST and may be linked with above normal rainfall along the coast of Angola and Namibia and sometimes also inland areas of Southern Africa, e.g. Zambia. However, rainfall anomalies during some events appear to depend on the intensity of the regional moisture convergence and atmospheric circulation anomalies (Rouault *et al.*, 2003). Though little has been done to understand the possible links between SST anomalies in the tropical Atlantic Ocean and southern African rainfall, warm events appear to have great impact on late austral summer rainfall. Therefore, a better understanding of these warm events is necessary for assessing impacts on regional rainfall and agriculture and for improving seasonal forecasting in the region (Rouault *et al.*, 2003).

This chapter has reviewed specific systems linked to rainfall production over southern Africa. However, the focus of this thesis is on Benguela Niños because the atmospheric anomalies associated with these systems and their impact on southern African rainfall are not well known. Until recently, little work has been on these systems since the work of Hirst and Hastenrath (1983).

2.6 Summary

Despite a great deal of research relating rainfall variability over southern Africa to ENSO and the Indian Ocean, extreme rainfall seasons in southern Africa still need to be better understood. This situation results from the fact that climate variability over southern Africa is complex with a multitude of forcing factors that interact with each other (Reason *et al.*, 2006). It is therefore important to also investigate possible contributions of the Atlantic Ocean to climate variability over southern Africa. Observational studies (e.g. Hirst and Hastenrath, 1983, Rouault *et al.*, 2003, Reason and Jagadheesha, 2005a) have shown that the SST in the South Atlantic Ocean may influence rainfall variability over southern Africa. However, the Atlantic Ocean exhibits several modes of variability, identified through observational and statistical methods, of comparable importance, although not all of them have been observed to have influence on southern Africa climate variability. Benguela Niños have been observed to influence late austral summer rainfall over coastal regions of Angola and Namibia and sometimes over inland regions

of South Africa. Preliminary results indicate that a nonlinear relationship may exist between Benguela Niño intensity and southern African rainfall and that SST in the Indian Ocean and other land-based processes during these events may modulate their impact on southern Africa. Therefore, this thesis investigates the impacts of the Benguela Niño on rainfall over southern Africa. In order to carry out this investigation, experiments with a numerical model are conducted and this is discussed in the next chapter.

Chapter 3

Methodology and Data

3.1 Introduction

Atmospheric general circulation models (AGCMs) have proven useful in many applications, particularly in weather and climate studies. These include weather and climate prediction, sensitivity/perturbation and simulation studies. AGCMs numerically solve fundamental or primitive equations describing the conservation of mass, energy, momentum and moisture for each atmospheric gridbox while taking into account the transfer of those quantities between gridboxes (Goddard Institute for Space Studies - GISS, 1999). General circulation models also consider, often in parameterized form, the physical processes within the boxes including sources and sinks of these quantities. AGCMs are either grid-point or spectral models.

Though knowledge of the model type does not have an obvious application to the interpretation of model output, there are many important reasons for knowing the type of model (University Corporation for Atmospheric Research - UCAR, 1999). For example, grid-point and spectral models differ in the way the primitive equations are solved, how data are represented and the type and scale weather features that can be resolved. Just as the model-type names imply, grid-point models represent data as discrete, fixed, grid points, whereas spectral models use continuous wave functions. AGCMs have historically been spectral because the wave functions and spherical harmonics in the spectral

formulation operate over a spherical domain, a good match for AGCMs. With the increase in computer resources, AGCMs are increasingly becoming grid-point (University Corporation for Atmospheric Research - UCAR, 1999).

In chapter two, it has been suggested that the relationship between Benguela Niño warm events in the southeast Atlantic and austral late summer rainfall over southern Africa is not linear and that the Indian Ocean SST may modulate their impact. This chapter presents an outline of experiments designed to attempt to answer the questions posed in chapter one. The main tool used for this purpose is the atmosphere component of the United Kingdom Met Office (UKMO) Hadley Centre Coupled Model version 3 (HadCM3), the Hadley Centre Atmospheric Model version 3 (HadAM3) general circulation model, forced with different prescribed SST patterns. We acknowledge the importance of coupling between the ocean and the atmosphere and the feedbacks involved, however, the focus in this thesis is on the processes hence the use of the atmospheric component only.

HadAM3 is a grid-point model and has been used in various African studies, for example, in investigating intraseasonal (Tennant, 2003) or interannual (Reason and Jagadheesha, 2005a,b) varibility, and in sensitivity studies (Washington and Preston, 2006) as well as for operational seasonal forecasting. Previous studies with this model (e.g. Reason *et al.*, 2003, Reason and Jagadheesha, 2005a,b, Washington and Preston, 2006) indicate that HadAM3 correctly simulates a unimodal annual cycle with maximum rainfall in the austral summer (October - March) over subtropical southern Africa and winter rainfall over southern South Africa. These authors indicate that the model does overestimate summer rainfall and this is most pronounced in the early summer season (October to December) with positive bias continuing into the late summer months (January to March).

Reason and Jagadheesha (2005a) also observed that the model is less successful with magnitudes of winter rainfall over the southwestern Cape region of South Africa for certain years between 1985 and 2000. Despite the model's shortcomings in simulating rainfall magnitudes correctly, it has some skill in capturing the observed interannual tendency in

rainfall over southern Africa (Reason and Jagadheesha, 2005a,b, Washington and Preston, 2006) for both the small winter rainfall dominated southwestern region and the summer rainfall region that exists over most of southern Africa. Given these strengths of the model, it seems appropriate to apply it to investigate the sensitivity of the regional atmosphere to idealized SST patterns. The following sections present a brief description of the model and the design of the experiments. A detailed evaluation of this model, its biases and the main parameterizations of the sub-grid-scale physics are provided in Pope *et al.* (2000).

3.2 Model Dynamics and Parameterisation Schemes

The HadAM3 model is the atmospheric component of the Hadley Centre Coupled Model version 3 (HadCM3), a coupled atmosphere-ocean general circulation model (AOGCM) also known as the Unified Model (UM, Pope *et al.*, 2000), developed at the Hadley Centre in the United Kingdom (UK) and used at UKMO. Coupling between the atmosphere and the ocean is not considered in this thesis, therefore no feedbacks are not taken into account. HadAM3 is a hydrostatic, grid point model using an Arakawa B grid and hybrid vertical co-ordinates. It uses an Eulerian advection scheme and has a horizontal resolution of $3.75° \times 2.5°$ in longitude $\times$ latitude, which gives it 96×73 grid points and about 416 km and 277 km longitudinal and latitudinal grid distance respectively. There are 19 levels in the vertical and 30 minutes timestep. The levels are spaced unevenly in the vertical to give the optimum resolution in terms of pressure in the upper troposphere and stratosphere, and near the surface (Lean and Rowntree, 1997).

The model uses a prognostic cloud scheme, which diagnoses cloud ice, cloud water and cloud amount from the primary model variables q_T (total moisture or water content, Senior and Mitchell, 1993, Pope *et al.*, 2000) and θ_L (liquid water potential temperature, Deardroff, 1976, Pope *et al.*, 2000). The scheme produces realistic cloud distributions and the predicted cloud water content verifies well against microwave radiometer data in all regions except the mid latitudes of the summer hemisphere (Smith, 1990). Here,

$$q_T = q + q_C \tag{3.1}$$

where q and q_C are the specific humidity and cloud water content respecitively.

$$\theta_L = \theta - \left(\frac{\theta}{T}\frac{L}{c_p}\right) q_l \tag{3.2}$$

where θ is the potential temperature, q_l the liquid water specific humidity, L the latent heat of vaporization, and c_p the specific heat at constant pressure.

The model's precipitation scheme uses the above cloud scheme together with the evaporation of precipitation scheme. The evaporation scheme uses different evaporation coefficients for ice (A_v^s) and water (A_v^w) (Gregory, 1995). The evaporation coefficient for ice is,

$$A_v^s(T,p) = (-5.2 \times 10^{-9}T^2 + 2.5332 \times 10^{-6}T - 2.9111 \times 10^{-4})\frac{10^5}{p} \tag{3.3}$$

and for water is,

$$A_v^w(T,p) = (2.008 \times 10^{-9}T^2 - 1.385 \times 10^{-6}T + 2.424 \times 10^{-4})\frac{10^5}{p} \tag{3.4}$$

where T(K) and p(Pa) are the temperature and pressure respectively. The model includes a prognostic ice microphysics large-scale precipitation scheme which uses variables representing vapour, liquid, ice and rain. This scheme is referred to as the mixed-phase scheme (MPS) or mixed-phase precipiation scheme (MPP). This scheme is used in all the experiments in this thesis.

Moist and dry convection are modelled using the mass-flux penetrative scheme, which uses a bulk cloud model to represent an ensemble of convective clouds and aims to represent shallow, deep and midlevel convection (Gregory and Rowntree, 1990). Convective downdrafts are also incorporated in this scheme. The bulk cloud model is derived by summation over an ensemble of convective clouds with differing characteristics. For a cloud I within the ensemble the equation governing cloud mass flux (M) is,

$$\frac{\partial M_{PI}}{\partial \sigma} = (E_I - N_I - D_I) \tag{3.5}$$

where

M = cloud mass flux

E = entrainment rate

N = mixing detrainment rate

D = forced detrainment rate

and summing over all cloud types lead to equation for the bulk cloud model:

$$\frac{\partial M_P}{\partial \sigma} = (E - N - D) \tag{3.6}$$

where

$E = \sum_I E_I$

$N = \sum_I N_I$

$D = \sum_I D_I$

The gravity wave drag (GWD) parameterization aims to represent the transport of momentum by unresolved gravity waves. Currently, only the impact of those gravity waves forced by orography is represented (Webster, 1998). There are three GWD schemes to choose from in the UM. The first scheme is what might be described as the classical first generation GWD scheme. This scheme assumes the surface stress is orientated in the same direction as the low level wind and is proportional to the sub-grid orographic standard deviation. The parameterization assumes that linear hydrostatic waves are generated and so the stress is deposited according to a simple saturation hypothesis. This scheme exerts most of the drag in the lower stratosphere (Webster, 1998).

The surface stress calculation for the second scheme is identical to that of the first. This scheme has a different stress deposition algorithm; the stress is linearly deposited between the surface and the top of the atmosphere, unless a critical level is encountered in which case all the remaining stress is deposited in the current level. This scheme, therefore, exerts a uniform drag through the full depth of the atmosphere.

The most widely used GWD scheme is the third version. This scheme builds on the first scheme and accounts for the anisotropy of the sub-grid orography in the calculation

of the surface stress (Webster, 1998). The model uses this anisotropic gravity-wave-drag parameterization scheme which represents high drag states modeled on hydraulic jump, flow blocking and internal-wave-reflection theory, including trapped lee-waves. The scheme represents the breaking of waves over mountains better (Gregory and Shutts, 1998) than previously.

Because of the earths surface interaction with the lowest part of the atmosphere, the bottom kilometer one or two of the atmosphere (the boundary layer) is often turbulent. Turbulent motions within the boundary layer are important because they transport momentum, moisture, heat, aerosol and pollutants mainly in the vertical. However, AGCMs are not able to resolve these motions adequately and therefore, turbulent motions are parameterized. The boundary layer scheme (version 3A or 6A) in the HadAM3 model is in two parts; the surface exchange scheme and the boundary layer turbulent mixing scheme (Smith, 1998). The surface exchange scheme determines the turbulent transport of surface variables and atmospheric variables at the bottom model level to/from the atmosphere. This scheme uses surface exchange coefficients, which are functions of the stability of the surface layer and quantities such as the surface roughness and wetness. Version 3A uses the bulk Richardson number of the surface layer as its stability parameter whereas version 6A uses the Monin-Obukhov length (Smith, 1998).

The boundary layer turbulent mixing scheme determines the turbulent transports above the surface layer. Version 3A uses the vertical profile of the locally determined Richardson number to determine the top of the turbulent boundary layer. This version also has the option of rapid mixing of scalar quantities from the surface throughout the boundary layer in unstable conditions. Stable boundary layers are determined from local Richardson number (Smith, 1998).

The 6A version classifies the boundary layer into six types:

I. Stable boundary layer

II. Boundary layer with stratocumulus over a stable surface layer

III. Well mixed boundary layer

IV. Boundary layer in a decoupled stratocumulus layer not over cumulus

V. Boundary layer with a decoupled stratocumulus over cumulus

VI. Cumulus capped boundary layer

In this version, the depths of the mixing layers are determined by testing the buoyancy of plumes rising from the surface or descending from cloud top. When a cumulus capped boundary layer is diagnosed the surface-based turbulent mixing is not applied above the lifting condensatioin level (Smith, 1998).

Edwards and Slingo (1996) have developed a radiation scheme designed to be flexible that it could be used in a wide range of applications. This scheme is based on the two-stream equations in both the long-wave and short-wave spectral regions. This implies that the processes that are important in both spectral regions, such as the overlapping of partially cloudy layers, are treated consistently. The two-stream equations are valid only for monochromatic radiation therefore the irradiance within a particular spectral band is calculated by performing a number of quasi-monochromatic calculations (Edwards and Slingo, 1996). Using $F^{\pm}$ and S to denote the upward and downward diffuse irradiances and solar irradiance respectively, the two-stream equations may be written:

$$\frac{dF^{+}}{d\tau} = \alpha_1 F^{+} - \alpha_2 F^{-} - Q^{+} \tag{3.7}$$

$$\frac{dF^{-}}{d\tau} = \alpha_2 F^{+} - \alpha_1 F^{-} + Q^{-} \tag{3.8}$$

and

$$\frac{dS}{d\tau} = -\frac{S}{\mu_0} \tag{3.9}$$

where τ is the optical depth measured downwards from the top of the atmosphere, $Q^{\pm}$ are source terms and α_1 and α_2 are coefficients defined in terms of the diffusivity factor D, which lies between 1.5 and 2. μ_0 is the cosine of the zenith angle ($\mu_0 \geq 0$).

This scheme has six shortwave bands and eight longwave bands. With increase in atmospheric aerosol concentrations and their importance in the atmospheric radiation budget, the scheme includes the effects of background aerosols, CFC11, CFC12, CH_4, CO_2, H_2O, N_2O, O_2 and O_3. Ice crystals and water droplets are treated separately in the scheme (Pope *et al.*, 2000).

The model uses an ozone climatology based on recent satellite measurements in the stratosphere and a limited set of ground based measurements in the troposphere. This climatology represents a realistic prescribed ozone distribution for GCMs and can be used as a reference for validation of GCM that treat ozone as prognostic variable (Li and Shine, 1995). As the climatology was constructed from different sources, the cubic spline interpolation scheme was used to interpolate the data onto the adopted grid.

The Meteorological Office surface exchange scheme (MOSES) is used for HadAM3's land surface scheme. MOSES includes a representation of the freezing and melting of soil moisture leading to better simulations of surface temperatures (Pope *et al.*, 2000). In addition to calculating water and energy fluxes, MOSES also calculates vegetation to atmosphere fluxes of CO_2 incorporating the direct physiological effect of atmospheric CO_2 concentrations of both photosynthesis and stomatal conductance (Cox *et al.*, 1999).

3.3 Data

3.3.1 Initial and boundary conditions

In order to start an AGCM simulation, it is necessary to supply the model with initial conditions and boundary conditions that define the initial state of all factors in the model that affect model calculations. An initial atmospheric state is prescribed at the start together with boundary conditions such as SST, vegetation and usage, soil moisture etc. Boundary conditions must be as realistic as possible and appropriate for the type of simulation planned. One of the most important boundary conditions is the SST data, since SST directly affects the moisture and energy fluxes at the ocean surface. The OISSTv2 data set, produced at the National Oceanic and Atmospheric Administration

(NOAA) was used to force the model. The same data set is used to identify Benguela Niños in chapter 2. This data set is produced using both in situ and satellite data and is interpolated on 1° latitude/longitude grid (Reynolds *et al.*, 2002). The in situ data are determined from observations from ships and buoys with the former depending on shipping traffic and is most dense in the midlatitude Northern Hemisphere. The ship data are very sparse in the midlatitude South Pacific east of the 180° meridian and in the tropical Pacific east of 160°E (Reynolds and Smith, 1994). The buoy data are designed to fill in some areas with little ship data and to monitor ENSO and this process has been most successful in the tropical Pacific compared to other areas such as the tropical Atlantic that have almost no buoys SST observations. Buoy observations are typically made by thermistor or hull contact sensor at an average depth of 0.5m compared to the 1 m and deeper measurements from ships. The random error from buoy observations is better (less then 0.5°C) than ship error (Reynolds *et al.*, 2002).

The satellite observations are obtained from the Advanced Very High Resolution Radiometer (AVHRR) on the U.S NOAA polar orbiting satellite. The SST satellite retrieval algorithms are tuned by regression against quality controlled drifting buoy data using the multichannel SST technique of McClain *et al.,* (1985) and Walton (1988) (cited in Reynolds and Smith, 1994). Note that the tuning is usually done when a new satellite becomes operational; November 1981 is used in this case, or when verification with the buoy data shows increasing errors. This procedure is done to eliminate cloud contamination in the data as the AVHRR cannot see the surface in cloud-covered regions. The in situ and satellite SST are then blended with ice sea data from the U.S National Meteorological Centre (NMC, later NCEP) using technique developed at the UKMO. This technique eliminates any high-latitude satellite biases and extends the analysis to the ice edge. This data set is widely distributed and used by researchers around the world.

Owing to HadAM3's coarser resolution than the OISST data set, OISST data is degraded by interpolating it to the model grid of 3.75° longitude by 2.5° latitude using bilinear interpolation. This method basically performs linear interpolation first in one direction, and then in the other direction; the order does not matter.

As mentioned above, an initial state of the atmosphere needs to be prescribed at the start of a model run. This atmospheric initial state is prescribed by initial condition data. In general, different data sets can be used for initial condition data in AGCMs. In HadAM3, initial data must be in the form of a dump file, but depending where the data originate and how they are generated, there is no general method of creating such a file (Robinson and Clark, 1998). Information related to boundary conditions and climatological values are contained in an ancillary file. However, ancillary files are only necessary in the absence of dump files or when model reconfiguration is necessary. Dump files or initial dumps, as they are sometimes referred, are data files containing initial conditions at particular dates from previously run experiments or simulations. In this thesis initial dumps from previously run experiments are used for the models initial condition data.

3.3.2 Observations

The NCEP/NCAR dataset is a product of a project undertaken by NCEP (formerly NMC) and NCAR in 1991 to produce a 40-year (1957-1996) record of global analyses of atmospheric fields in support of the needs of the research and climate monitoring communities (Kalnay *et al.*, 1996). This project involved the recovery of land surface, ship, raobs (rawinsonde observations), pibal (pilot balloon), aircraft, satellite, and other data; quality controlling and assimilating these data. The NCEP/NCAR 40-yr reanalysis uses a frozen state-of-the-art global analysis/forecast and data assimilation system and a database as complete as possible. The data assimilation system uses past data, from 1957 to the present and uses the same horizontal resolution of about 210 km with 28 vertical levels as the NCEP global spectral model. The database is enhanced with many sources of observations provided by different countries and organizations (Kalnay *et al.*, 1996).

Complex and optimal interpolation quality control (CQC and OIQC, respectively) methods are used to quality control rawinsonde heights and temperatures and all data respectively. CQC first computes residuals from several independent checks (i.e., it computes the difference between an observation and the expected value for that observation from each check). The residuals are used together with the decision making algorithm

(DMA) to accept, reject or correct data. OIQC detects and withhold from the assimilation data containing gross errors generated by instrumental, human, or communication-related mistakes that may occur during the process of making or transmitting observations. It also withholds observations with large errors of representativeness that are accurate but whose measurements represent spatial and temporal scales impossible to resolve properly in the analysis-forecast system (Kalnay *et al.*, 1996).

The reanalysis gridded fields have been classified into four classes, depending on the relative influence of the observational data and the model on the gridded variable. An **A** indicates that the analysis variable is strongly influenced by observed data, and hence it is the most reliable class (e.g., upper-air temperature and wind). The designation **B** indicates that, although there are observational data that directly affect the value of the variable, the model also has a strong influence on the analysis value (e.g., specific humidity and surface temperature). The letter **C** indicates that there are no observations directly affecting the variable, so that it is derived solely from the model fields forced by the data assimilation to remain close to the atmosphere (e.g., clouds, precipitation and surface fluxes). Finally the letter **D** represents a field that is obtained from climatological values and does not depend on the model (e.g., plant resistance and land-sea mask) (Kalnay *et al.*, 1996).

Although the reanalysis should be a research quality dataset suitable for many uses, including weather and short-term climate research, it should be used with caution as the different outputs are not uniformly reliable (Kalnay *et al.*, 1996). For example, fields in class **B** are not as equally influenced by observations as those in class **A**. Those in **A** are generally well defined by the observations and, given the statistical interpolation of observations and first guess, provide and estimate of the state of the atmosphere better than would be obtained using observations alone. Those in **B** are partially defined by the observations but are also strongly influenced by the model characteristics (Kalnay *et al.*, 1996).

CMAP global monthly precipitation has been constructed on a 2.5° latitude-longitude grid by merging several kinds of information sources with different characteristics. The

sources are mainly from gauge observations, satellite estimates and output from a numerical model (Xie and Arkin, 1997). Gauge observations are gauge-based analysis from the Global Precipitation Climatology Center (GPCC) and the Global Historical Climatology Network (GHCN) of the Carbon Dioxide Information Center (CDIC) of U.S. Department of Energy (DOE) and the Climate Anomaly Monitoring System (CAMS) of the Climate Prediction Center (CPC) of National Oceanic and Atmospheric Administration (NOAA). The GPCC analysis is constructed by interpolating quality-controlled observations from over 6700 stations globally using the spherical version of the Shepard scheme (Xie and Arkin, 1997). The GHCN/CAMS gauge-based data is constructed by interpolating station observations of monthly precipitation for over 6000 gauges using the same algorithm as used by the GPCC.

The quality of gauge-based analysis depends primarily on the gauge network density and random error decreases with increasing gauge network density (Xie and Arkin, 1997). Significant bias exists over grid boxes without gauges because values over these areas are determined by interpolating observations over the surrounding areas. GPCC and GHCN/CAMS analyses do not cover the oceans, therefore observations from over 100 gauges located on atolls and small islands are used over oceanic areas. However, these atoll gauges are mainly located in the western Pacific Ocean (Xie and Arkin, 1997).

Estimates inferred from satellite observations include the infrared (IR)-based Geostationary Operational Environmental Satellite (GOES) Precipitation Index (GPI), the Outgoing Longwave Radiation (OLR)-based Precipitation Index (OPI), the Microwave Sounding Unit (MSU)-based Spencer, the Special Sensor Microwave/Imager (SSM/I)-scattering-based NOAA/NESDIS (National Environmental Satellite, Data, and Information Services), and the SSM/I-emission-based Chang (Xie and Arkin, 1997). Satellite estimates are available from 60°N to 60°S. Though satellite observations are used to retrieve precipitation information over many parts of the globe, the estimates made from satellite observations contain non-negligible random errors and bias because inadequate sampling and imperfect algorithms (Xie and Arkin, 1997).

Since none of the above data sources is able to monitor precipitation with reasonable quality over mid- and high-latitude oceanic areas, precipitation distributions produced by numerical models are included to ensure full global coverage of precipitation (Xie and Arkin, 1997). The model-produced precipitation data used in the CMAP dataset is that from the NCEP/NCAR reanalysis, which is defined by assimilating quality-controlled observations from all possible sources.

To produce the CMAP dataset, gauge observations, satellite estimates and numerical model predictions are merged and this is done in two steps. In the first step, the satellite estimates and the model predictions are combined linearly through the maximum likelihood estimation method, in which the weighting coefficients are inversely proportional to the error variance for the individual data source. This mode helps to reduce random errors in the dataset. However, the bias in the individual datasets remains in the combination, therefore the output from the first step is blended with the gauge observations to remove that bias. The gauge data is used to define the amplitude of the finial precipitation field and the first-step-output is used to define the distribution (Xie and Arkin, 1997). Therefore the CMAP dataset contains precipitation distributions with full global coverage and improved quality.

3.3.3 Model data

For model validation purposes in chapter 4, the data used in Reason and Jagadheesha (2005a,b) for the climatology is used in this thesis. This data was contructed by forcing the HadAM3 model with a 10-year Reynolds OISSTv2 monthly climatology and integrated for 15 year, from January 1985 to December 1999.

3.4 Experimental design

In an SST forcing experiment, an AGCM is forced using a prescribed SST pattern and the idea behind this is normally to try and work out what influence a given pattern of SST has on the atmosphere. Usually this pattern is constructed from a climatological SST

pattern with a SST anomaly superimposed that is an idealized representation of some observations. In order to ascertain the impacts of the Benguela Niños on southern Africa rainfall and whether the Indian Ocean modulates these impacts, idealized experiments with different SST anomaly patterns are carried out in this thesis. These anomalies are smoothed representations of the observed patterns and are about twice as large as the actual magnitudes. The SST forcing is increased so as to reduce the noise and help isolate the model response to the forcing (Reason and Jagadheesha, 2005a). In this thesis, the forcing is introduced in the model via ancillary files. The experiments are an idealization of the most recent observed strong (1995) and weak (2001) Benguela Niño events which had opposite signed SST anomalies in the south Indian Ocean.

In order achieve the objective of the research, model experiments are designed to address the questions posed in **Chapter 1**.

In many studies investigating the influence of prescribed SST patterns on the atmosphere, a kind of a control experiment is required. This control run acts like a base against which all other experiments can be compared. In this thesis, the control run is referred to as Experiment 1. Nine runs with idealised patterns of SST anomalies are designed to address the subsidiary questions above and are referred as Experiment 2-10. These experiments consist of five ensemble members, each initialized with different initial conditions arbitrarily picked. The use of a five-member ensemble is barely viable for significance test. However, limited computer facilities could not allow the use of a larger number of ensemble members.

The idealized SST anomaly patterns are shown in Figure 3.1 and the following section presents descriptions of each experiment.

In this thesis, the control experiment is one in which the model is forced with 24-yr (1982-2005) global climatology OISSTV2 (Reynolds and Smith, 1994, Reynolds *et al.*, 2002) at the sea surface and integrated for twelve months from November. Thus, the model run simulates the atmospheric state corresponding to the 24-yr mean of SST. As mentioned above, this experiment consists of five ensemble members, each initialized with different initial conditions arbitrarily picked.

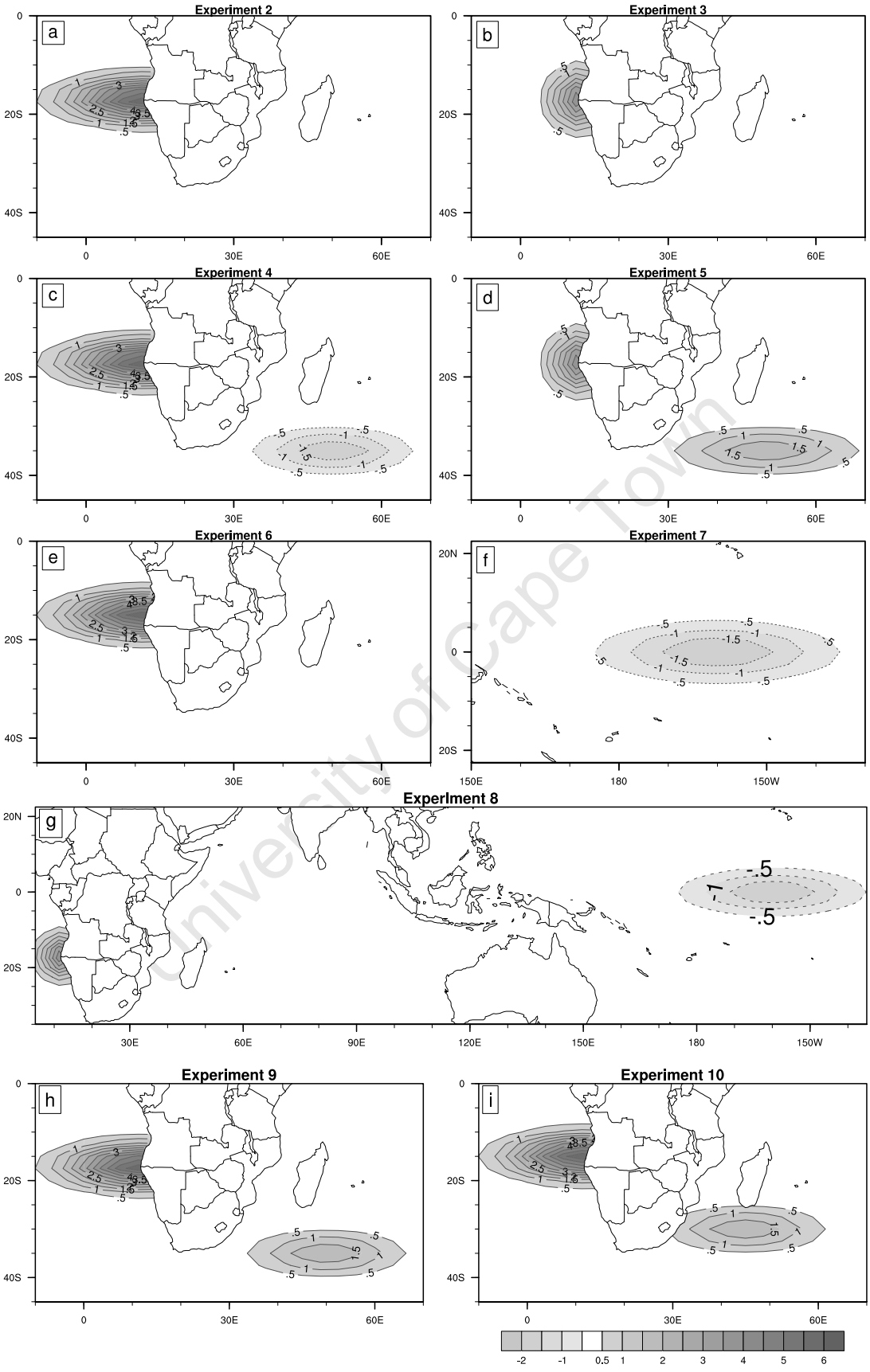

Figure 3.1: Idealized SST anomaly patterns for idealized exeriments

In Experiment2, the SST anomaly pattern is an idealized representation of the observed pattern in the southeast Atlantic Ocean during the 1995 Benguela Niño event. This experiment will try to examine circulation changes over southern Africa due to the southeast Atlantic Ocean forcing only. The forcing is centered at 17°S, 12°E and extends westward to about 10°W and the size is +6°C (Figure 3.1**a**), about twice the observed (Figure 2.2). This experiment represents an intense Bengula Niño and therefore the purpose of this experiment is to address the strong intensity aspect of the first question in the subsidiary questions.

Experiment 3 (Figure 3.1**b**) is similar to Experiment 2 except that the intensity of the anomaly forcing is weaker, +4°C, than in Experiment 2 and does not extend westward as much as in Experiment 2. This experiment is an idealized representation of the 2001 Benguela Niño event SST warm anomaly pattern in the southeast Atlantic Ocean. The purpose of this experiment is to address the weak intensity aspect of the first question in the subsidiary questions. Therefore, together with Experiment 2, this experiment will try to address subsidiary question 1 and the impacts of Benguela Niño on southern African rainfall.

As suggested in chapter two, warming or cooling in the southwest Indian Ocean may modulate the impact of Benguela Niños on southern African rainfall. In Experiment 4, in addition to the southeast Atlantic Ocean, warming in Experiment 2 cooling is imposed in the southwest Indian Ocean. The cooling is centered at 50°E, 35°S and -2°C in size (Figure 3.1**c**). This experiment is an idealization of the 1995 Benguela Niño event, which was characterized by cool SST anomalies in the southwest Indian Ocean. This experiment will try to address the effects of cooling in the southwest Indian Ocean in association with a strong Benguela Niño in the southeast Atlantic Ocean.

Experiment 5 is similar to Experiment 3 except that a warm SST anomaly centered at 50°E, 35°S and +2°C in size is imposed in the southwest Indian Ocean (Figure 3.1**d**). Experiment 5 is an idealization of the 2001 Benguela Niño event, which was characterized by warm SST anomalies in the southwest Indian and southeast Atlantic Oceans. This

experiment will try to address the effect of warming in the southwest Indian Ocean in association with a weak Benguela Niño. Therefore, this experiment together with Experiment 4 will try to address subsidiary question 2.

Though tropical regions do not show much spatial variability in SST, weak SST gradients may influence atmospheric circulation over these areas and the neighbouring continents. In Experiment 6, the SST anomaly forcing is shifted northward, centered at 15°S, 12°E (Figure 3.1**e**). This experiment is similar to Experiment 2 except for shifted forcing and will try to address question 3 of the subsidiary questions. Note that some observed Bengula Niños (e.g. the 2001 event) do occur further north than others.

During the 2001 Benguela Niño event, cool SST anomalies of about -1°C were observed in the equatorial Pacific Ocean (see Figure A.1 in Appendix A). These SST anomalies extend northeastwards from about 160°E to the Southwest coast of North Amerimca and signify a La Niña event. Therefore, the 2001 Bengula Niño event coincided with a La Niña event. The La Niña event also may have contributed to the atmospheric circulation, and hence rainfall over southern Africa during the 2001 Benguela Niño. In Experiment 7, the influence of cooling in the central equatorial Pacific Ocean on southern African circulation is examined. Note that this experiment does not include any forcing elsewhere except the central equatorial Pacific (Figure 3.1**f**). Given the large spatial extent of the cool SST anomalies in the equatorial Pacific Ocean during the La Niña, a small region in the central equatorial Pacific is arbitrarily chosen to force the model with cool SST anomalies (see Figure A.1 in Appendix A). This is needed to simulate the atmospheric response over southern Africa to a cool SST forcing emanating only from the central Pacific Ocean. This experiment is an idealization of the observed anomaly in the central Pacific Ocean. The idealized anomaly is centered at the Equator, 160°W and -2°C in size. Therefore, Experiment 7 partly addresses the last subsidiary question.

Experiment 8 is similar to Experiment 7 except that a positive anomaly 4°C is imposed in the southeast Atlantic Ocean (Figure 3.1**g**). This experiment is an idealization of the 2001 Benguela Niño, except that the southwest Indian Ocean forcing is removed. In this experiment, the influence of cooling in the central equatorial Pacific on southern African

circulation in relation to the Benguela Niños is examined. Therefore, this experiment and Experiment 7 will try to address question 4 in the subsidiary questions.

In Experiment 9, the model is forced with the same SST anomalies as in Experiment 6 but with a warm anomaly added in the southwest Indian Ocean (Figure 3.1**h**) This experiment is conducted on the premise that warm SST anomalies in the subtropical southwest Indian Ocean may generate increased rainfall over southern Africa and hence could augment those due to SST anomalies in the southeast tropical Atlantic Ocean. Both observations and GCM results in Reason and Mulenga (1999), Reason (2001) and Hansingo and Reason (2006) have shown that warming in the subtropical South West Indian Ocean during austral summer leads to enhanced rainfall over large areas of south-eastern Africa. Further, Behera and Yamagata (2001) and Reason (2001, 2002) have shown that anomalous rainfall is produced over southern Africa during the positive phase of a South Indian Ocean subtropical dipole event in summer. This phase is characterised by warm SST anomalies south of Madagascar and cool anomalies off the western coast of Australia. Therefore, this experiment further addresses the second subsidiary question.

Experiment 10 is similar to Experiment 9 except that the SST anomaly forcing in the subtropical southwest Indian Ocean is shifted closer to the subcontinent(Figure 3.1**i**). Previous experiments with a numerical model suggest that the positive rainfall anomalies are further enhanced over southern Africa when the warm SST anomalies in the subtropical southwest Indian Ocean are close to the subcontinent (Reason, 2002). Therefore, one expects this experiment to generate more rainfall over the subcontinent than Experiment 9. This experiment aslo addresses the second subsidiary question.

A summary of the above above experiments is shown in Table 3.1.

3.5 Model configuration and method

It is standard practice that the simulations should begin at least one month before analyzable data begins to be produced. This is referred to as a spin-up period, during which numerical noise in the atmosphere subsides. This noise is associated with the fact that the initial conditions and boundary conditions are not in perfect equilibrium with each other

Table 3.1: Thesis Experiments

Experiment #	Atlantic Anom °C	Indian Anom °C	Pacific Anom °C
2	+6	0	0
3	+4	0	0
4	+6	−2	0
5	+4	+2	0
6	+6 (equatorwards)	0	0
7	0	0	−2
8	+4	0	−2
9	+6 (equatorwards)	+2	0
10	+6 (equatorwards)	+2 (closer to subcontinent)	0

at the start. Within a month, this noise is hopefully negligible and meaningful output my be obtained from the model.

Errors evolve in simulations with AGCMs because of incomplete physical understanding and limited knowledge of past (or future) climate forcing (Smith *et al.*, 2002). In addition, uncertainty related to climate chaos occurs in a model because of nonlinear interactions in the climate system. Murphy *et al.* (2004) suggest modeling uncertainties also arise from fundamental choices made when building the AGCM (for example, grid resolution), and from the parameterization of processes unresolved at the grid scale (for example cloud formation). Because of uncertainty from internal variability of the model, ensemble experiments are done to reduce chaos errors. Traditionally, the focus has been on repeating runs with the same forcing and varying the initial conditions, to sample internal climate variability. However, this method may not adequately sample the range of possible initial conditions when a small ensemble size is used. To minimize uncertainties related to climate processes, more accurate parameterizations for use in AGCMs are required (Murphy *et al.*, 2004).

In this thesis, each idealized experiment is an ensemble consisting of five integrations (Hansingo and Reason, 2006), each integrated for twelve months (November to October). As suggested above, November is the spin-up month. Each ensemble member is initialized with different initial dumps randomly picked from previous HadAM3 experiments. These initial dumps are used for all the idealized experiments. Because the model is forced with

different SST anomaly pattern for each experiment, the model is run in reconfiguration mode. There are of the order of 100 parameters in HadAM3, consisting of logical switches or variable coefficients or thresholds (Murphy *et al.*, 2004). There are also well over 250 windows to go through, with almost no default settings, if a run has to be set from scratch. De Witt (1998) suggests that doing this is not only time consuming and wasteful but also error prone. This author advises to copy a run or job from a colleague who is doing similar work or use one of the Standard Experiments provided and modify it. For this thesis a job used in Reason and Jagadheesha (2005a) was copied and modified. Major modifications were in the initial and boundary conditions and the integration period.

3.6 Summary

In this chapter, a number of subsidiary questions were posed in order to address the aim of this research, and total of ten model experiments were designed to address these questions. The UKMO grid-point AGCM, HadAM3 model, was proposed and used to run a control experiment and nine idealized experiments, forced with different prescribed SST anomaly patterns. A 24-yr OISST climatology was used to force the model at the boundary in the control experiment and different initial dump files from previously run jobs were used for the initial conditions for ensemble members of the idealized experiments. This chapter has presented descriptions of quality-controlled datasets used to identify anomaly patterns to force the model with. In chapter 5 and the chapters that follow, differences between ensemble means and the control-run mean will be used to analysis the output. In the next chapter, the ability of the HadAM3 GCM to adequately represent the climate of the southern African region is evaluated with NCEP-NCAR reanalyses and CMAP precipitation.

Chapter 4

Model Validation

4.1 Introduction

In idealized numerical model experiments, it is necessary to first establish that the model qualitatively simulates the observed climate and its variability. The ability of an AGCM to simulate the observed climate is important to establish the appropriateness of its application to climate variability studies. It is therefore desirable that the model simulates the observed climate and its variability well, giving confidence in its applicability (Cavalcanti *et al.*, 2002).

Climate simulations (e.g. Hurrell *et al.*, 1998, Gates and Coauthors, 1999, Johns *et al.*, 1997, Pope *et al.*, 2000, Cavalcanti *et al.*, 2002) have shown the ability of different models to represent observed features of the atmospheric circulation and precipitation. However, the intensity and geographical distribution of these variables in the various models may differ greatly from observations. For example, GCMs used in the Atmospheric Model Intercomparison Project (AMIP) produced varying results for the global mean surface air temperature and precipitation over land (Gates, 1992). Although outdated, this study indicates the importance of assessing the performance of GCMs in simulating regional and general circulation features. In this chapter, the ability of the HadAM3 GCM to adequately represent the climate of the southern African region is evaluated by comparing geographical maps and zonally averaged statistics of the model climatology used in Reason and Jagadheesha (2005a,b) with NCEP-NCAR reanalyses and CMAP precipitation. The

ability of the model to simulate general circulation features is presented first, followed by its ability to simulate regional circulation.

4.2 Global zonally averaged statistics and spatial distributions

Although there are various GCM validation methods, it is common practice to directly compare spatial distributions of long-term means for various variables computed from observed data and GCM simulations (e.g. Hulme, 1994, Ponater *et al.*, 1994, Cubasch *et al.*, 1996). Though this method is old, it is probably the most appropriate if there is not much data and thus far has remained the standard procedure (von Storch and Navarra, 1999, chap. 8). However, this method is not quantitative or completely objective, and it is prone to individual, subjective biases of interpretation. This may lead to an incorrect assessment of agreement of the simulated and observed states (von Storch and Roeckner, 1983) and therefore it should be used with caution.

Other methods involve analyses of the main features of the spatial variability (usually given by the most important empirical orthogonal function (EOF) patterns) and large-scale mechanisms controlling the regional climate variability given by canonical correlation analysis (CCA) (von Storch *et al.*, 1993, Ponater *et al.*, 1994, Kharin, 1995, Busuioc *et al.*, 1999a).

Statistical methods such as the students t-test have also been widely employed in climate modeling particularly in studies involving the test of statistical significance of model responses to SST forcing (e.g. Chervin and Schneider, 1976, Chervin *et al.*, 1976, Livezey, 1985, Reason and Jagadheesha, 2005a). This method basically assesses the statistical difference between two means (climatologies in this case). However, this method assumes that the two means to be tested come from normally distributed populations (parameterized populations). Some variables like precipitation cannot be compared using this method because they are not normally distributed (von Storch and Navarra, 1999). Therefore, non-parameterized methods are used on such variables. The alternative to the

students t-test method is the Mann-Whitney U test (von Storch and Zwiers, 1999) or Wilcoxon test which tests the null hypothesis that two samples have the same median. For simple analysis, the sample t-test method is used on rainfall and other variables in this thesis.

As described in chapter three, obtaining the model climatology involved forcing the model with a 10 year Reynolds OISSTv2 monthly climatology and integrated for 15 years, from January 1985 to December 1999. Therefore not much variability is expected in the model for the 15 year period as compared to the same period of observations. As a result, the EOF and CCA methods cannot be used here.

For the statistical method, the single-sample t-test is used to show statistically significant differences between the model and observed precipitation climatology and other variables. The single-sample t-test is used because the 15 years of the model climatology are considered as the climatological sample (i.e. the sample size is 15). The mean of these climatologies is compared with the observed (NCEP-NCAR) climatology. The differences between the two climatologies are also analysed.

As mentioned above, the main goal of the comparison is to provide a global view of the climatological features simulated by the model and to evaluate the ability of the model to reproduce the annual cycle. Emphasis is given to the FMA season over southern Africa since this is the main rainy season in the Angolan area of most interest to this study and because previous studies have already shown that the model represents the main circulation during winter (JJA) (Reason *et al.*, 2003) and DJF (Reason *et al.*, 2005) adequately.

4.2.1 Zonal means

An overview of the accuracy of the model climatology is given by zonally averaged statistics of precipitation, sea level pressure, near-surface specific humidity and zonal moisture flux, geopotential height and upper level zonal winds. Zonal mean values for various patterns for FMA are shown in Figure 4.1. The zonally averaged precipitation is better simulated in FMA in the Northern Hemisphere (NH) and compares very well with

the CMAP climatology (Figure 4.1**a**), but overestimates the precipitation in comparison with the observed dataset in the extra-tropics. The equatorial double maximum, which reflects the southern and northern equatorial location of the ITCZ in the eastern and western hemisphere respectively during this season, is captured by the model. However, the model underestimates the northern equatorial maximum by about 1 mm/day. Another important precipitation feature captured by the model is the minima associated with the subtropical highs which have closer values to CMAP in the NH than in Southern Hemisphere (SH). There are more discrepancies between the model and CMAP rainfall in the SH than in the NH, particularly in the mid and higher latitudes. HadAM3 underestimates the minimum associated with subtropical highs in the SH and overestimates and misplaces the maximum associated with the westerly storm-track region.

The equatorial trough as well as the subtropical highs and the Circumpolar Trough near 60°S are well simulated in the zonal mean sea level pressure (SLP, Figure 4.1**b**). Although the model estimates higher (lower) polar SLP in the NH (SH) than the observations, it shows some skill in capturing important features elsewhere. Low pressure around 60° in both hemispheres, which may represent the location of the ascending arms of the Ferrel and Polar cells, is not as pronounced in the model as observed in the NH. The model also overestimates (underestimates) the NH (SH) polar high, but correctly estimates FMA SLP in the lower and mid-latitudes in both hemispheres.

Figure 4.1**c** indicates that the model reasonably simulates the 850 hPa specific humidity in both hemispheres and captures the equatorial maximum during FMA. This plot suggests that the model has some success in simulating mean meridional moisture. However, the model overestimates the equatorial near-surface specific humidity maximum by about 1 g/kg.

The zonally averaged zonal moisture flux field at 850 hPa is shown in Figure 4.1**d**. The model shows reasonably good skill in simulating the overall structure and the seasonal locations of the maxima and minima are represented. The low level easterly and westerly moisture fluxes in the tropics and high latitudes respectively are well reproduced by the

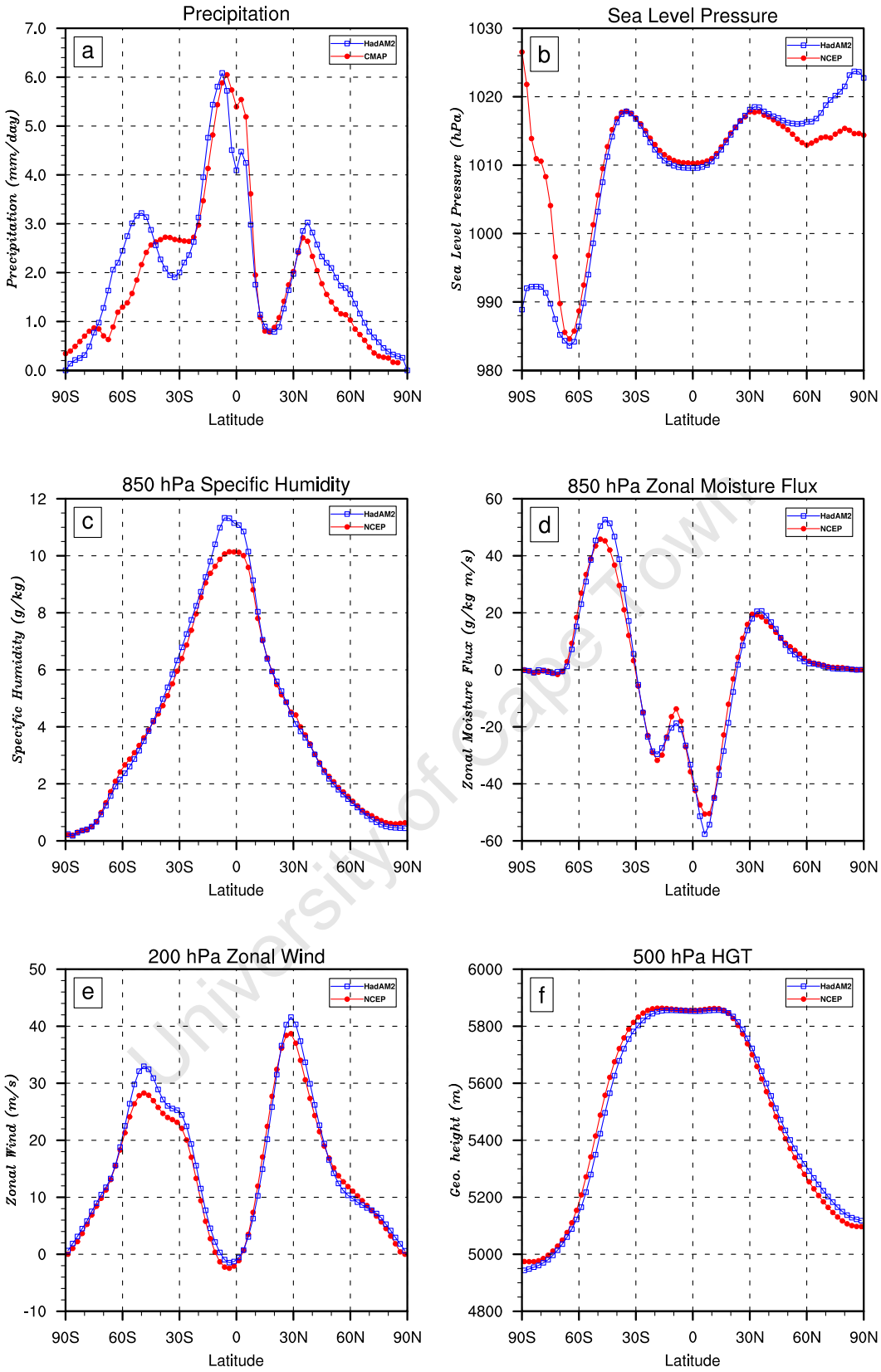

Figure 4.1: HadAM3 and NCEP/NCAR reanalysis FMA zonal means: (**a**) precipitation, (**b**) sea level pressure, (**c**) 850 hPa specific humidity, (**d**) 850 hPa moisture flux, (**e**) 200 hPa wind, (**f**) 500 hPa geopotential height. Precipitation is from CMAP and units are shown on the Y-axis.

model. However, HadAM3 slightly overestimates the near surface zonal moisture fluxes in the SH.

The model reproduces very well the structure of the upper level zonal winds, but in comparison with NCEP/NCAR reanalysis, tends to overestimate the intensity of the westerlies in both hemispheres as shown in Figure 4.1**e**. Jet stream regions and tropical easterlies are well captured by the model. Generally, the model shows success in simulating the 200 hPa zonally averaged zonal winds.

Figure 4.1**f** shows the zonally averaged 500 hPa level geopotential height. This figure suggests that the model has skill in capturing mid-troposphere features. HadAM3 correctly estimates the location and magnitude of the geopotential height extremes in the higher and lower latitudes during FMA season. A closer examination of Figure 4.1**f**, however indicates that the model tends to underestimate (overestimate) the geopotential height in the southern (northern) polar region.

4.2.2 Mean vertical structure of zonal wind

Vertical structures of mean zonal wind from the model and from NCEP-NCAR are shown in Figure 4.2. The jet streams in both hemispheres of the model climatology (Figure 4.2**a**) are slightly stronger than in the reanalysis dataset (Figure 4.2**b**) although the model reproduces their positions well. In both the model and the observation, the NH jet stream is stronger than the SH during FMA. Overall, the differences are larger in the mid- and higher troposphere in the mid latitudes of both hemispheres (Figure 4.2**c**). These differences are statistically significant at 90% significant level as indicated by the stippled regions. The model underestimates (overestimates) the zonal winds in the mid (higher) troposphere.

4.2.3 Seasonal precipitation, sea level pressure, geopotential height and wind

The main features of the seasonal cycle of precipitation are well represented by the model as shown Figure 4.3**a**, **c** and **e**. The ITCZ and its southward location during FMA are

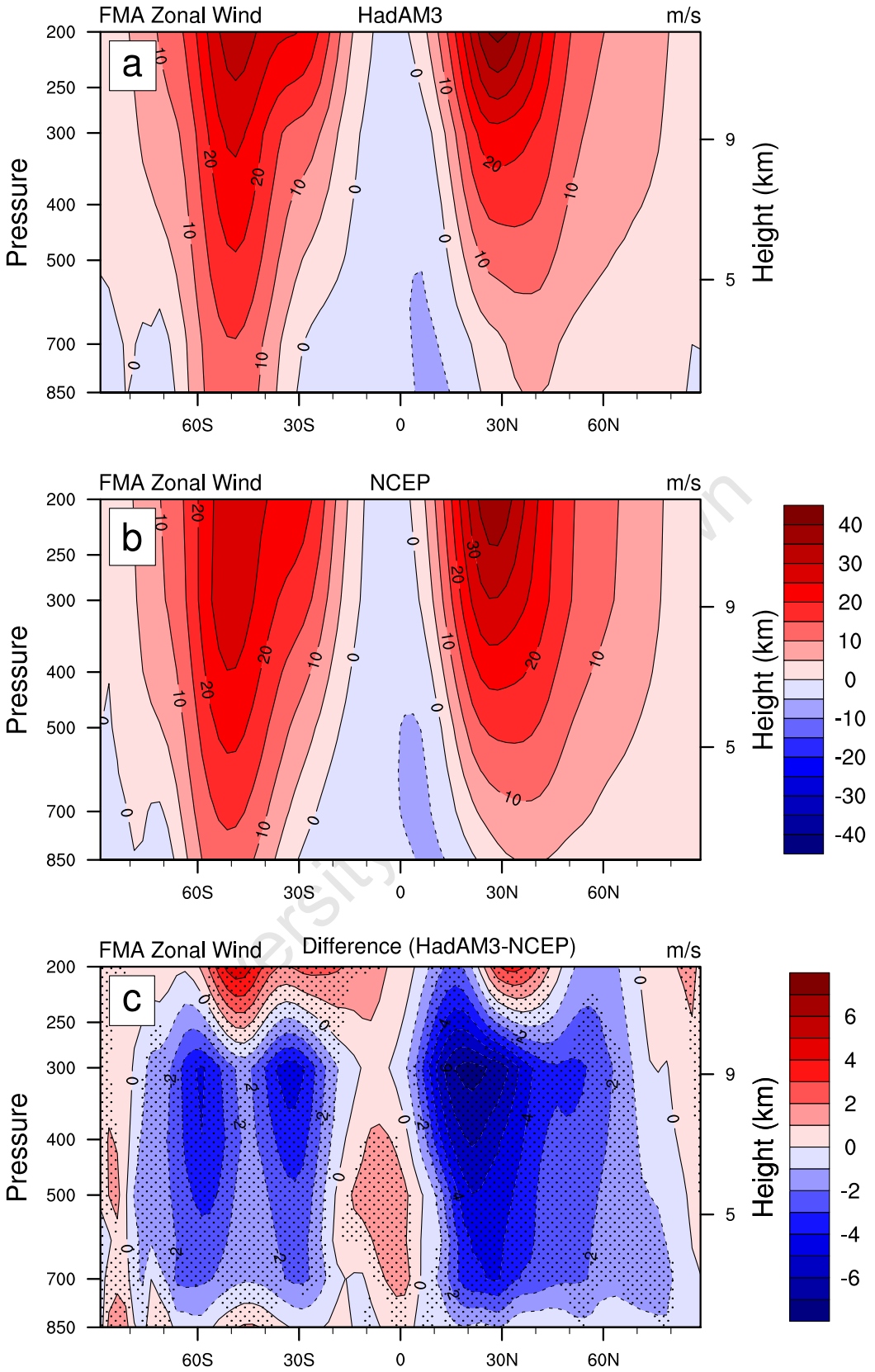

Figure 4.2: FMA climatological vertical structure of zonal wind (m/s): (**a**) HadAM GCM, (**b**) NCEP-NCAR Reanalysis, (**c**) Difference between model and reanalysis. Stippled regions indicate statistically significant differences at 90% significant level.

well depicted by the model in Figure 4.3**a**. However, the model fails to capture the precipitation bands related to the South Pacific Convergence Zone (SPCZ) and South Indian Convergence Zone (SICZ) over southeastern Africa (Figure 4.3**c**). The model also overestimates precipitation over central equatorial Asia, Pacific and Atlantic Oceans. Furthermore, Figure 4.3**e** indicates that precipitation over the eastern (western) Indonesian continent is underestimated (overestimated) by the model as well as over southern Africa and Brazil. Cavalcanti *et al.* (2002) reported that other GCMs, such as the European Center for Medium range Weather Forecasting (ECMWF) model, NCAR Community Climate Model Version 3 (NCAR CCM3) and Geophysical Fluid Dynamics Laboratory (GFDL) model produce erroneous precipitation over the Amazonian region during the DJF season. These authors further report that HadAM3, when coupled with the ocean model produces results closer to the observations than the models mentioned above. They have attributed HadAM3s ability to simulate Amazonian precipitation during DJF to the mass-flux penetrative convective scheme used in this model.

The SH subtropical high pressure centers are reproduced in the sea level pressure field (Figure 4.3**b**, **d** and **f**). In general the pressure in the model is higher than in the NCEP-NCAR reanalysis over most of the NH region except over Asia where it is lower. In the SH, the model produces lower pressure over the polar regions than the reanalysis.

The near-surface flow (850 hPa) over the oceans (Figure 4.4**a**, **c** and **e**) shows the circulation associated with the subtropical highs. The general seasonal characteristics of the subtropical highs are well represented by the model. Also the extra-tropical circulation in the SH north of 60°S is well simulated by the model. Noted circulation differences between the model and reanalysis (Figure 4.4**e**) are observed over east of Australia and the western equatorial Atlantic Ocean near Brazil (Nordeste). The circulation east of Australia is southeasterly in the model compared to the easterly flow in the reanalysis. This may have implications over moisture advection over eastern and northern Australia during FMA. Over the western equatorial region, the flow is northeasterly in the model and easterly in the reanalysis. This may contribute to precipitation differences between

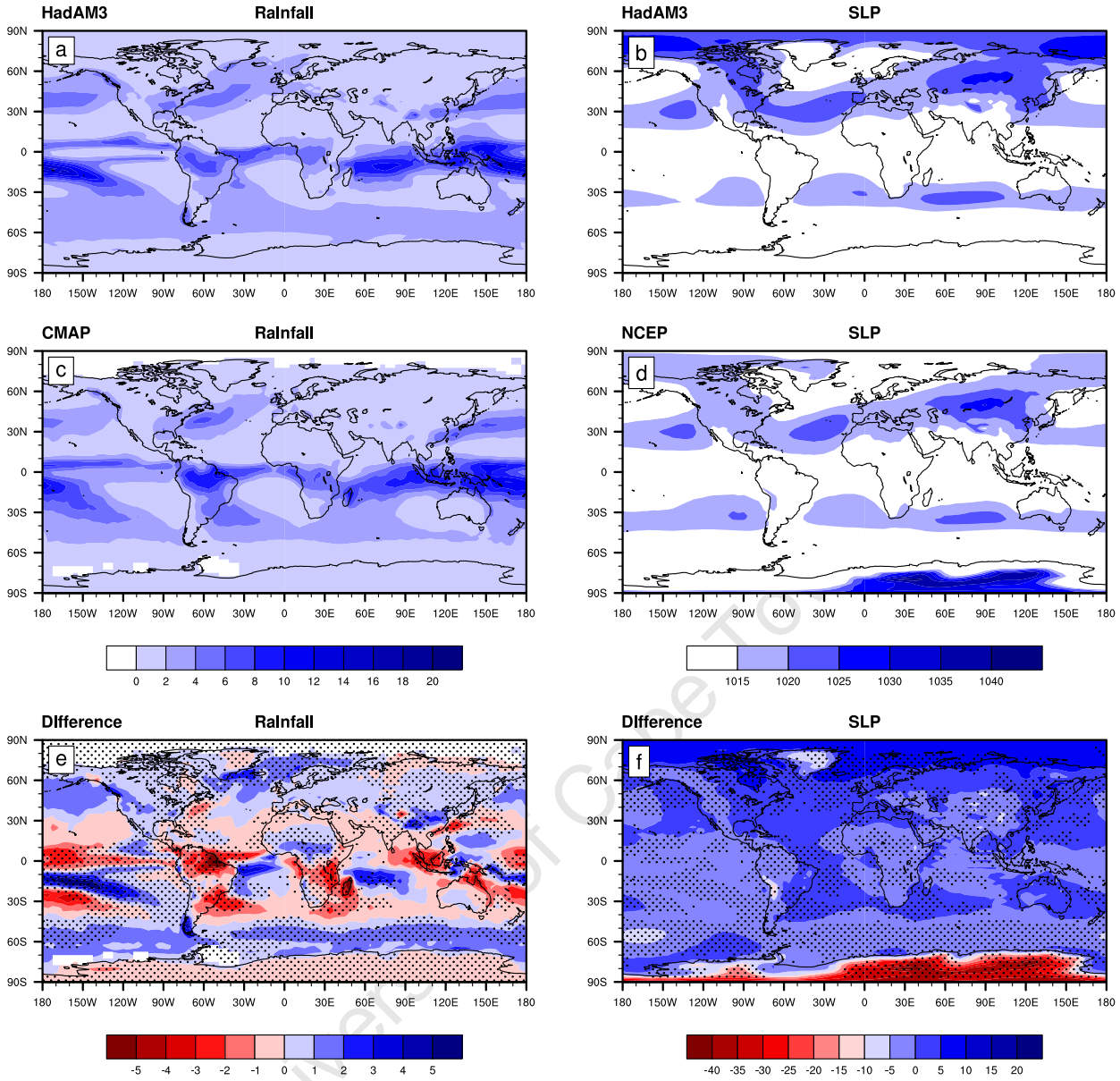

Figure 4.3: FMA climatological precipitation (mm/day, left panel) and sea level pressure (hPa, right panel): (**a**), (**b**) HadAM3, (**c**) CMAP, (**d**)NCEP-NCAR reanalysis. (**e**), (**f**) The difference between model and reanalysis. Stippled regions indicate statistically significant differences at 90% significant level.

the model and CMAP over the Nordeste region in Figure 4.3. The differences in near-surface flow between the model and NCEP-NCAR reanalysis data show the Indian and the western Pacific trade winds are stronger in the model than in the reanalysis. The Atlantic trade winds are however weaker in the model than in the reanalysis. The strong equatorial westerlies north of Madagascar in Figure 4.4**e** may be responsible for wet conditions north of Madagascar (Figure 4.3**e**).

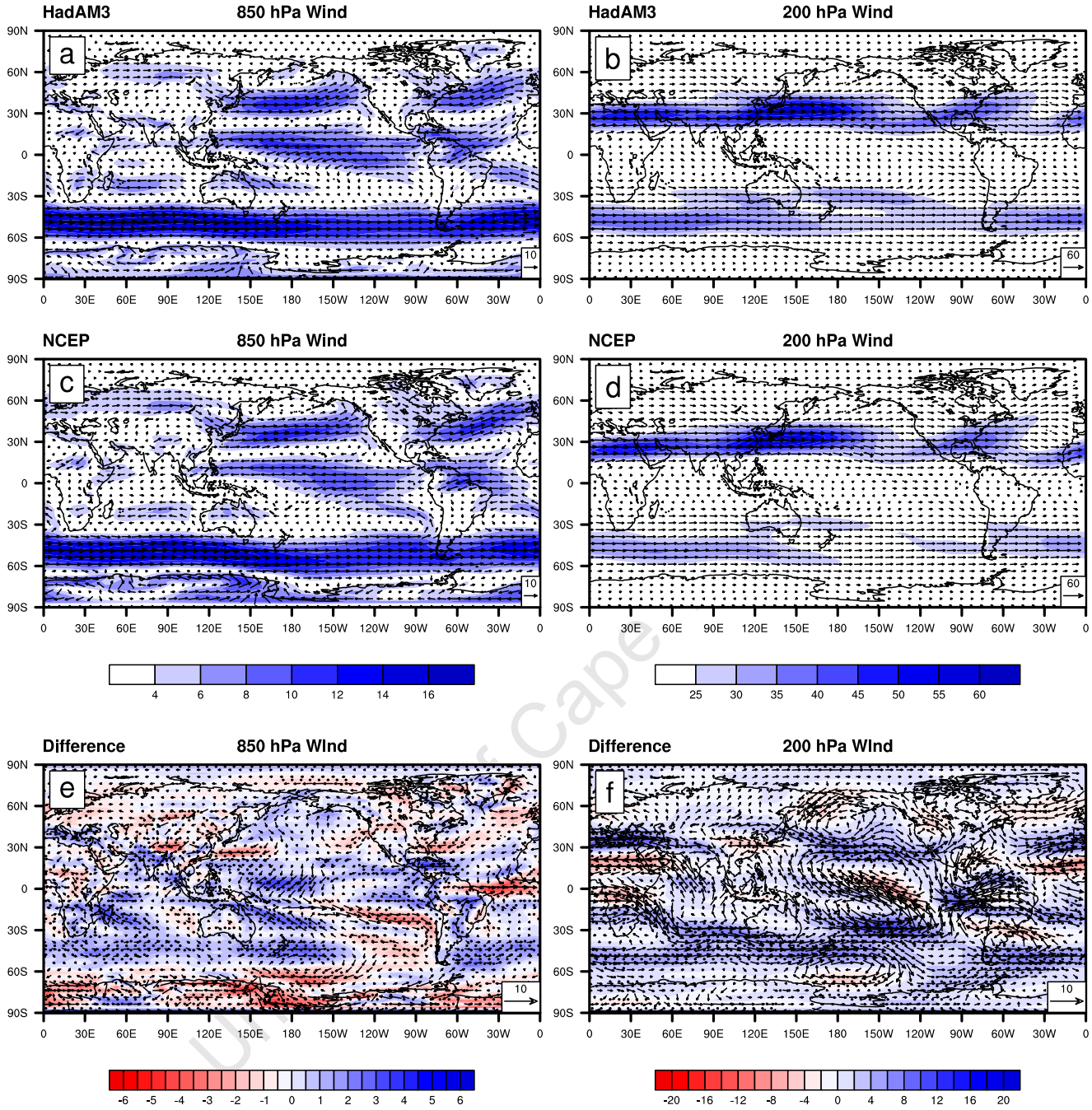

Figure 4.4: Vectors and magnitude of FMA climatological wind field at 850 hPa (left panel) and 200 hPa (right panel) m/s: (**a**), (**b**) HadAM3 and (**c**), (**d**)NCEP-NCAR reanalysis. (**e**), (**f**) The difference between model and reanalysis. The magnitudes are shaded and stippled regions indicate statistically significant differences at 90% significant level.

The model wind field at 200 hPa (Figure 4.4**b**, **d** and **f**) shows the main global circulation features, such as the summertime subtropical jet streams and anticyclonic circulations associated with summertime deep convection. The subtropcal jet stream in the NH

is stronger than the SH one in both the model and the reanalysis. The anticyclonic circulation centres over South America, southern Africa and western Pacific region in FMA are associated with summertime convection in the SH. The anticyclonic centre over South America is not well simulated in the model. The main differences between the model and the reanalysis over South America may be related to the intensity of the anticyclonic circulation. The cyclonic circulation seen in the difference field, over southeastern Africa and southwestern subtropical Indian Ocean means less intense anticyclonic circulation in the model results than in the analysis. The anticyclonic circulation to the southeast of South America in the difference field can be as a result of the SACZ enhancement in the model. The subtropical jet streams in both hemispheres are stronger in the model than in the reanalysis between 60°E and 120°W.

The zonal means are removed from geopotential fields to enhance the stationary climatological features, which are shown in Figure 4.5 for the southern hemisphere (Cavalcanti *et al.*, 2002). The wavenumber 1 observed in the reanalysis in mid high latitudes is reproduced in the model results, but there are some differences related to the intensity and position of zonal anomaly centres. The anomalous centres at mid- and high latitudes are stronger in the model than in the reanalysis, representing the stronger amplitude of the stationary wave in the model. The trough over the South Pacific and the ridge east of South Africa is shifted eastward when compared with the reanalysis.

The difference between the model and reanalysis fields of geopotential zonal anomaly is shown in Figure 4.5**c**. At high latitudes of the SH, the largest errors occur over the South Pacific Ocean and they extend over southern Australia and South America. Cavalcanti *et al.* (2002) suggest that the errors in the intensity and position of the main centers of the stationary features may be associated with the poor representation of the model topography because the atmospheric stationary waves are in part related to orography.

4.3 Regional maps

Particular atmospheric circulation and continental features and rainfall patterns inherent to southern Africa and the adjacent oceans occur during summer are now discussed. These

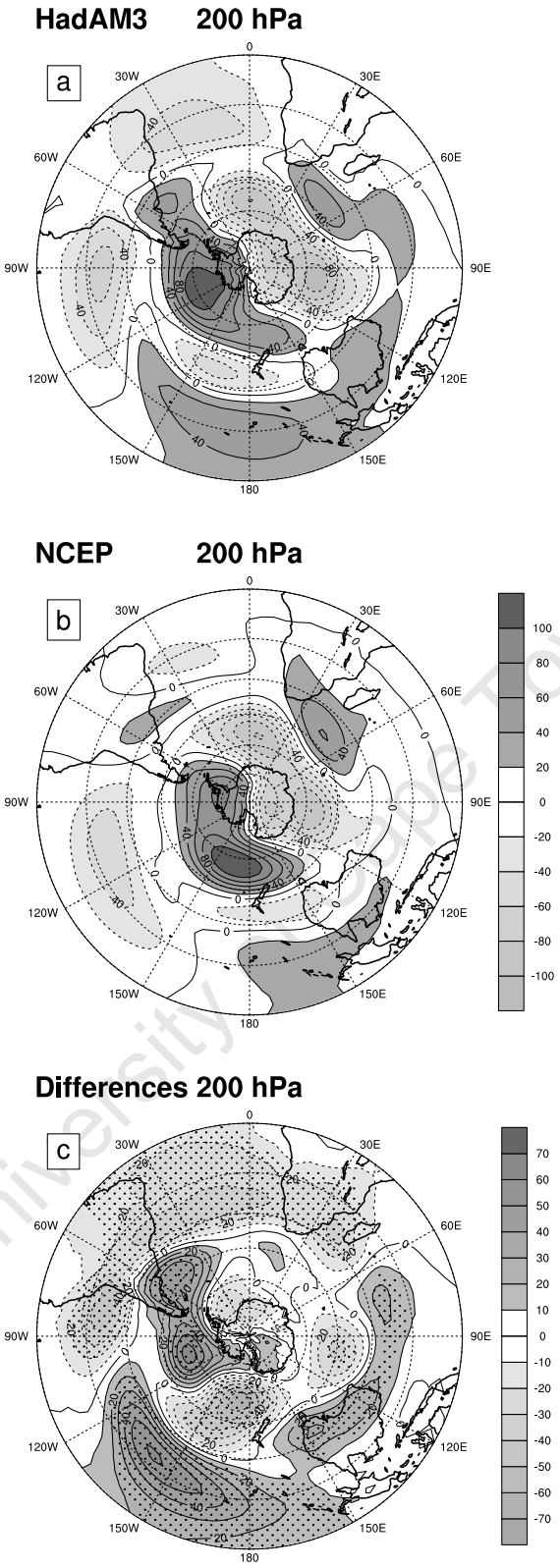

Figure 4.5: FMA climatological zonal geopotential height anomaly (m) at 200 hPa for the southern hemisphere:(**a**) HadAM3, (**b**) NCEP-NCAR reanalysis. (**c**) difference between model and reanalysis. Stippled regions indicate statistically significant differences at 90% significant level

features may play an important role in modulating the magnitude and distribution of rainfall over the subcontinent. Therefore, it is important that the ability of any GCM used in regional climate studies to simulate these features is assessed. Because the subcontinent is narrow and its location is essentially subtropical- tropical circulation features inherent to this region may be thermally related. This section presents thermal and dynamical features that characterize the FMA season of southern Africa and the adjacent oceans. The domain used for the validation of the HadAM3 model over southern Africa extends from 50°S to 10°N and from 40°W to 80°E.

4.3.1 Precipitation, sea level pressure, temperature and outgoing longwave radiation

Globally, the model has some skill in capturing rainfall distribution patterns during the FMA season. Over southern Africa and the surrounding oceans, Figure 4.6 (left panel) shows that the model captures the location of the precipitation bands associated with the ITCZ and the desert and semi-desert areas over southwestern Africa. However, the region of minimum precipitation extends further east in the model (Figure 4.6**a**) than in the observations (Figure 4.6**c**). The model also produces a region of minimum precipitation southwest of Madagascar, which is present in the observations. The region of minimum precipitation in the South Atlantic Ocean extends further west in the observations than in the model. Minimum precipitation in this region may be as a result of the influence of the cold Benguela current and the South Atlantic subtropical high. Cold current regions are not favourable regions for precipitation as these regions are cold and dry and subsidence dominates high pressure regions.

Like in the global plots, Figure 4.6**c** indicates that the model overestimates precipitation over the maritime ITCZ region and underestimates this variable over the central and eastern regions of the subcontinent and Madagascar. The models inability to correctly estimate precipitation over Madagascar may be associated with the strong easterlies north of Madagascar (Figure 4.10**a**).

The South Indian and Atlantic Ocean subtropical high pressure systems are dominant circulation features during the FMA summer season. The intensity and location of these features play an important role in advecting moist air, the Indian Ocean high in particular, from the surrounding ocean to the subcontinent. The right panel in figure 4.6 shows the model (Figure 4.6**b**) and NCEP-NCAR reanalysis (Figure 4.6**d**) climatologies of sea level pressure for the FMA season. The model shows success in capturing the subtropical high-pressure systems, but overestimates the pressure south of South Africa. The model

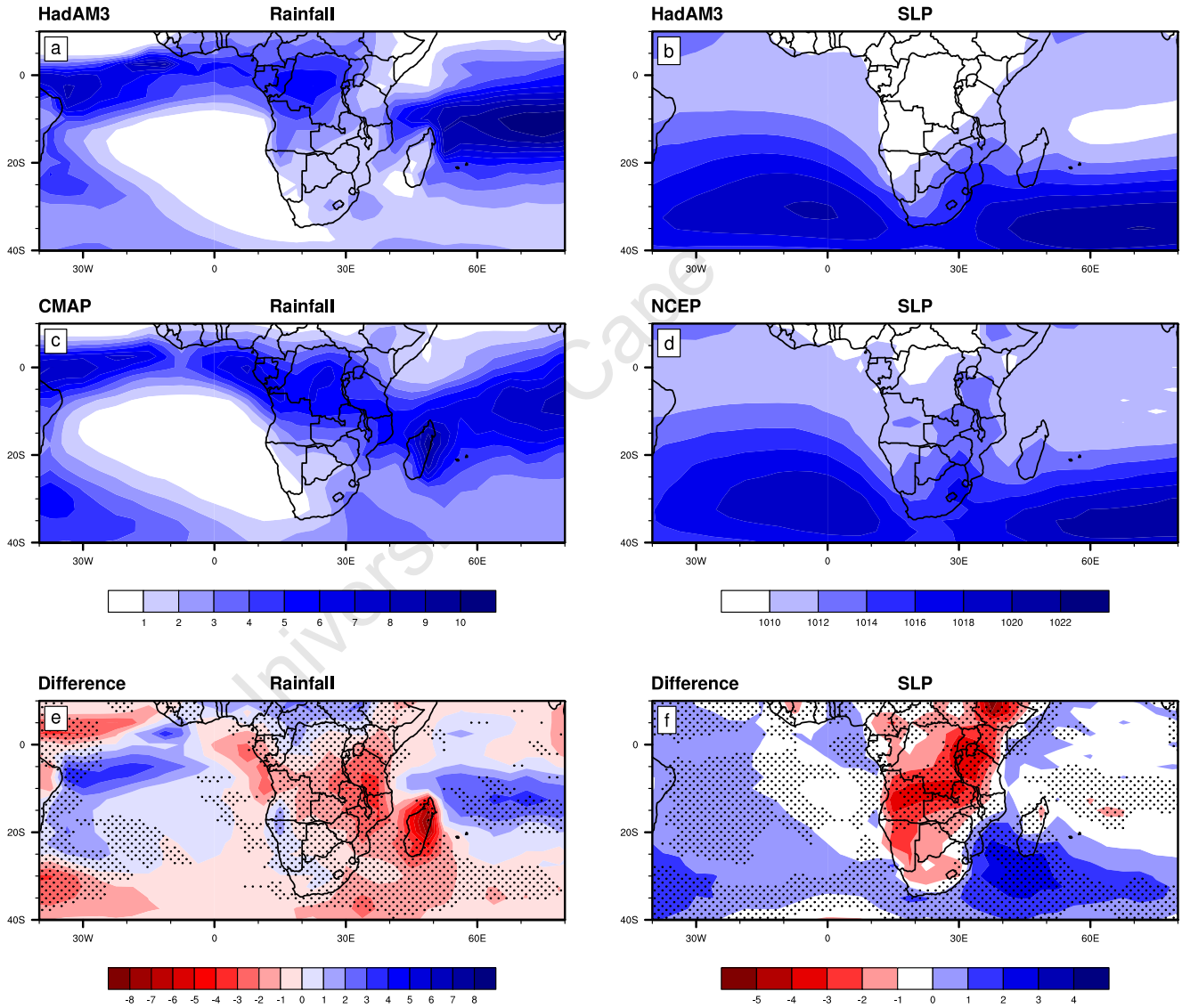

Figure 4.6: FMA precipitation (in mm/day, left panel) and SLP (in mb, right panel) climatology over southern Africa: (**a**), (**b**) HadAM3, (**c**) CMAP, (**d**) NCEP-NCAR reanalysis. (**e**), (**f**) differences between model and reanalysis. Stippled regions indicate statistically significant differences at 90% significant level

also overestimates the strength of the Indian Ocean subtropical high and produces low pressures over the subcontinent as shown in the difference plots in Figure 4.6**c**.

Figure 4.7 (left panel) shows the distribution of 850 hPa surface temperature from the model (Figure 4.7**a**) and observations (Figure 4.7**c**). This level is representative of the surface in some regions with height close to 1500 meters and thus coincides with some continental features (Mulenga, 1998). The highest temperature ($> 24°$C) is found over the Kalahari Desert and lowest temperature ($< 10°$C) over the southern oceans in the midlatitudes. The temperature over the subcontinent is above 18°C except for the eastern coastal region with temperature below 18°C.

The feature of highest temperature over the Kalahari, which also relates to the Angola-Low to some extent, is captured by the model but, this feature does not extend southeastward in the model as in the reanalysis. Overall, the model simulates the temperature over the subcontinent quite well, but overestimates (underestimates) it over eastern Zambia and northern Tanzania and Madagascar (South Africa) (Figure 4.7**e**).

As can be seen in Figure 4.7 (right panel), both the model (Figure 4.7**b**) and the reanalysis (Figure 4.7**d**) indicate that the climatological field of FMA Outgoing Long-wave Radiation (OLR) is similar to the precipitation. High values (260 Wm^{-2}) are observed over regions of minimum precipitation, over the South Atlantic Ocean and southwestern Africa and may be associated with clear skies. Note that high OLR values may be expected over the subtropical high-pressure areas, for example over the South Atlantic subtropical high in Figure 4.7**d**. However, this is not so over the South Indian Ocean subtropical high even when the intensity of this system is as strong as its counterpart in the South Atlantic Ocean.

Low values ($<$230 Wm^{-2}), which are associated with convective systems, are observed over central Africa and the ITCZ. The feature of low OLR values over central Africa is smaller in extent in the model than in the observed. Over the oceans, features of low OLR are stronger in the model than in the reanalysis and are associated with strong convection. Overall, the model overestimates OLR over the subcontinent and the subtropical Indian Ocean.

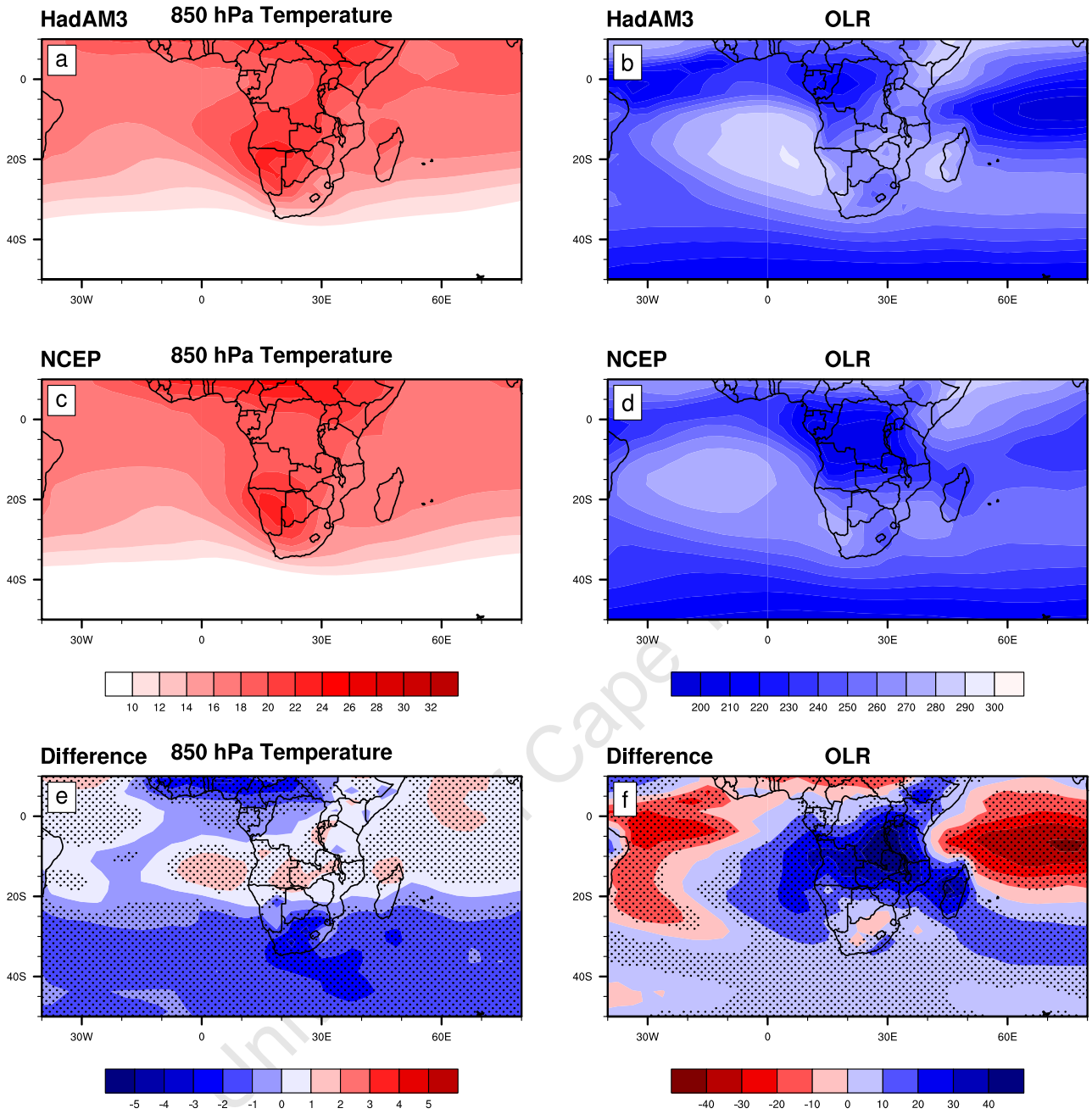

Figure 4.7: FMA climatological 850 hPa temperature (in °C, left panel) and outgoing long-wave radiation (in Wm^{-2}, right panel): (**a**), (**b**) HadAM3; (**c**), (**d**) NCEP-NCAR reanalysis. (**e**), (**f**) differences between model and reanalysis. Stippled regions indicate statistically significant differences at 90% significant level

4.3.2 Zonally averaged zonal moisture flux, vorticity and wind

It is well known that the Indian Ocean is the primary source of moisture over southern Africa and the ability of a GCM to reproduce this fact is important for determining the success of the model in simulating southern African climate variability. Figure 4.8 shows zonally averaged (40°W to 80°E) climatological zonal moisture flux over southern Africa

(50°S to 10°N) for the FMA season from the model (Figure 4.8**a**) and NCAR-NCEP reanalysis (Figure 4.8**b**). As can be seen from the observations, most moisture in the atmosphere is found in the lower and middle troposphere (below about 500 hPa). The advection of moist air from the Indian Ocean extends to about 30°S over southern Africa. The South Atlantic Ocean is the primary source of moist air south of this latitude. This suggests that only the southern tip of the subcontinent gets the majority of its moisture from the South Atlantic Ocean. The model captures this scenario quite well, but shows a break in the easterly flow between 8°S and the equator. The difference between the model and the reanalysis (Figure 4.8**c**) suggests that the model underestimates (overestimates) the zonal moisture flux north (south) of 10°S in the lower troposphere.

Synoptic and mesoscale weather systems over southern Africa are linked to vertical motion of moist air at the surface and associated relative vorticity. The vorticity field at 850 and 200 hPa levels for the HadAM3 and NCEP-NCAR reanalysis is show in Figure 4.9. Negative values at 850 hPa coincide with areas of cyclonic and upward motion; hence these areas may be associated with active weather. Over southern Africa, these areas are observed over northern Namibia, Angola, the Mozambique Channel, and over the Tanzania-Uganda-Congo (DR) border in the reanalysis (Figure 4.9**c**). These features are weakly simulated and misplaced in HadAM3 (Figure 4.9**a**). As found from the precipitation and OLR fields, the model overestimates this upward vertical motion over the ITCZ regions in the western Indian Ocean. This is because the ITCZ is stronger in the model. Thus, caution must be taken in analyzing the difference field of this parameter in Figure 4.9**e**. Positive differences over Angola, the Mozambique Channel and the Tanzania-Uganda-Congo (DR) suggest stronger upward motion over these regions in the reanalysis than in model. However, positive differences over South Africa suggest stronger downward (anticyclonic) motion in the model than in the reanalysis. Overall the model captures the cyclonic (anticyclonic) motion over the lower (subtropical) latitudes at the 850 hPa level.

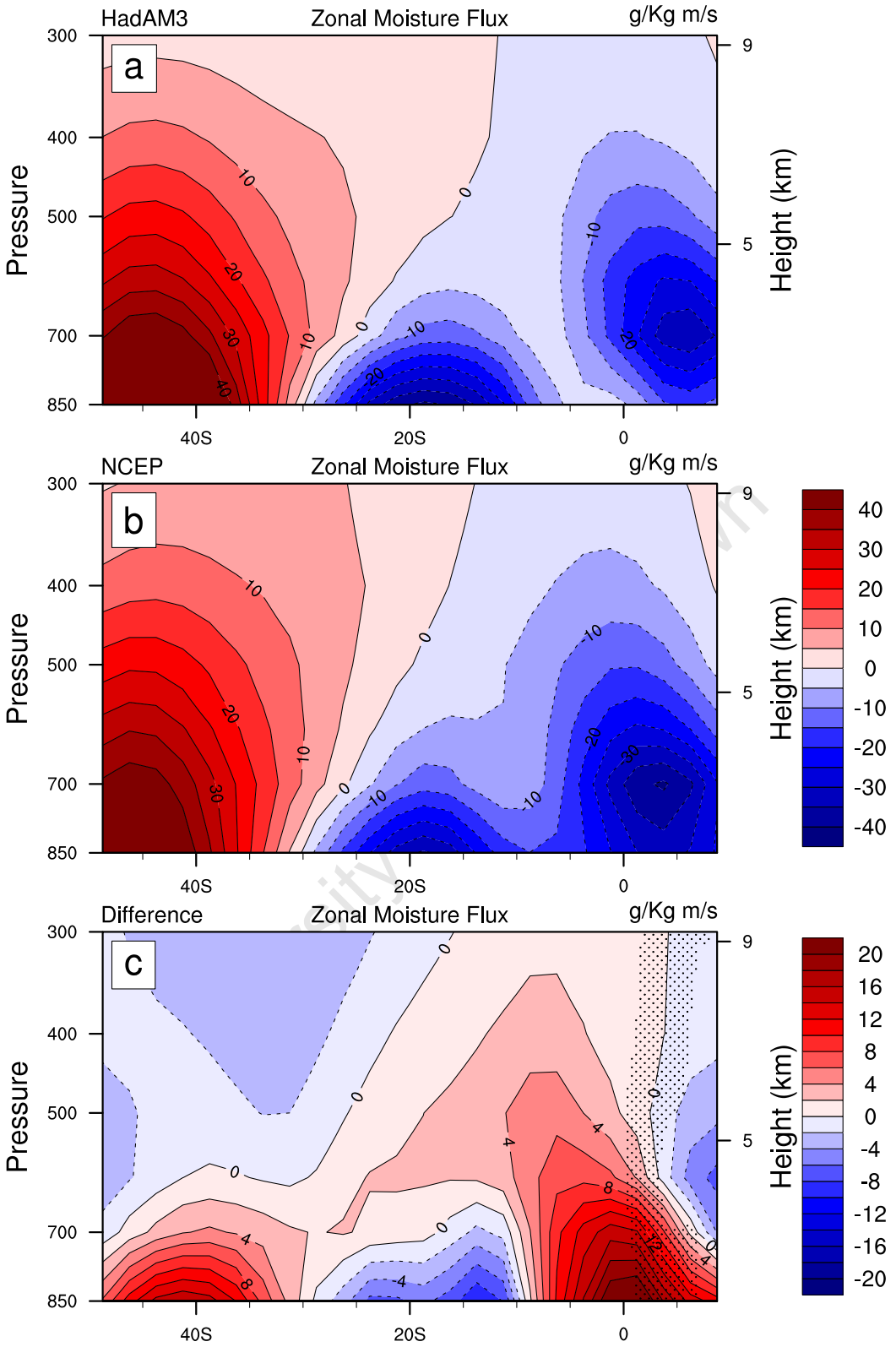

Figure 4.8: FMA climatological of zonal moisture flux zonally averaged between -40°W and 80°E: (**a**) HadAM3, (**b**) NCEP-NCAR reanalysis, (**c**) differences between model and reanalysis. Stippled regions indicate statistically significant differences at 90% significant level

At the 200 hPa level, strong anticyclonic circulation (positive values) is observed over tropical southern Africa and Indian Ocean in both the model and NCEP-NCAR reanalysis. Cyclonic circulation at the surface (850 hPa) and anticyclonic circulation aloft (200 hPa) over these regions provide favourable conditions for moisture ascent and the formation of deep convection. Over central Africa, this circulation may influence rainfall variability over Angola and western Zambia. However, the upper level anticyclonic features are located further south in the model and the cyclonic circulation also extend further south compared to the reanalysis which indicates an equatorially confined cyclonic circulation. The difference field suggests the model produces weaker downward motion over the northern region of southern Africa than observed.

Finally, observed and model vector winds at 850 and 200 hPa levels are shown in Figure 4.10. Also, moisture flux vectors at 850 hPa are shown in Figure 4.11. The observed (blue vectors) and model (red vectors) winds are on one plot. This is done to examine the models ability in simulating the direction of the wind at the above pressure levels. At 850 hPa (Figure 4.10**a**), the model shows some skill in simulating the direction and magnitude of the wind over midlatitudes (south of 35°S), the Atlantic equatorial region and east of Madagascar. However, the model fails to simulate the wind correctly over southern Africa and Madagascar. Monsoonal westerlies north of Madagascar are too strong in the model. This may be the reason the model ITCZ and rainfall are too strong in the western tropical Indian Ocean. For example over Angola, the model wind direction over a small area is infact opposite to the observed, this is because the model does not simulate the Angola-Low properly (see Reason and Jagadheesha, 2005a). Over eastern Africa, the model wind direction is southeasterly while the observed is easterly. At 200 hPa level (Figure 4.10**b**), the model shows success in simulating the flow across the midlatitude South Atlantic and Indian Oceans, but shows less skill in simulating the tropical and subtropical flow. The model flow is less zonal in the eastern subtropical Atlantic Ocean and east of Madagascar. Reason and Jagadheesha (2005a) observed similar differences in the moisture flux field at 500 hPa in the austral winter season. Figure 4.11 shows the moisture flux field at 850 hPa for the FMA season. Like in the wind field at 850 hPa, the model shows succes in

simulating the flow across the midlatitudes in the South Atlantic and Indian Oceans, but show less skill in simulating the tropical and subtropical flow.

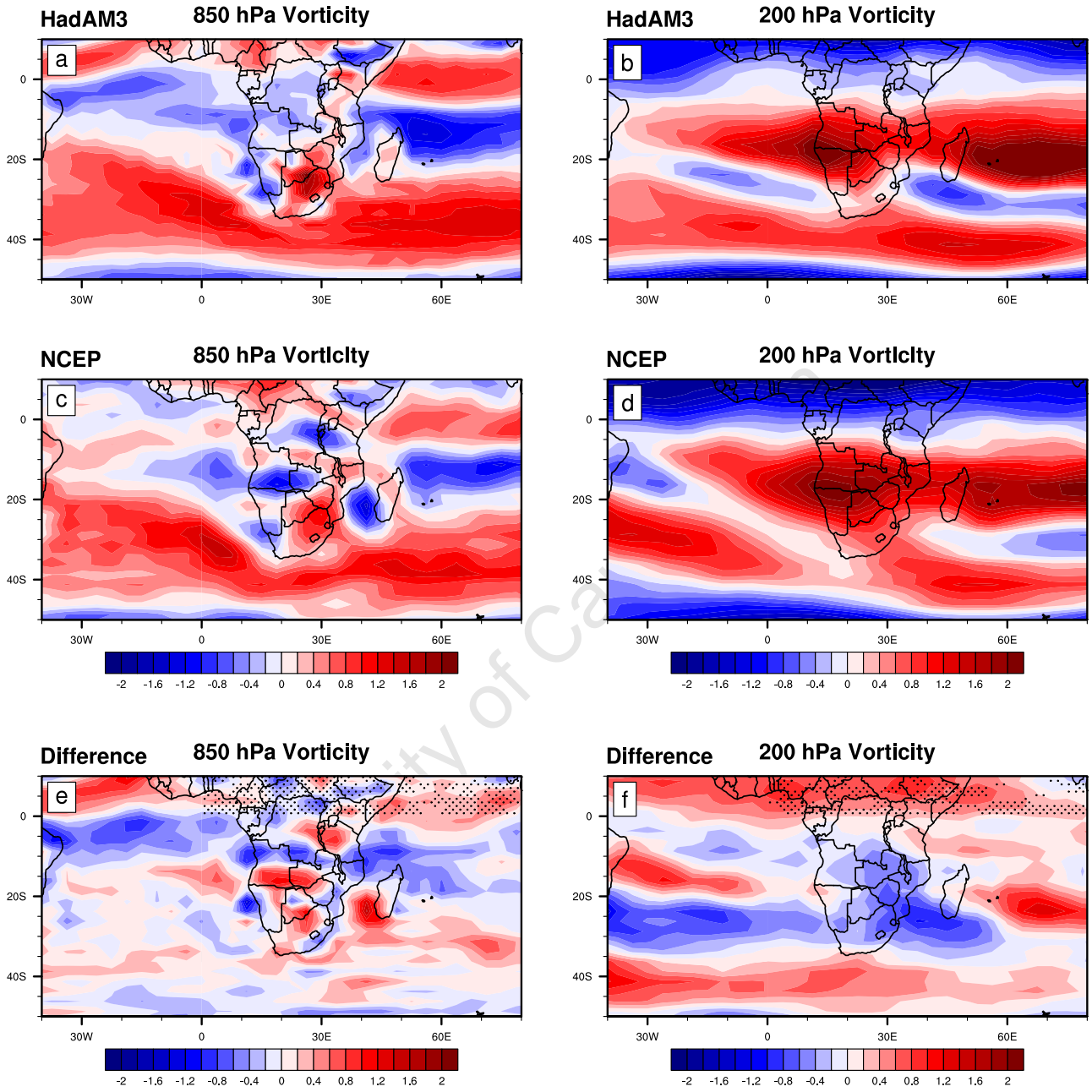

Figure 4.9: FMA climatology of vorticity at 850 hPa (left panel) and 200 hPa (right panel): (**a**), (**b**) HadAM3; (**c**), (**d**) NCEP-NCAR reanalysis. (**e**), (**f**) differences between model and reanalysis. Stippled regions indicate statistically significant differences at 90% significant level

4.4 Summary and Conclusion

The global and regional atmospheric features simulated by the HadAM3 AGCM are shown in this chapter, with emphasis on the southern hemisphere and FMA season. The model is able to reproduce the precipitation annual cycle and the main seasonal global climatological features of the circulation. Precipitation bands associated with the ITCZ are depicted well by the model, though the model overestimates these features over the ocean. Precipitation within the tropics is simulated reasonably well, but precipitation in the extra-tropics in both hemispheres is overestimated. However, the model underestimates precipitation over central and eastern Africa probably due to monsoonal westerlies north of Madagascar being too strong.

The major high- and low-level circulation features such as the subtropical highs and jet streams are captured well by the model although with different intensities when compared with the reanalysis. HadAM3 overestimates the jet streams in both hemispheres between 60°E and 120°W, i.e. over the ocean. The dominance of wavenumber 1 in the zonal geopotential anomaly indicates the ability of the model to simulate the main stationary waves of this hemisphere.

The model also shows some skill in capturing regional scale features, important for rainfall, over southern Africa, although it appears to misplace and underestimate them. The model shows less skill in simulating lower and upper level tropospheric wind direction correctly over southern Africa, therefore this field must be interpreted with caution.

Based on the above comparisons, there is generally reasonable agreement of the FMA climatology between NCEP-NCAR reanalysis and HadAM3. In addition to the above analysis, results from Johns *et al.* (1997), Reason *et al.* (2003), Reason and Jagadheesha (2005a) and Washington and Preston (2006), there is some confidence in the ability of this model to represent the climate of southern Africa reasonably well and therefore it is used in this thesis to perform the sensitivity experiments described in chapter 3.

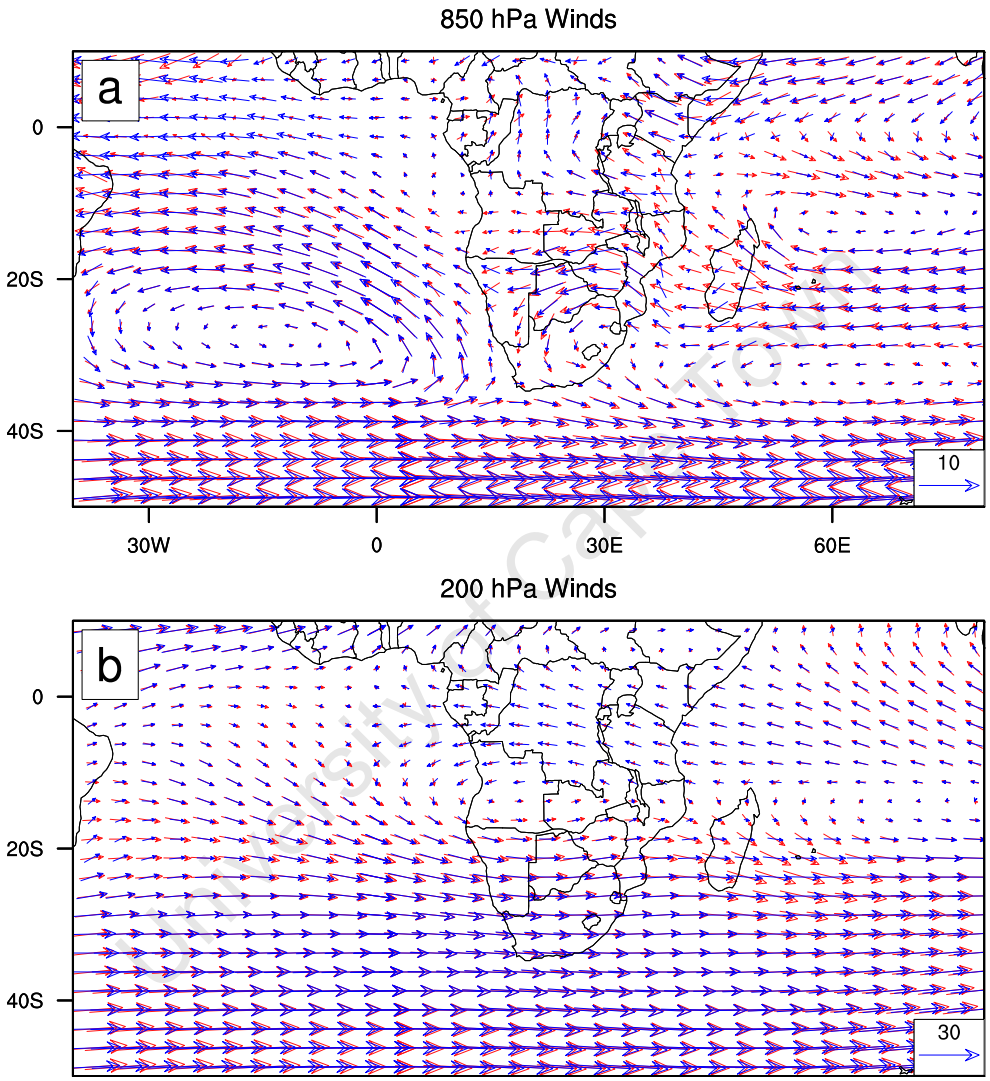

Figure 4.10: FMA wind climatology for NCEP-NCAR reanalysis (blue vectors) and HadAM3 (red vectors) at: (**a**) 850 hPa, (**b**) 200 hPa. Arrow size is shown.

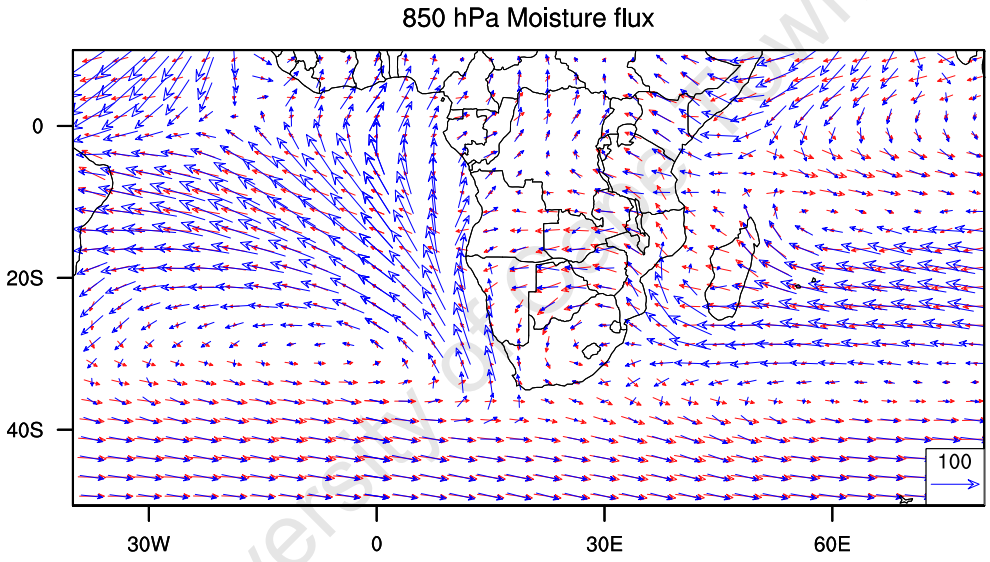

Figure 4.11: FMA Moisture flux climatology for NCEP-NCAR reanalysis (blue vectors) and HadAM3 (red vectors) at 850 hPa. Arrow size is shown.

Chapter 5

Sensitivity to Atlantic Ocean SST

5.1 Introduction

This chapter presents results from Experiments 2, 3,and 6 in which the HadAM3 GCM is forced with various idealized positive SST anomaly patterns only in the southeast tropical Atlantic Ocean. These patterns vary in location and intensity in each experiment. Therefore this chapter will try to address the sensitivity of the atmosphere over southern Africa to location and intensity of Benguela Niño events and addresses the first and third questions posed in chapter 1.

The results in this chapter and the chapters that follow present the February-March-April (FMA) mean differences between each experiment and the control experiment (Experiment 1). Section 5.2 discusses results from Experiment 3 in which the GCM is forced with a moderate idealized SST anomaly, about 4°C, and centred around 12°E, 17°S (Figure 3.1**b**). This experiment represents the case of a weak Benguela Niño. Experiment 2 similar is to Experiment 3 except that the forcing is stronger, about 6°C and more extensive (Figure 3.1**a**). This experiment represents a strong and extensive Benguela Niño and results from this experiment are discussed in section 5.3. The above experiments therefore, address the case of atmospheric sensitivity to SST intensity.

The results from Experiment 6 (Figure 3.1**e**) in which the model is forced with a SST anomaly similar to that in Experiment 2, but slightly shifted north (12°E, 15°S), are discussed in section 5.4. This experiment addresses the sensitivity of the atmospheric

model to the location of the SST forcing. The summary and conclusion of this chapter are presented in section 5.5.

5.2 Sensitivity to Benguela Niño SST: Experiment 3

As mentioned in chapter 3, this experiment is an idealized representation of the 2001 Benguela Niño event when positive SST anomalies of about 2°C were observed over the Benguela Niño region. The SST forcing in this experiment is double the SST anomalies observed during this event. Previous work (Marlow *et al.*, 2000, Kandiano *et al.*, 2004) has shown that SST has varied by up to ±10°C during the past, throughout various parts of the Atlantic. But variations in the tropical Atlantic Ocean during the more recent instrumental period have been smaller, varying from ±3°C (Williams *et al.*, 2008).

The GCM's response to the SST anomaly in Experiment 3 (Figure 3.1**b**) consists of a low pressure anomaly near the SST anomaly that extends westwards (Figure 5.1**b**) and a high pressure aloft downstream to the southwest of the forcing (Figure 5.1**c**). This response is somewhat similar to the baroclinic response obtained by Haarsma *et al.* (2003) and Robertson *et al.* (2003) to a regional SST anomaly in the South Atlantic Ocean during summer. Reason and Jagadheesha (2005a) also obtained a baroclinic-type response when the HadAM3 model was forced with warm SST anomalies during the winter season over the subtropical South Atlantic Ocean. Anomalous circulation provided by warming due to enhanced moisture convection associated with warm SST may result in anomalous regional rainfall (Moura and Shukla, 1981). SST anomalies may force surface convergence and strong cyclonic vorticity (Wagner and da Silva, 1994). Other mechanisms which may contribute to variability relate to the role of SST in determining evaporation rates and vertical stability (Wagner and da Silva, 1994). In addition to the above response, two noticeable low-level cyclonic circulation anomalies are generated just one in the tropical Atlantic centred around the 0° longitude and another over the Mozambique channel (Figure 5.1**e**). Also an anticyclonic circulation anomaly is generated just north of the SST forcing.

The 2001 Benguela Niño event was characterised by anomalous rainfall over southern Africa (Figure 2.2**h**). This event coincided with the weakening a strong and prolonged La Niña event of 1998-2001. During this event, abnormal sea level heights near equatorial Africa propagated southwards along the the Angola Benguela Frontal Zone and caused seasonal warm and salty water of tropical origin to penerate into the Angola and Benguela upwelling system (Rouault *et al.*, 2007). This had impact on the Benguela ecosystem and the fishing industry. Further inland, parts of central southern Africa received anomalous rainfall, probably in association with a La Niña occurring in 2000/2001. From this finding, it is not clear as to how influential a Benguela Niño is in forcing anomalously wet conditions further inland.

Figure 5.1 shows rainfall, sea level pressure, geopotential height, omega and low level moisture flux and divergence anomalies generated by the model when forced with the SST anomaly pattern in Figure 3.1**b**. The stippled regions in the plots of Figure 5.1 denote statistically significant differences at 90%. The model produces positive rainfall anomalies over the SST forcing and northern Angola. These anomalies stretch westward over the tropical Atlantic, with other areas of increased rainfall over parts of the south Sahel region, Congo basin, Zambia, Zimbabwe, south Mozambique and southwest Indian Ocean (Figure 5.1**a**). Positive anomalies over the Gulf of Guinea and neighbouring coastal West Africa are consistent with the observations in Reason and Rouault (2006) who found a strong positive correlation between rainfall there and SST anomalies in the tropical southeast Atlantic. Note that only the anomalies stretching eastwards from the Cameroonean coast and those near the SST forcing are statistically significant.

Associated with rainfall anomalies over the equatorial Atlantic are low sea level pressure, weak upper level pressure, enhanced uplift and low-level moisture convergence anomalies (Figures 5.1**b,c,d and f** respectively). Negative values in the omega field at 500 hPa in Figure 5.1**d** imply increased uplift and positive imply subsidence. Figure 5.1**e** indicates that near surface moist air from the equatorial Atlantic is advected towards the continent by the westerly anomalies. These anomalies appear to converge over the equatorial Atlantic as they advect moist air towards the continent. Together

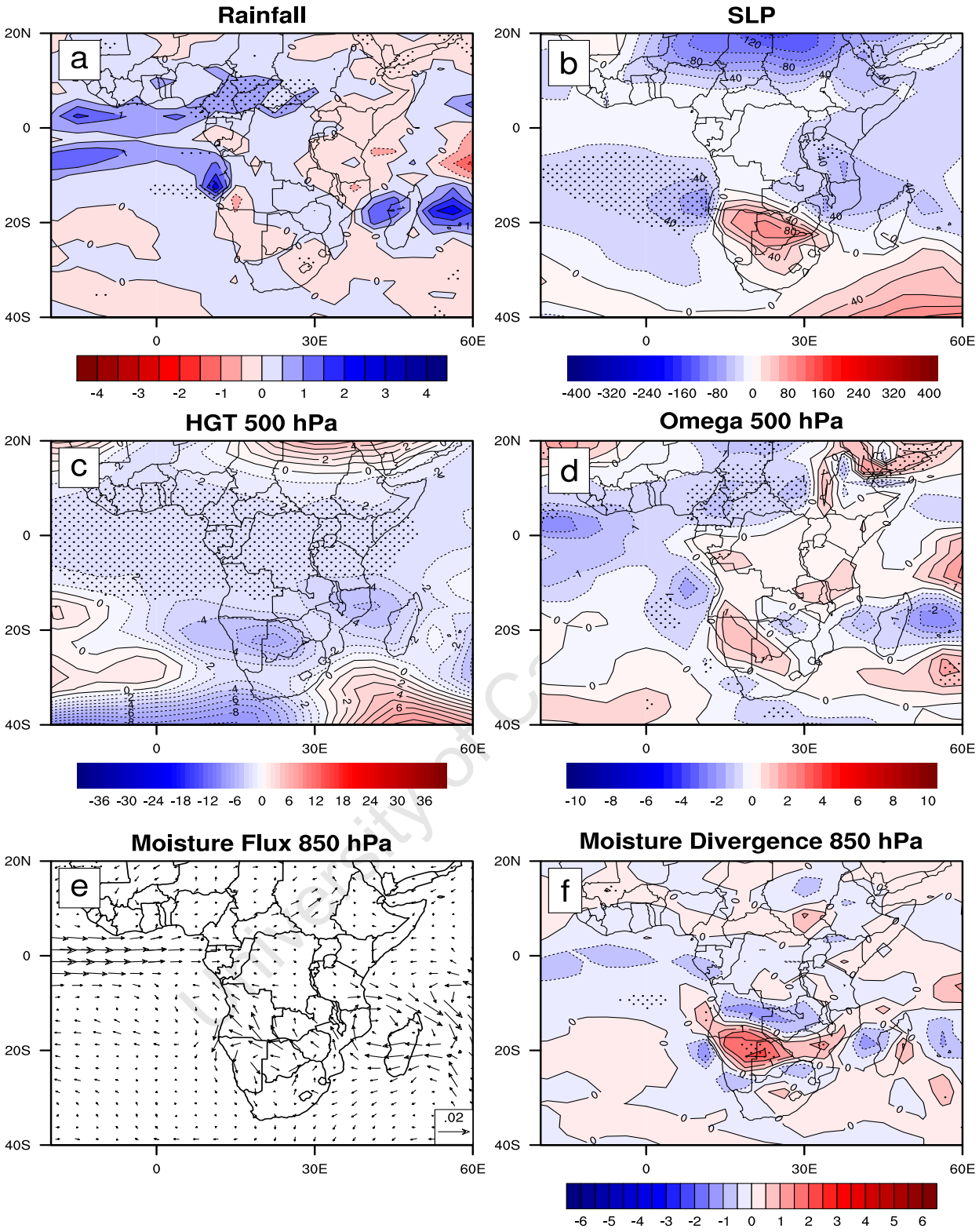

Figure 5.1: Experiment 3 anomalies: (**a**) precipitation at 0.5 mm/day contour interval, (**b**) sea level pressure at 20 Pa contour interval, (**c**) 500 hPa geopotential height at 1m contour interval, (**d**) 500 hPa omega at 0.5×10^{-2} contour interval, (**e**) 850 hPa Moisture flux the vector size is shown, (**f**) 850 hPa Moisture divergence at 0.5×10^{-8} contour interval. Stippled regions denote statistically significant differences at 90%.

with enhanced uplift over this region, this circulation anomaly favours the formation of rain through convective and convergence processes and thus positive rainfall anomalies observed over this region (Figure 5.1**a**). Positive rainfall anomalies extend further inland over equatorial Africa despite enhanced low-level moisture divergence there. This suggests that convective processes are play a major role in producing anomalous rainfall over land.

The low-level cyclonic and anticyclonic circulation anomalies generated near the SST forcing (Figure 5.1**e**) appear to lead to relative convergence northwest of the forcing (Figure 5.1**f**). Though this convergence is weak, it is statistically significant. Figures 5.1**d** and **f** indicate that the forcing enhances uplift and weakens low-level moisture convergence, respectively, locally near the forcing. With the anomalous surface latent heat flux generated over the the SST forcing (see Figure B.1**b** Appendix B), this suggests that convective processes contribute more to rainfall formation over this area. Therefore, Benguela Niño SST in the tropical southeast Atlantic may generate anomalous rainfall locally via convective processes.

The large cyclonic anomaly centred over the Mozambique Channel leads to relative convergence over Zambia and other areas of tropical eastern Africa and the tropical southwestern Indian Ocean on its northern arm with associated positive rainfall anomalies there. Anomalous circulations over the southwest Indian Ocean are produced in all the experiments and seems to be as a result of the SST forcing modulating the standing waves in Southern Hemisphere that are known to be important to southern African climate (Mason and Jury, 1997). These modulations are consistent with similar results obtained by Williams *et al.* (2008).

Anomalous positive sea level pressure anomalies over the region extending southeastward from southern Angola (Figure 5.1**b**) and the associated level low pressure anomaly aloft (Figure 5.1**c**) represent an equivalent barotropic response. Rainfall over this region is usually associated with tropical-extratropical cloud bands or tropical-temperate troughs (TTTs) which extend from the Angola low to a westerly disturbance passing south of Africa. However, Figure 5.1**a** shows negative rainfall anomalies over this region, suggesting weakening of TTT activity. This may be due to the barotropic conditions observed

over this region as a result of the forcing. Also associated with these rainfall anomalies is low-level moisture divergence (Figure 5.1**f**) and subsidence (Figure 5.1**d**) oriented in the NW-SE direction over this region.

The following section presents results of Experiment 2 in which the SST anomaly and the spatial extent are increased. This experiment is an idealized representation of the observed Benguela Niño SST in the southeast tropical Atlantic Ocean during the 1995 Benguela Niño event.

5.3 Sensitivity to a strong Benguela Niño: Experiment 2

The 1995 Benguela Niño had a very strong impact on the Benguela ecosystem and the fishing industry and also led to extensive floods in western Angola and northern Namibia. Further east, many parts of southern Africa received below average summer rainfall (Rouault *et al.*, 2003), in association with an El Niño occurring in 1995. This finding suggests that a Benguela Niño is capable of forcing anomalously wet conditions over western Angola/Namibia on its own. Again, it is not clear as to how influential it is on the rainfall further inland. During the 1995 Benguela Niño event, extensive floods were reported over western Angola and northern Namibia, but further east, many parts of southern Africa received below average rainfall. Experiment 2 is an idealization of this event, in which the AGCM is forced with SST anomalies as in Figure 3.1**a**.

Figure 5.2 shows rainfall, sea level pressure, low level moisture flux and divergence, 500 hPa geopotential height and omega anomalies generated by the model when forced with the SST anomaly pattern in Figure 3.1**a**. Like in the previous experiment, the GCM's reponse to this forcing consists of a low pressure anomaly (Figure 5.2**b**) near the SST forcing and a high pressure anomaly aloft (Figure 5.2**c**) southwest downstream of the forcing. Associated with the low pressure anomaly is a low-level cyclonic moisture flux anomaly (Figure 5.2**e**) near the forcing. Statistically significant relative low-level moisture convergence and divergence are generated by the model over the central south

and southeastern Atlantic (Figure 5.2**f**) in association with the cyclonic anomaly. This anomaly is stronger in this experiment than in the previous.

The cyclonic anomaly over the Mozambique Channel in Experiment 3 has weakened and slightly shifted southwards in Experiment 2. Further, this anomaly together with the easterly circulation anomaly north of Madagascar, enhance low-level moisture convergence over southwest tropical Indian Ocean, Tanzania, Zambia and northern Mozambique. Enhanced low-level moisture convergence and uplift (Figure 5.2**d**) over this region provide favourable conditions for rainfall there (Figure 5.2**a**). Note that over the subcontinent, statistically significant rainfall anomalies are observed only over Zambia. The model generates positive rainfall anomalies over eastern Africa and the southwest tropical Indian Ocean when forced with intense SST in southeast tropical Atlantic. Negative rainfall anomalies are generated over eastern Africa and the southwest tropical Indian Ocean when forced with weaker SST in the southeast tropical Atlantic Ocean. This indicates a positive correlation between SST in the southeast tropical Atlantic Ocean rainfall over eastern Africa.

Like in the previous Experiment, statistically significant positive rainfall anomalies are generated near the SST forcing. These anomalies extend westward from the Angolan coast. The mechanisms producing rainfall over this region are similar in both experiments. Enhanced uplift (Figure 5.2**d**), latent heat flux (see Figure B.1**a** Appendix B), low sea level pressure (Figure 5.2**b**) and low-level moisture divergence (Figure 5.2**f**) are observed over the region of SST forcing in Experiment 2 and 3. This suggests that convective processes dominate the mechanisms producing rainfall there.

NCEP re-analyses for austral summer 1995 indicate strongly negative anomalies in the 500 hPa omega field over the tropical southeastern Atlantic and Angola/Namibia. Thus, rising air was also observed near the warm SST during the 1995 Benguela Niño and hence led to the increased precipitation there. With a baroclinic type of response in the model and rising air at 500 hPa over the tropical South East Atlantic, this suggests strong convective processes near the region of the forcing. Over tropical eastern Africa and the tropical southern Indian Ocean, increased moisture convergence and uplift leads

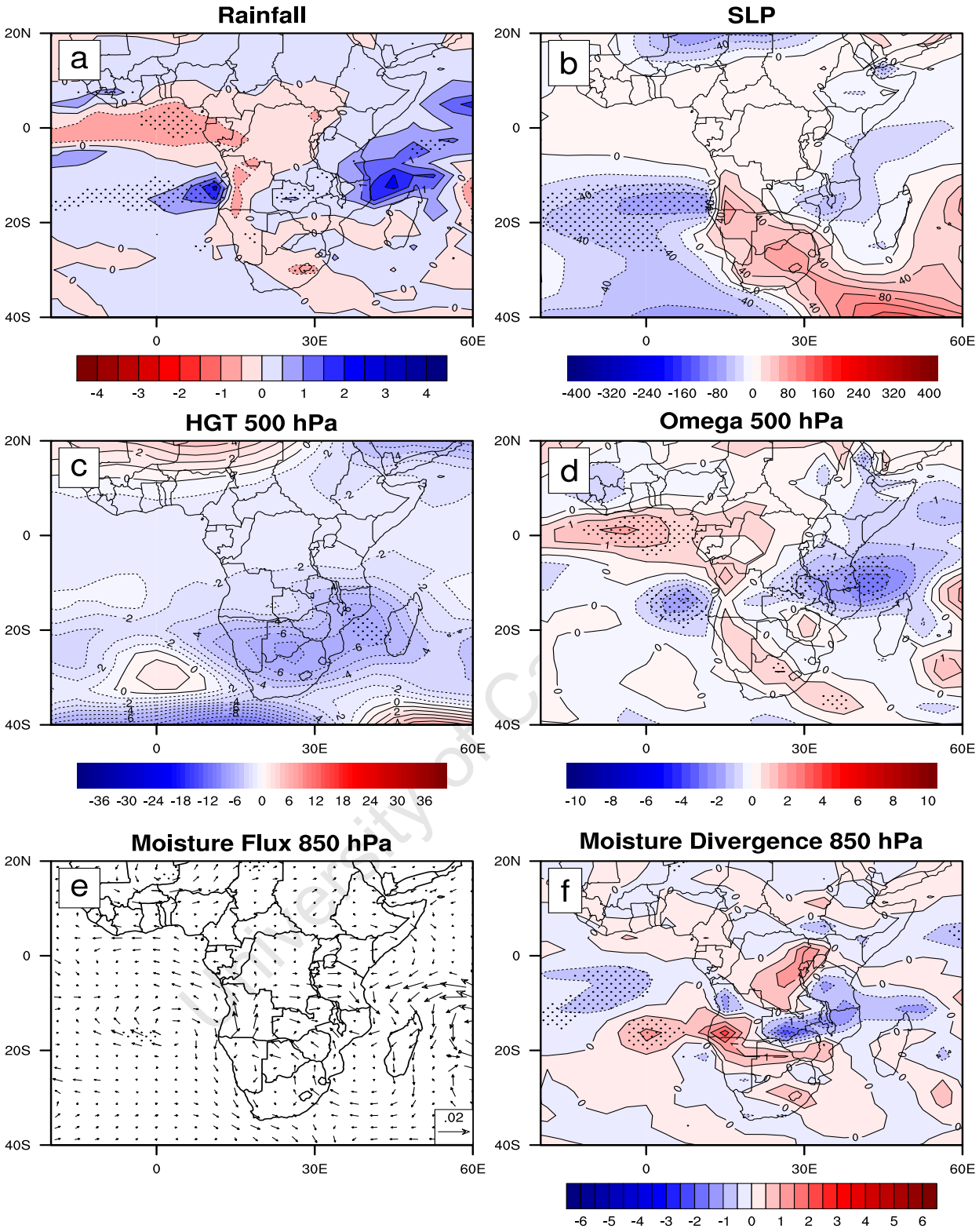

Figure 5.2: Same as 5.1 except for Experiment 2.

to anomalous rainfall there. On the other hand, strong relative subsidence over the equatorial South Atlantic leads to reduced rainfall over this region.

Given the positive rainfall anomalies generated near the SST forcing in Experiment 3, one expects even more rainfall anomalies to be generated near the forcing in Experiment 2 in which the forcing is increased. However, the magnitudes of the rainfall, sea level pressure and omega anomalies over this region are about the same in the two Experiments. This suggests that there exists a SST threshold in this region above which no further increase in rainfall is observed. This kind of response may be related to an SST threshold for convection that leads to saturation (Hoerling *et al.*, 2001). However, an examination of latent heat flux anomalies of both experiments shows that the increase in SST results in a corresponding increase in latent heat flux. Areas of increased latent heat flux may serve as sources of moisture and energy for storms as a result of enhanced surface evaporation.

Although not the subject of this study, it is important to mention that the relationship between SST and latent heat flux is complex and cannot be explained by thermodynamic considerations alone (Zhang and McPhaden, 1995). In investigating relationships between SST and latent heat flux in the equatorial Pacific, Zhang and McPhaden (1995) found that at low SST, the latent heat flux increases with SST whereas at high SST the latent heat flux decreases with SST. Other parameters such as wind speed and humidity need to be considered as well in order to understand this relationship. The latent heat results (see Figure B.1**a** Appendix B) are in agreement with this relationship because the ABF is a region of relatively lower SST than in the equatorial western and central Pacific. Another thing to note is that since this is an atmosphere only experiment, feedbacks between the ocean and the atmosphere which take place in the real world through surface flux interactions, are not taken into account. Therefore the results need to be interpreted in that light.

Figure 5.2**a** shows that the model generates negative rainfall anomalies over the equatorial Atlantic, the Gulf of Guinea, the Congo basin, parts of Angola and over the TTT region when forced with SST anomalies in Figure 3.1**a**. Statistically significant negative rainfall anomalies over the Gulf of Guinea in this experiment appear to contradict results in Experiment 3 and observations in Reason and Rouault (2006). These authors observed a strong positive correlation between SST over southeast Alantic and rainfall

over the Gulf. The apparent contradiction supports the above suggestion of the existance of a threshold SST. In this case, the positive-correlation relationship between SST in the southeast Atlantic and rainfall over the Gulf does not hold above the threshold SST.

The model produces high sea level pressure anomalies (Figure 5.2**b**) over the TTT region, that extend southeast from Angola to the southeast coast of South Africa. Like in the previous experiment, an upper level low pressure (Figure 5.2**c**), subsidence and low-evel moisture divergence (Figure 5.2**f**) over this region provide unfavourable conditions for TTT activity and formation of cloud bands.

In the following section results from Experiment 6 are presented. In this Experiment the model was forced with the SST anomaly similar to Experiment 2 except that the anomaly is slightly shifted northward in Experiment 6.

5.4 Sensitivity to location of Benguela SST anomaly: Experiment 6

In Experiment 6 (Figure 3.1**e**), the forcing in the southeast Atlantic is shifted equatorward. This experiment is conducted on the premise that tropical forcing may produce a stronger atmospheric response locally, similar to over Peru during an El Niño in the Pacific. Because of higher SST in the tropics, a warm SST anomaly located further into the tropics raises the actual surface temperature to a correspondingly higher level than one located more polewards, thereby, increasing the chances of deep atmospheric convection developing in its vicinity. Therefore, it is expected that Experiment 6 will generate more rainfall along the Angolan coast than Experiment 2 and 3. Figure 5.3 shows the model's response to this northward shifted SST forcing. Consistent with the more tropical SST anomaly, anomalously positive rainfall anomalies of more than 5 mm/day (or about twice the magnitude of that in Experiment 2, Figure 5.2**a**) are generated near the SST forcing and along the Angolan coast (Figure 5.3**a**). Rainfall anomalies of greater than 0.5-1 mm/day extend from this region westward to the central tropical Atlantic Ocean.

In general, substantially more widespread rainfall is generated over the subcontinent in this experiment than in the previous two.

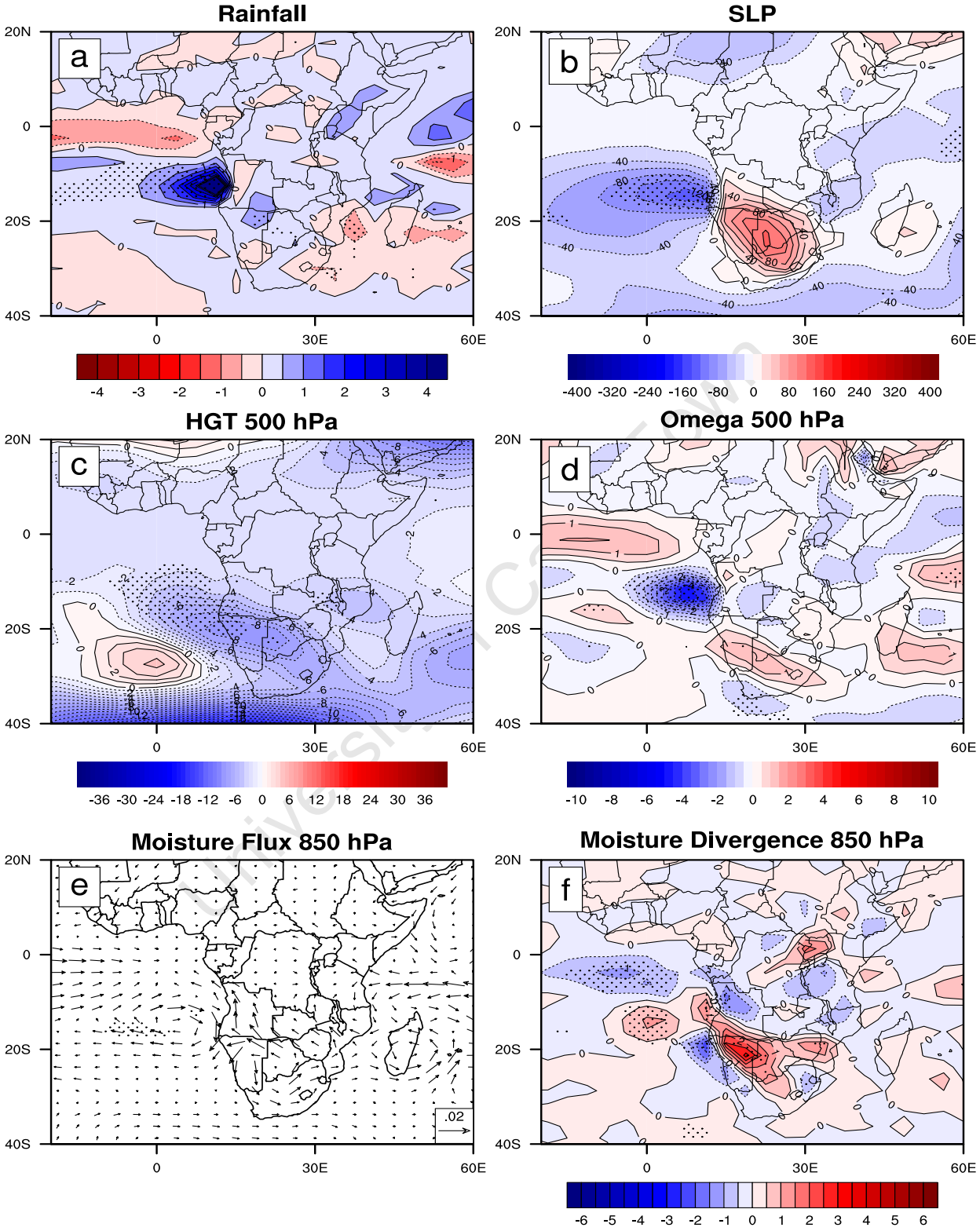

Figure 5.3: Same as 5.3 except for Experiment 6.

These results suggest that a Benguela Niño with maximum SST anomaly slightly farther north may produce more anomalous rainfall over western Angola/northern Namibia and elsewhere than if the SST forcing is situated further poleward. The cyclonic (anticyclonic) anomaly centred off Angola (over Madagascar) lead to low level moisture convergence anomalies over northern Angola (eastern tropical Africa) (Figures 5.3**e** and **f**). Although the cyclonic circulation anomaly is also produced in the above experiments, it appears to be stronger in Experiment 6. However, a cyclonic anomaly is produced over the Mozambique channel in the previous two experiments. This indicates that SST in the southeast tropical Atlantic may influence circulation in the southwest tropical Indian Ocean. However, the mechanisms producing the change in circulation over the Mozambique channel/Madgascar in this experiment remain obscure.

The cyclonic anomaly off Angola tends to reduce the low level moisture flux off the subcontinent onto the South Atlantic Ocean (cf Figure 2.3) whereas the anticyclonic anomaly over Madagascar tends to enhance moisture flux from the subtropical southwest Indian Ocean, thus leading to more widespread rainfall south of Zambia in this experiment. However, the sea level pressure high anomalies (Figure 5.3**b**), upper level low pressure anomalies (Figure 5.3**c**), increased subsidence (Figure 5.3**d**) and strong low-level moisture divergence (Figure 5.3**f**) over the TTT region suggest unfavourable rainfall conditions over this region. Therefore, other processes may be behind the observed rainfall there. Stronger uplift near the SST forcing (Figure 5.3**d**) compared to the previous experiments contributes to the large anomalous rainfall observed over this region.

In general a stronger response is observed near the SST forcing in Experiment 6 than in the previous two experiments. This is evident in the rainfall, sea level pressure, 500 hPa geopotential height and omega and near surface moisture flux and divergence anomalis shown in Figure 5.3.

5.5 Summary and Conclusion

This chapter has presented results for experiments in which the HadAM3 GCM is forced with various idealized SST patterns only in the southeast tropical Atlantic Ocean. The

results presented in this chapter are those from Experiments 2, 3 and 6. These experiments are used to explore the sensitivity of the regional atmosphere to SST forcing in the southeast tropical Atlantic Ocean. In Experiment 2 the model was forced with an idealization of the SST anomaly pattern in the southeast tropical Atlantic observed during the 1995 Benguela Niño. The anomaly is centred around 12°E, 17°S and about 6°C in magnitude (Figure 3.1**a**). Experiment 3 involved forcing the model with idealized representation of the SST anomaly pattern observed during the 2001 Benguela Niño event. In this experiment the anomaly is centred as in Experiment 2, but has a magnitude of about 4°C and is less extensive (Figure 3.1**b**). Experiment 6 is similar to Experiment 2 except that the forcing is slightly shifted equatorward to about 15°S (Figure 3.1**e**).

The model's response to the SST anomaly forcing in the tropical southeast Atlantic Ocean consists of positive rainfall anomalies over western Angola and near the SST forcing. The positive rainfall anomalies over western Angola and the SST forcing are associated with enhanced surface latent flux over the SST forcing and uplift near the SST forcing in the tropical southeast Atlantic Ocean. Positive anomalies in low level moisture divergence suggest that the enhanced surface latent heat flux and local uplift contribute more to the positive rainfall anomalies over western Angola and the SST forcing than do changes in moisture convergence. In addition, the enhanced uplift over this region favours stronger convective rainfall there. Circulation changes over southern Africa resulting from the SST forcing in the southeast Atlantic suggest that Benguela Niño events tend to suppress TTT occurrence.

The model results suggest that a Benguela Niño is capable of forcing anomalous wet conditions over western Angola on its own. However, it is less clear as to how influential it is on the rainfall further inland. Statistically significant postive (negative) rainfall anomalies are generated over Zambia and parts of eastern Africa (equatorial Atlantic) when the intensity of the southeast tropical Atlantic anomaly is increased. However, strong positive correlation exists between SST over the southeast tropical Alantic and the Gulf of Guinea. Therefore the results suggest that there exists a threshold SST above which the observed correlation ceases. The resulting changes in the atmospheric

circulation lead to changes in low-level moisture convergence and uplift over Zambia and eastern Africa that appear to contribute to positive rainfall anomalies there. Therefore, this suggests that a Benguela Niño is capable of influencing anomalous rainfall both over western Angola and much further inland when the intensity is increased.

Widespread weak positive rainfall anomalies are generated over southern Africa when the maximum SST anomalies are located further north in the South East Atlantic. Stronger positive anomalies are produced over western Angola and near the SST forcing. Consistent with observational studies (Hirst and Hastenrath, 1983, Rouault *et al.*, 2003), these model results imply that the western Angola region is susceptible to flood events during Benguela Niño. Since the onset of these events is typically around December/January, monitoring the tropical southeast Atlantic Ocean could provide an early warning system that could be beneficial to the Angolan economy.

Chapter 6

Sensitivity to Indian Ocean SST

6.1 Introduction

The previous chapter discussed the regional atmospheric response to SST forcing only in the southeast tropical Atlantic Ocean. In this chapter, the results of the models response to various regional idealized SST patterns in the southeast tropical Atlantic and subtropical southwest Indian Ocean (SWIO) are presented. These SST patterns vary in location, sign and magnitude. Observational work (Reason and Mulenga, 1999, Behera and Yamagata, 2001) and studies with numerical models (Reason, 2001, 2002, Hansingo and Reason, 2006) have found that SST in the subtropical SWIO may influence austral summer rainfall over southern Africa. The results discussed in this chapter are those from Experiments 4, 5, 9 and 10. The SST forcing in the southeast tropical Atlantic in these experiments is the same as discussed in the previous chapter. In the subtropical SWIO, the SST forcing varies in location and sign in the experiments discussed here. The purpose of this chapter is to study how cooling or warming in the subtropical SWIO that often occurs during Benguela Niño events may modulate the rainfall impacts over southern Africa. Therefore, this chapter addresses the second question posed in chapter 1. Section 6.2 considers cool SST forcing in the SWIO whereas section 6.3 discusses the results for warm SST forcing here. The summary and conclusions are presented in section 6.4.

6.2 Sensitivity to Negative SST Anomalies : Experiment 4

In Experiment 4, the model is forced with positive SST anomalies, up to about 6°C, in the southeast tropical Atlantic Ocean centred around 12°E, 17°S and negative SST anomalies, up to about −2°C, in the subtropical SWIO centred around 50°E, 35°S (Figure 3.1**c**). This experiment is similar to Experiment 2 except that cool SST anomalies are added south of Madagascar. During the 1995 Benguela Niño, cool SST anomalies occurred in the SWIO south of Madagascar together with strong warming in the tropical Southeast Atlantic. As mentioned in chapter 5, extensive floods were reported over western Angola and northern Namibia, but further east, many parts of southern Africa received below average rainfall. Experiment 4 (Figure 3.1**c**) is an idealization of this event.

When forced with the SST anomalies in Figure 3.1**c**, the model produces rainfall anomalies similar to those in Experiment 2. However, a small reduction in the positive rainfall anomalies seen in Experiment 2 (Figure 5.2**a**) is observed over the Mozambique/Tanzania border (Figure 6.1**a**). The reduction in rainfall anomalies over this region may be associated with relative reduced low-level moisture convergence (Figure 6.1**d**) and uplift (Figure 6.1**b**) there as result of these features slightly shifting eastward. There is reduced evaporation south of Madagascar due to reduced surface latent heat flux (see Appendix B) as a result of the negative SST forcing in the subtropical SWIO. Because of reduced evaporation south of Madagascar as result of cool SST, the cyclonic low-level moisture flux anomaly (Figure 6.1**c**), centred over the southern Mozambique Channel, advects cool and less moist air over South Africa. The model generates statistically significant negative rainfall anomalies over the southeast coast of South Africa as result of cool SST forcing in the subtropical SWIO in Experiment 4. Note that Behera and Yamagata (2001) and Reason (2001, 2002) have shown that negative rainfall anomalies are generated over southern Africa during the negative phase of a South Indian Ocean subtropical dipole event in summer. This phase is characterised by cool SST anomalies south of Madagascar and warm anomalies off the western coast of Australia.

Anomalous rainfall is generated over the tropical SWIO in Experiment 4 compared to Experiment 2. These anomalies extend southwest across the subcontinent in Experiment 4. An increase in rainfall over north eastern Namibia corresponds with an increase in surface latent heat flux (see Appendix B) over this region. The low-level westerly moisture flux anomalies over the equatorial Atlantic (Figure 6.1**c**) appear to reduce the advection of moist air away from West African regions. This circulation, together with enhanced uplift off the Liberia/Sierra Leone coast and parts of West Africa, generates positive rainfall anomalies over these regions. Negative rainfall anomalies seen over the Gulf of Guinea extending westward in Experiment 2 have weakened in Experiment 4. This may be as result of the westerly low-level moisture flux anomalies there which act to weaken the advection of moist air away from this region. Note that the anomalies are easterly in Experiment 2.

Noticeable differences in low-level moisture flux anomalies between Experiment 2 (Figure 5.2**e**) and 4 (Figure 6.1**c**) are observed over the SWIO.. The anomalies over the tropical SWIO are northeasterly in Experiment 4 and northerly in Experiment 2. The cyclonic anomaly over the subtropical SWIO is centred over the southern Mozambique Channel in Experiment 2 and weak and closer to the subcontinent in Experiment 4. Thus, these results suggest that a cool SST anomaly in the subtropical SWIO may lead to its own response over the region that can augment or oppose the rainfall impacts of a Benguela Niño over southern Africa. Note that previous AGCM experiments with SST anomalies imposed in this part of the SWIO (e.g. Reason and Mulenga, 1999, Reason, 2001, 2002) have shown a significant circulation and rainfall response over southern Africa.

One would also expect anomalous rainfall to occur over northern Angola as a result of enhanced low level moisture convergence there (Figure 6.1**d**). However, relative subsidence there and over most parts of Southern Africa south of Zambia (Figure 6.1**b**) may lead to the negative rainfall anomalies seen in this region. Note that during the 1995 Benguela Niño, below average rainfall was observed over these regions and also Zimbabwe/Mozambique but wetter than average conditions occurred over eastern South Africa and Tanzania (Rouault *et al.*, 2003). Figure 6.1**a** also shows above average rainfall

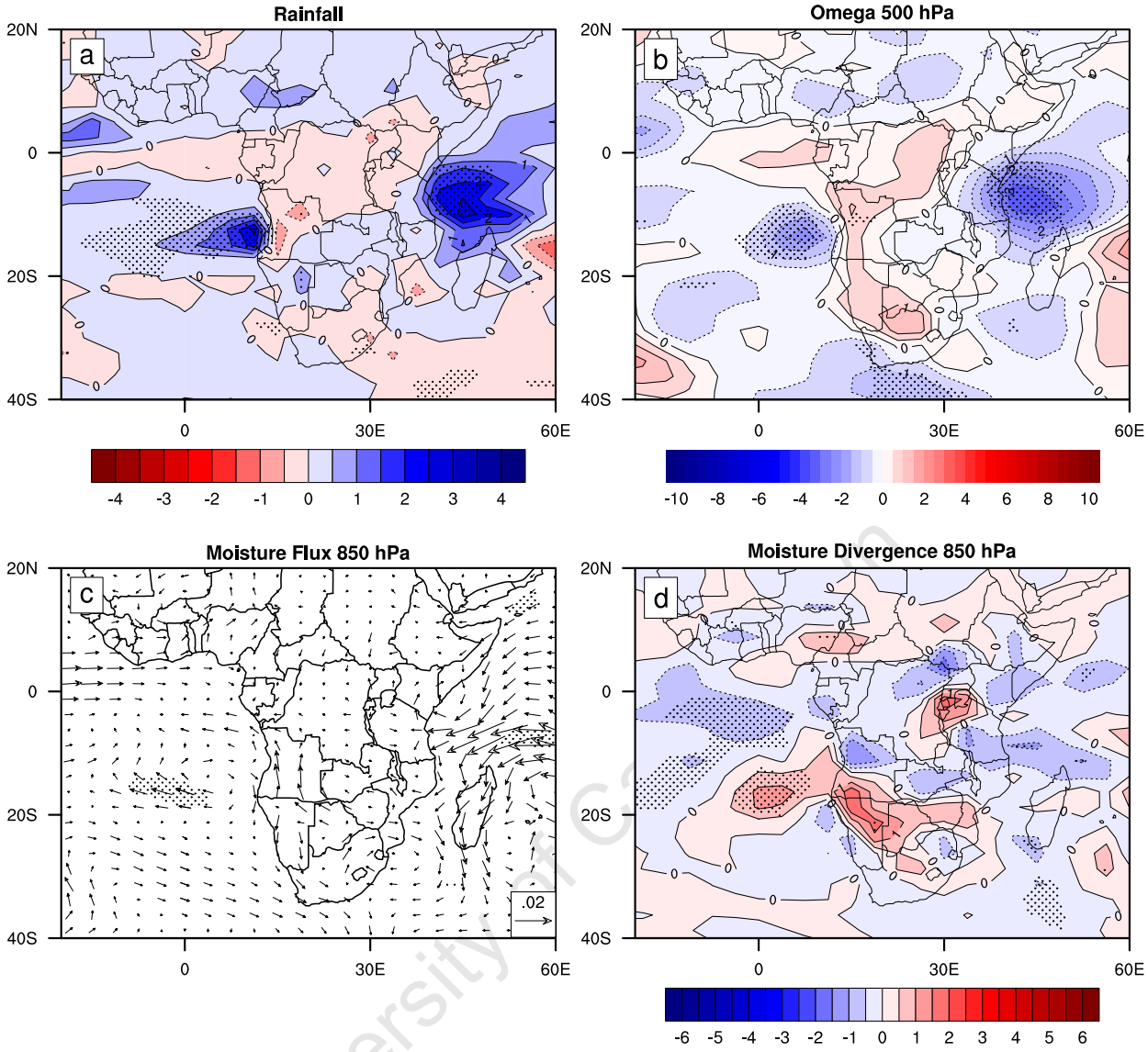

Figure 6.1: Experiment 4 anomalies for, (**a**) Rainfall with contour interval of 0.5 mm/day, (**b**) 500 hPa Omega, (**c**) 850 hPa Moisture flux and d 850 hPa Moisture divergence.

over western South Africa and eastern Tanzania but dry conditions over eastern South Africa and western Tanzania. This result suggests that some other forcing besides the SST anomaly idealized in Figure 3.1c may have contributed to the observed rainfall anomalies. Note that the 1995 Benguela Niño event also coincided with a protracted El Niño event in the Pacific but that the corresponding Pacific or tropical Indian SST anomalies are not included in the model experiment. Thus, these model results suggest that independent of ENSO, a Benguela Niño is capable of producing anomalous rainfall over southern Africa despite cooling in the Indian Ocean which is normally associated with below average rainfall over the subcontinent. However, the results also suggest that the 1995 observed

rainfall anomalies were not solely due to regional Atlantic or South Indian Ocean SST forcing but were also contributed to by other SST forcing (e.g., associated with the ENSO event) or by other factors not included here.

6.3 Sensitivity to Positive SST anomalies: Experiments 5, 9 and 10

In this section, results from Experiments 5, 9 and 10 are presented. In these experiments, the HadAM3 GCM is forced with positive SST anomalies in the southeast tropical Atlantic Ocean which vary in location and magnitude and in SWIO which vary only in location. In Experiment 5, the forcing in the southeast tropical Atlantic has a magnitude of up to about 4°C and centred around 12°E, 17°S while the forcing in the SWIO reaches a magnitude of about 2°C and is centred around 50°E, 35°S. The SST forcing in Experiment 9 is similar to Experiment 5 except that the forcing in southeast tropical Atlantic reaches about 6°C, and its location is shifted slightly northward (12°E, 15°S). Experiment 10 is similar to Experiment 9 except that the forcing in the subtropical SWIO is located closer to the subcontinent (45°E, 32°S). These experiments are conducted on the premise that warm SST anomalies in the subtropical SWIO may generate increased rainfall over southern Africa and hence could augment those due to SST anomalies in the South East Atlantic. Note that during certain Benguela Nino events, SST anomalies of similar magnitude and location have been observed.

Both observations and GCM results in Reason and Mulenga (1999), Reason (2001) and Hansingo and Reason (2006) have shown that warming in the subtropical SWIO during austral summer leads to enhanced rainfall over large areas of southeastern Africa. Furthermore, Behera and Yamagata (2001) and Reason (2001, 2002) have shown that anomalous rainfall is produced over southern Africa during the positive phase of a South Indian Ocean subtropical dipole event in summer. This phase is characterized by warm SST anomalies south of Madagascar and cool anomalies off the western coast of Australia.

Therefore, given this previous research and the results in experiments 2-4, with the SST forcing in the tropical southeast Atlantic shifted northward plus warm SST forcing imposed south of Madagascar (Figures 3.1**d**, **h** and **i**), one expects these experiments to generate more rainfall over southern Africa than Experiments 2-4 and 6.

Warm SST anomalies were observed over the southeast tropical Atlantic and the southwest subtropical Atlantic Oceans during the 2001 Benguela Niño event. This event was characterised by above average rainfall over southern Africa. Therefore, Experiment 5 is an idealization of the observed regional SST anomalies during the 2001 Benguela Niño. When forced with SST anomalies of Experiment 5 (Figure 3.1**d**), the model, however, generates relatively reduced rainfall (Figure 6.2**a**) over southern Africa compared to the previous experiments. In particular, negative anomalies are produced over the Congo basin and the equatorial Atlantic Ocean compared to Experiment 3 (Figure 5.1**a**) in which the model is forced with only Benguela Niño SSTs in the southeast tropical Atlantic Ocean. However, the model generates positive rainfall anomalies over Kenya and parts of Tanzania in Experiment 5. The westerly low-level moisture flux anomalies over the equatorial Atlantic Ocean seen in Experiment 3 (Figure 5.1**e**) have become northwesterly and stronger in Experiment 5 (Figure 6.2**c**). These circulation anomalies tend to weaken the advection of low-level moist air away from the subcontinent. However, enhanced subsidence (Figure 6.2**b**) and relatively reduced moist air convergence (Figure 6.2**d**) over the equatorial Atlantic and the Congo basin do not favour rainfall, thus the negative rainfall anomalies observed over this region in Experiment 5.

The cyclonic low-level moisture flux anomaly over the Mozambique Channel extends further south and appears to advect moist air from the south of Madagascar to central and eastern southern Africa. The warm SST forcing in the southwest SWIO enhances evaporation to the south of Madagascar as a result of enhanced surface latent heat flux there (see Appendix B). Statistically significant rainfall anomalies of only about 0.5 mm/day are produced over this region compared to about 2 mm/day produced over the SST forcing in the southeast tropical Atlantic Ocean. The SST forcing over the two regions differ by about 2°C. Relatively strong low-level convergence of the subtropical SWIO

sourced moist air and uplift over central and eastern southern Africa leads to relatively increased rainfall over Tanzania and Zambia.. The SST forcing in the subtropical SWIO appears to generate anomalous rainfall local to the region of the forcing. This is also observed in Experiments 9 and 10.

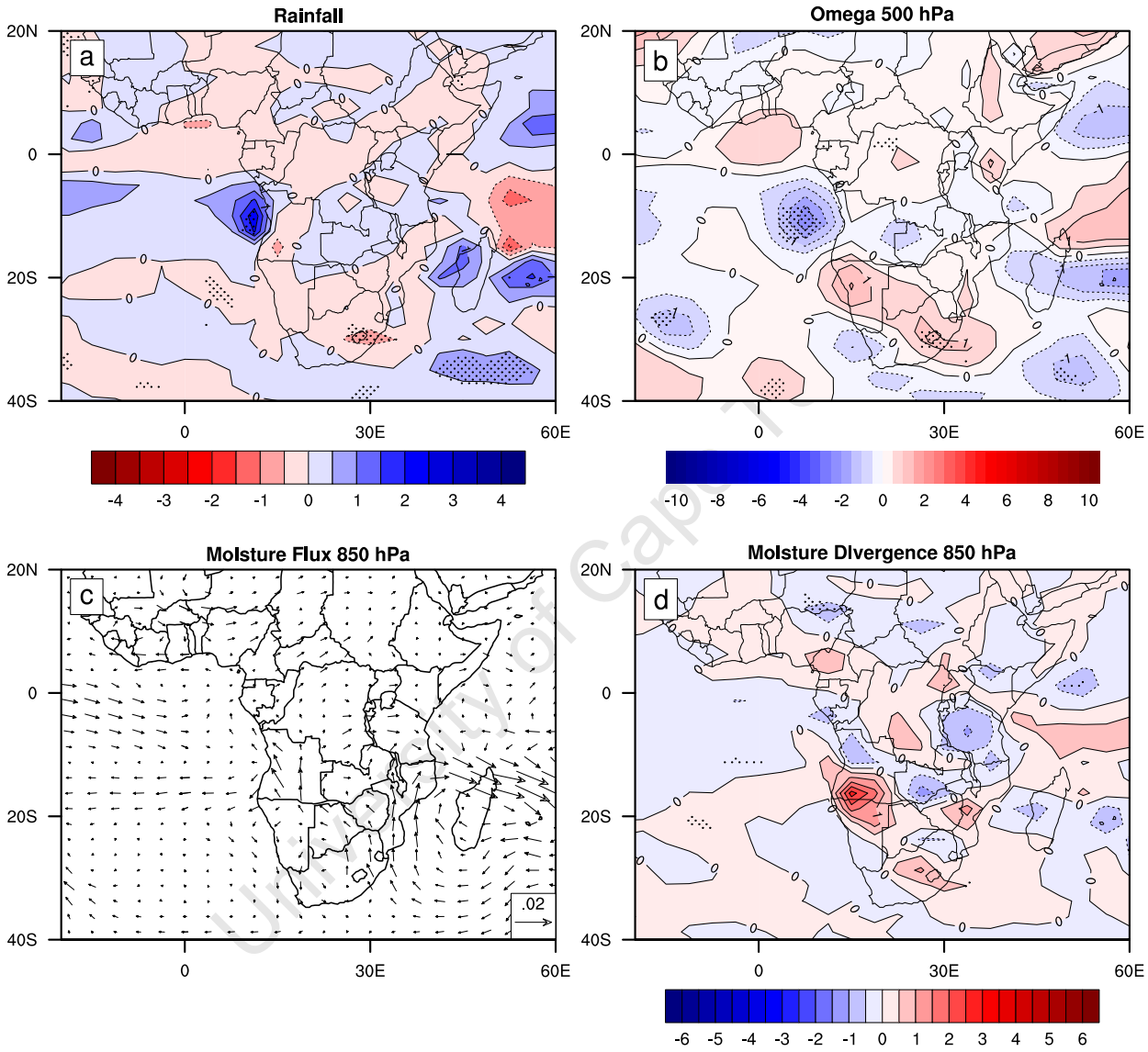

Figure 6.2: Same as Figure 6.1, but for Experiment 5.

When forced with SST anomalies of Experiment 9 (Figure 3.1**h**), like in Experiment 5, the model generates statistically significant positive rainfall anomalies of about $0.5mm/day$ over the SST forcing in the subtropical SWIO (Figure 6.3a). However, these anomalies are less extensive in Experiment 9. As expected, widespread and more rainfall is generated over southern Africa in Experiment 9 than in Experiments 4 and 5. This

increased rainfall response occurs because the forcing in the southeast tropical Atlantic Ocean is slightly shifted northward and is more extensive in Experiment 9. It is found, in chapter 5, that a more tropical and extensive positive SST forcing in the tropical southeast Atlantic generates more and widespread rainfall over southern Africa.

Somewhat larger positive rainfall anomalies are generated over the Mozambique Channel and east of Madagascar compared to Experiment 5. Anomalies of about 0.5 mm/day are generated over northern Namibia/southeastern Angola/ western Zambia and Tanzania. Reason and Mulenga (1999), Behera and Yamagata (2001) and Reason (2001, 2002) attributed anomalous rainfall over southeastern Africa during warm events in the subtropical SWIO to enhanced low-level tropospheric easterlies transporting surplus moisture to this region, and hence enhanced moisture convergence and convection there. The warm SST anomaly in the SWIO acts as the source of surplus moisture. This mechanism is observed in Figures 6.3**b**, **c** and **d** over eastern Zambia, Mozambique and Tanzania. Relative low-level moisture convergence results because the northwesterly anomalies over and north of Madagascar (Figure 6.3**c**) oppose the mean easterly flux in this region (Figure 2.3). Over eastern South Africa, relative subsidence (Figure 6.3**b**) and low-level moisture divergence (Figure 6.3**d**) may contribute to reduced rainfall there. As in Experiments 2-6, enhanced uplift near the forcing in the southeast Atlantic contributes to anomalous rainfall there and over coastal Angola.

Experiment 10 (Figure 3.1**i**) is similar to Experiment 9 except that the SST anomaly forcing in the subtropical SWIO is shifted closer to the subcontinent. Previous experiments with a numerical model suggest that the positive rainfall anomalies are further enhanced over southern Africa when the warm SST anomalies in the subtropical southwest Indian Ocean are close to the subcontinent (Reason, 2002). Therefore, one expects this experiment to generate more rainfall over the subcontinent than in Experiment 9. Rainfall anomalies over southern Africa are similar to Experiment 9 except that positive rainfall anomalies are now also produced over Zimbabwe and those over Zambia are larger and more widespread (Figure 6.4**a**). The size of the rainfall anomalies over the SWIO is now generally greater than in Experiment 9 and negative anomalies are generated over

the western equatorial regions of Africa, northern Angola and eastern South Africa. The cyclonic anomalies over the tropical southeast Atlantic and the Mozambique Channel are generally weaker in Experiment 10.

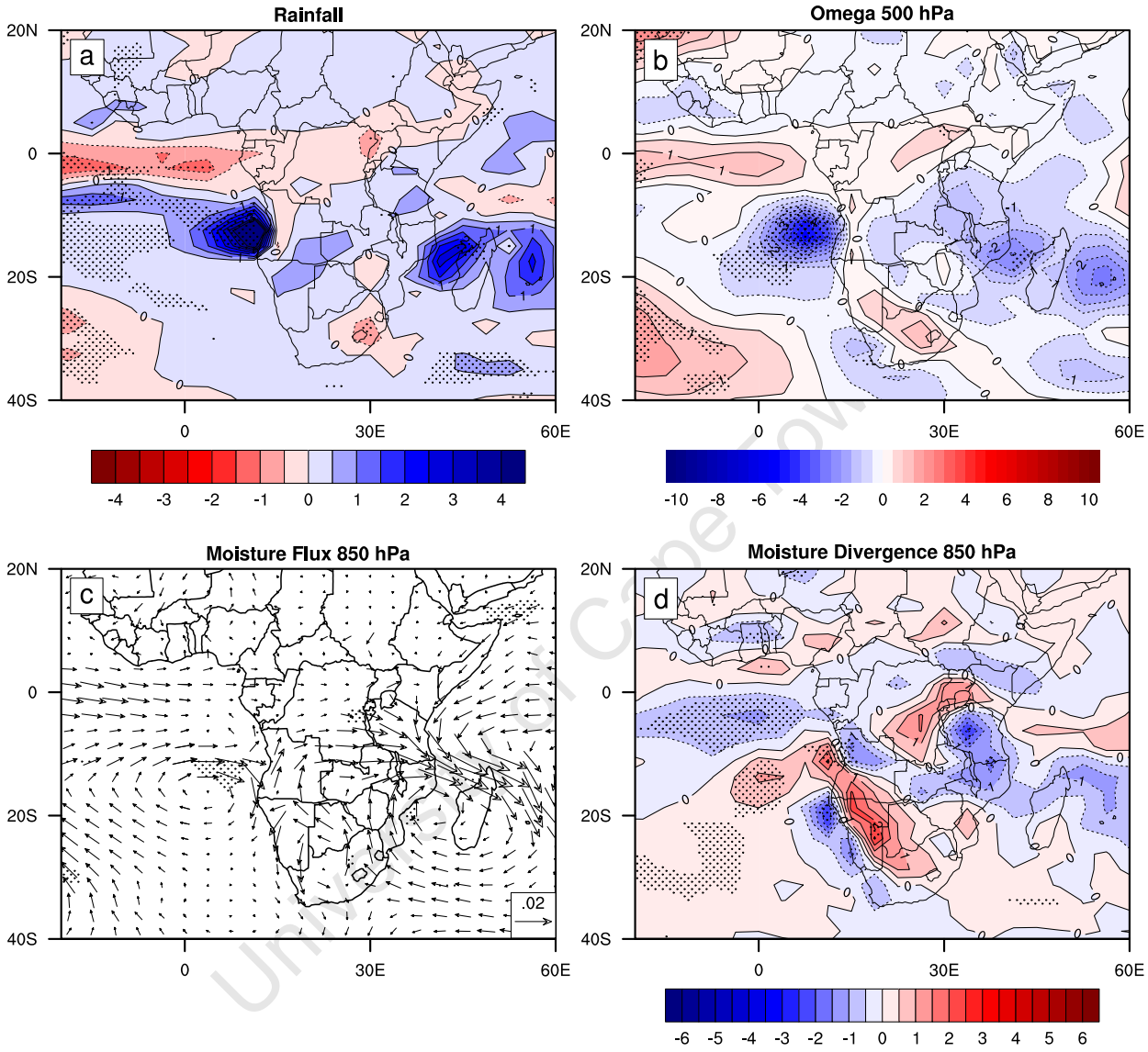

Figure 6.3: Same as Figure 6.1, but for Experiment 9.

An examination of the low-level moisture flux anomalies in Figure 6.4**c** indicates that the cyclonic anomaly centred over the southern Mozambique Channel and the anticyclonic anomaly to the northeast of Madagascar advect surplus moist air from the subtropical and tropical SWIO towards some areas of eastern Africa. In addition to moisture advection over this region, increased low-level convergence (Figure 6.4**d**) and uplift (Figure 6.4**b**) generate enhanced rainfall there. However, the convergence and uplift are

relatively weaker in Experiment 10 than in Experiment 9. The negative rainfall anomalies over eastern South Africa are as a result of relative subsidence, moisture divergence and reduced latent heat flux (see Appendix B). These conditions are also observed over the western equatorial regions of Africa and may be associated with the observed negative rainfalls there.

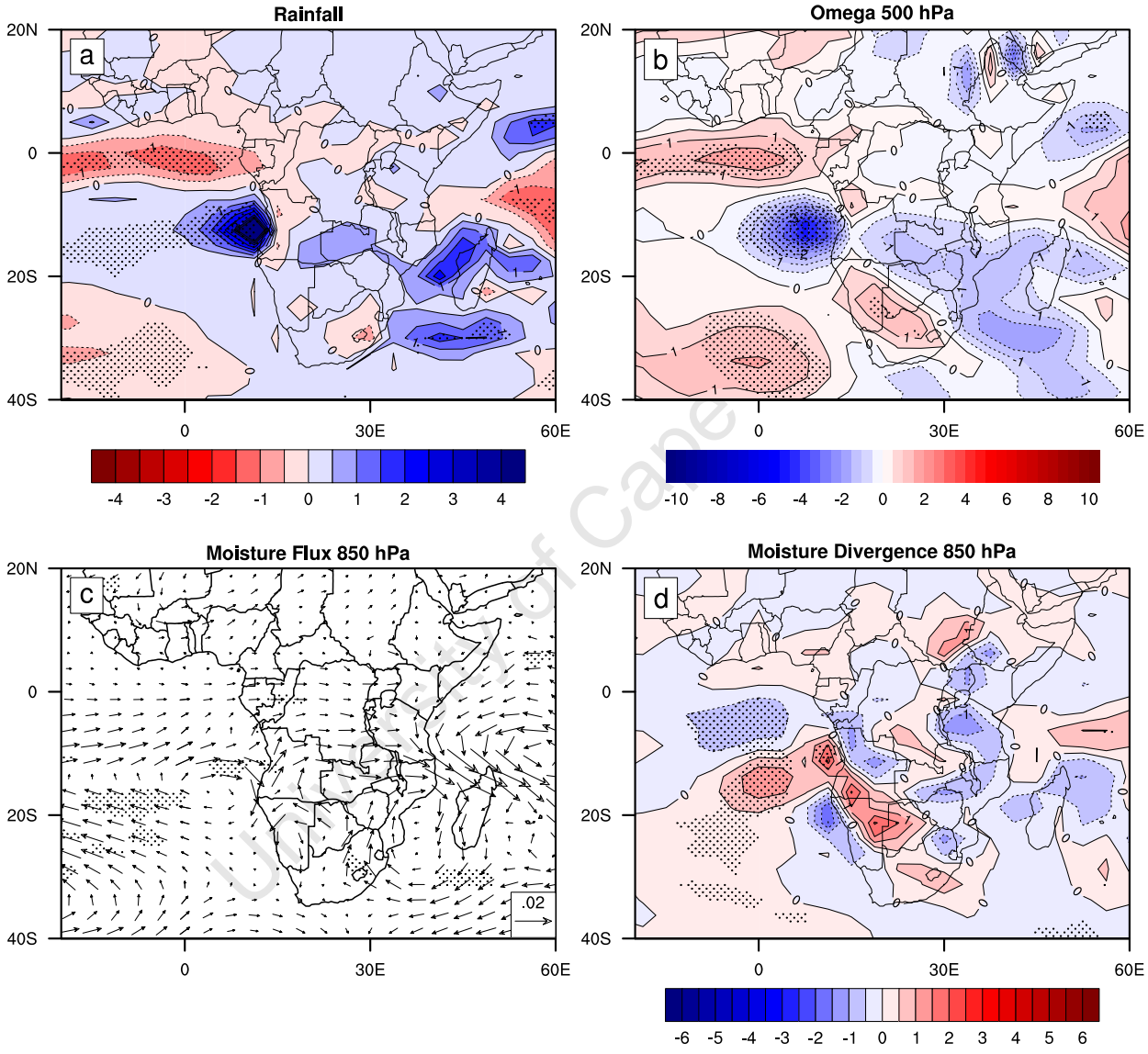

Figure 6.4: Same as Figure 6.1, but for Experiment 10.

Weak positive rainfall anomalies are observed over Botswana and parts of Namibia despite enhanced subsidence and moisture divergence. However, increased latent heat flux is observed over this region (see Appendix B). This result suggests that latent heat

and processes other than moisture convergence and uplift may produce the observed rainfall over this region.

6.4 Summary and Conclusion

Results from Experiments 4, 5, 9 and 10 have been presented in this chapter. These experiments involve forcing the HadAM3 with various patterns of SST anomalies in the tropical southeast Atlantic and subtropical southwest Indian Oceans (SWIO). The purpose of these experiments was to investigate in an idealized way the changes in rainfall response over southern Africa that may occur during Benguela Niño events that coincide with significant SST anomalies in the SWIO. In Experiment 4, the model was forced with positive SST anomalies of magnitude up to about 6°C, in the southeast tropical Atlantic Ocean centred around 12°E, 17°S. The forcing in the subtropical SWIO was negative, with magnitude up to about −2°C, centred around 50°E, 35°S. In Experiment 5, the forcing in the southeast tropical Atlantic reached up to about 4°C and was centred around 12°E, 17°S while the forcing in the subtropical SWIO had a magnitude of about 2°C and was centred around 50°E, 35°S. The SST forcing in Experiment 9 was similar to Experiment 5 except the forcing in southeast tropical Atlantic reached a magnitude of about 6°C, was more extensive and shifted slightly northward (12°E, 15°S). Experiment 10 was similar to Experiment 9 except that the forcing in the subtropical SWIO was located closer to the subcontinent (45°E, 32°S). These idealised SST anomalies are similar in magnitude and location to what is observed during certain Benguela Niño events.

Relatively reduced positive rainfall anomalies are produced over the Mozambique/Tanzania border (Figure 6.1**a**) while negative anomalies are generated over eastern South Africa, when the model is forced with SST anomalies in Experiment 4 (Figure 3.1**c**). There is reduced evaporation south of Madagascar due to reduced surface latent heat flux (see Appendix B) as a result of the negative SST forcing in the subtropical SWIO. The cyclonic low-level moisture flux anomaly (Figure 6.1**c**) centred over the southern Mozambique Channel advects cool and less moist air over South Africa. This result is consistent with the observations of Behera and Yamagata (2001) and numerical model experiments of

Reason (2001, 2002). These authors showed that negative rainfall anomalies are generated over southern Africa during the negative phase of a South Indian Ocean subtropical dipole event in summer.

When forced with SST anomalies of Experiments 5, 9 and 10, the model produces positive rainfall anomalies over southern Africa similar to experiment 4, except these are widespread in Experiments 9 and 10. When forced with SST anomalies of Experiment 5 (Figure 3.1**d**), the model, however, generates relatively reduced rainfall (Figure 6.2**a**) over southern Africa compared to the other experiments. Like in the southeast tropical Atlantic, positive rainfall anomalies are generated over the SST forcing in the subtropical SWIO in Experiments 5, 9 and 10. Statistically significant rainfall anomalies of only about 0.5 mm/day are produced over this region compared to about 2 mm/day produced over the SST forcing in the southeast tropical Atlantic Ocean in Experiment 5. Anomalous rainfall is generated over the forcing in the subtropical SWIO in Experiment 10 compared to Experiments 5 and 9. The model generates more widespread positive rainfall anomalies over southern Africa in Experiment 10 (Figure 6.4**a**) in which the forcing in the southwest subtropical Indian Ocean is closer to the subcontinent.

Taken together, the results of Experiments 4, 5, 9 and 10 suggest that, depending on their sign and location, SST forcing in the SWIO may augment or oppose the rainfall impacts over southern Africa during a Benguela Niño event. For both the SWIO and southeast Atlantic SST anomalies, a more tropically located pattern tends to produce a larger response in the model.

Chapter 7

Potential Influence of La Niña: Experiments 7 and 8

7.1 Introduction

The previous chapters have examined the sensitivity of the atmospheric response over southern Africa to regional SST forcing. The SST forcing in the experiments of the previous chapters was either only in the southeast tropical Atlantic Ocean or in both southeast tropical Atlantic and the southwest subtropical Atlantic Ocean. These experiments are idealized representations of observed SST anomalies in the neighbouring oceans during the Benguela Niño events occurring during 1995 and 2001. These events coincided with warm (1995) or cool (2001) SST anomalies occurring in the equatorial Pacific Ocean. Therefore, SST anomalies in the Pacific Ocean may have influenced the regional circulation and rainfall over southern Africa during the 1995 and 2001 Benguela Niño events, and therefore made the impacts of these Benguela Niños less transparent. It has long been recognised that the Pacific El Niño has a close association with rainfall variability in many parts of Africa (Nicholson and Selato, 2000, Reason *et al.*, 2000). In view of this association, an influence of La Niña during the 1995 and 2001 Benguela Niños might also be anticipated. This chapter examines the potential influence of cool SST anomalies in the central equatorial Pacific Ocean on southern Africa during a Benguela Niño event.

Thus, results from Experiments 7 and 8 are presented in this chapter. These experiments assume that the ENSO signal's influence on southern Africa is directly from the tropical Pacific Ocean and not via the Indian Ocean. Therefore, the objective is to isolate the effect of Pacific Ocean SST on southern African circulation.

In Experiment 7, the model is forced with negative SST anomalies only in the central equatorial Pacific Ocean. These anomalies have a minimum of about -2°C centred on the equator around 160°W (Figure 3.1**f**). The objective of this experiment is to isolate the effect of the SST anomalies in the central equatorial Pacific on southern African circulation. In Experiment 8, the model is forced with SST anomalies as in Experiment 3 but with the SST anomalies elsewhere in the equatorial Pacific included (Figure 3.1**g**). This chapter examines the model's response over southern Africa to Benguela Niño SST anomalies when there are also La Niña (cool) SST anomalies in the equatorial Pacific). Therefore, this chapter will try to answer the fourth question in chapter 1 and the results from Experiments 7 and 8 are presented in section 7.2. The summary and the conclusion are presented in section 7.3.

7.2 Possible Influence of La Niña

Figure 7.1 shows the model's response to the SST anomalies displayed in Figure 3.1**f**. When forced with these anomalies, the model generates positive rainfall anomalies over eastern Africa and parts of West Africa but reduced rainfall over subtropical southern Africa, Angola and central Africa (Figure 7.1**a**). These results are consistent with the findings of Nicholson and Selato (2000). In a study of the influence of La Niña on Africa rainfall using harmonic analysis, the above authors found that weak positive rainfall anomalies appear in the December-February season over most parts of the eastern half of southern Africa during most La Niña events. Similarly, Reason *et al.* (2000) found that increased rainfall tended to occur over southeastern Africa during the January-March season following the first appearance of cool SST anomalies in the equatorial Pacific (the mature phase).

The results shown in Figure 7.1**a** are consistent with the general observation that a La Niña event generates above average rainfall over southeastern Africa. However, dry conditions are produced over subtropical southern Africa and Angola Positive rainfall anomalies over Tanzania, Zambia and Kenya appear to be as a result of increased low-level moisture convergence (Figure 7.1**d**) and enhanced uplift (Figure 7.1**b**). These results are consistent with the observed links between SST in the equatorial Pacific Ocean and southern African circulation via modulations to the Walker circulation. The cool SST anomalies in the equatorial Pacific are typically associated with an enhanced strength of the equatorial Walker circulation (Allan *et al.*, 1996)

The southeasterly moisture flux anomalies over the subtropical southwest Indian Ocean (SWIO) (Figure 7.1**c**) act to strengthen the climatological westwards flux of Indian Ocean sourced moisture across subtropical southern Africa whereas the westerly anomalies over central southern Africa appear to weaken the mean southeasterly moisture flux away from Africa over the southeast Atlantic, thus leading to low level moisture convergence over Zambia, northern Mozambique and Tanzania with increased rainfall there.

Dry conditions over subtropical southern Africa seem to be as a result of enhanced subsidence and relatively weak moisture convergence. It is not obvious how SST forcing in the central equatorial Pacific can produce the rainfall anomalies in this region in this experiment. Note that similar anomalies are seen in previous experiments which do not include the forcing in the Pacific Ocean. However, weak anomalies over parts of West Africa seem to suggest a lack of influence of SST in the central equatorial Pacific on this region consistent with the finding of Ropelewski and Halpert (1989) for La Niña and the findings of Ropelewski and Halpert (1989) and Nicholson and Kim (1997) for El Niño events. Note that the model generates statistically significant rainfall anomalies over eastern South Africa, central Tanzania and the western equatorial Indian Ocean.

When the forcing in the southeast tropical Atlantic Ocean is included (Experiment 8, Figure 3.1**g**), the model generates statistically significant positive rainfall anomalies near the SST forcing in the southeast tropical Atlantic Ocean, and over eastern Angola

extending northeastward to northern Zambia and central Tanzania (Figure 7.2**a**). Statistically significant negative anomalies are generated over eastern South Africa, central Angola and Congo-Brazzaville. Rainfall anomalies generated in Experiment 8 are similar to Experiment 7 except that anomalous rainfall is generated over the tropical western Indian Ocean, and also over the Angolan coast as result of the SST forcing included just off that coast. An examination of rainfall anomalies in Experiments 3 (Figure 5.1**a**), 7 (Figure 7.1**a**) and 8 (Figure 7.2**a**) low-level moisture flux anomalies (Figure 5.1**e**, Figure 7.1**c** and Figure 7.2**c** respectively), reveals that, the La Niña signal seems to dominate the Benguela Niño signal over southern Africa. Note that the SST forcing in the southeast tropical Atlantic Ocean in Experiment 3 is similar to that in Experiment 8 in this region.

The positive rainfall anomalies of about 0.5 mm/day over Tanzania in Experiment 7 extend southwestward over Zambia in Experiment 8, while the negative anomalies of a similar magnitude over Angola and South Africa are now smaller in spatial extent. These results seem to suggest that when a Benguela Niño event occurs together with a La Niña event, the positive rainfall anomalies over Zambia and the western Indian Ocean are increased. In other words, the influence of a La Niña event in the equatorial Pacific on southern African circulation tends to dominate the influence from Benguela Niño event. This confirms the finding of Nicholson and Selato (2000) that La Niña appears to have the greatest influence on rainfall in southern Africa. Furthermore, AGCM studies with SST in the Pacific and Indian Ocean (Goddard and Graham, 1999, Washington and Preston, 2006) show that SST variability in the tropical Pacific exerts some influence over the African region.

The reduction in spatial extent of the negative rainfall anomalies over Angola and South Africa in Experiment 8, seem to suggest that a Benguela Niño opposes the influence of a La Niña over these regions. Compared to Experiment 3, negative rainfall anomalies are generated over equatorial western Africa in Experiment 8. Again, the strong La Niña signal seems to outweigh the Benguela Niño signal here.

The model generates similar low-level moisture flux anomalies over subtropical southern Africa in Experiments 7 (Figure 7.1**c**) and 8 (Figure 7.2**c**). Over eastern Africa, the

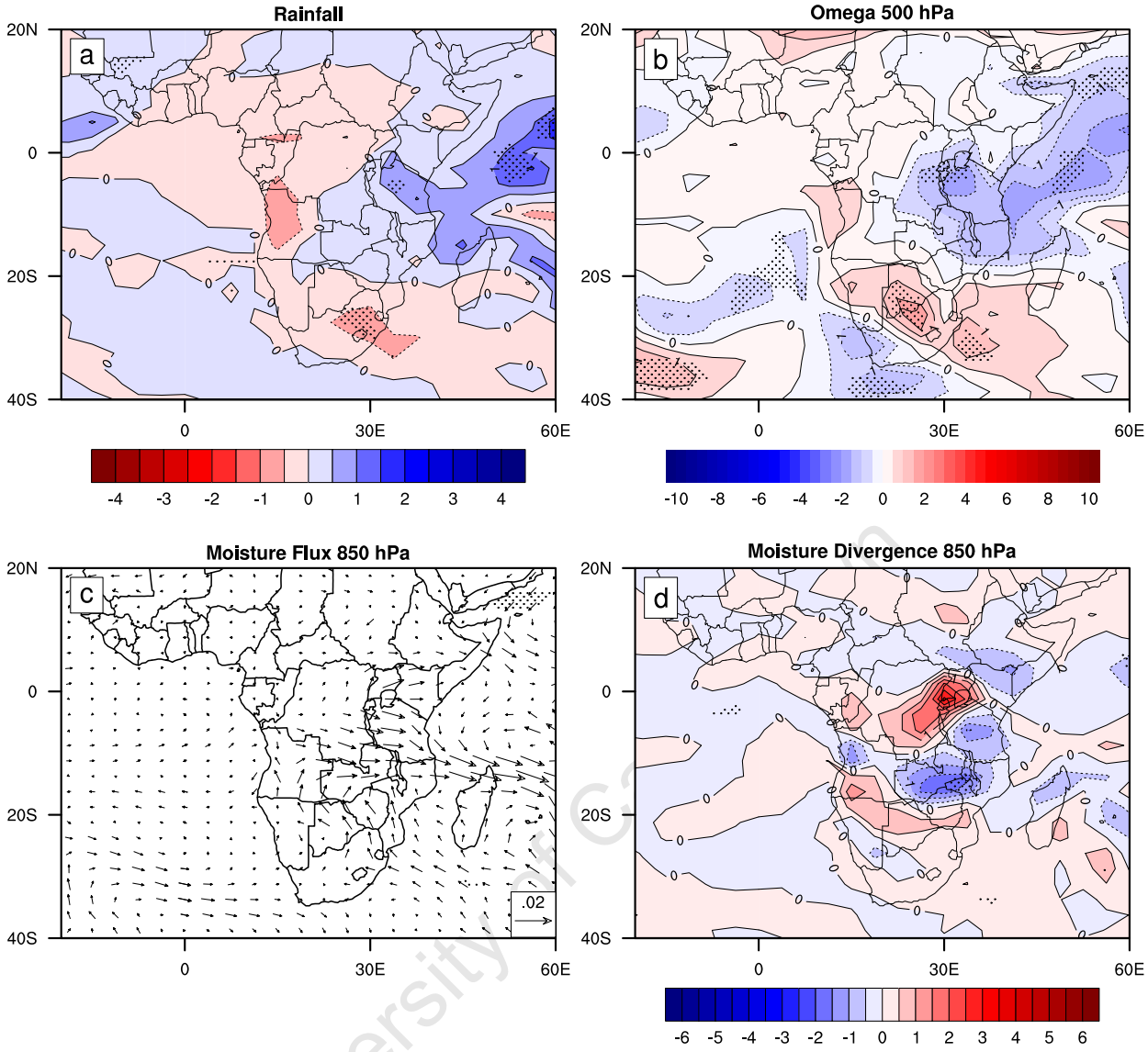

Figure 7.1: Experiment 7 anomalies: (**a**) Rainfall 0.5 *mm/day* contour interval, (**b**) Omega 500 hPa, (**c**) Moisture flux 850 hPa, (**d**) 850 hPa Moisture divergence. Stippled regions indicate statistically significant differences at 90% level.

westerly anomalies act to weaken the predominantly westerly moisture flux away from East Africa over the equatorial Indian Ocean. As a result, there is enhanced low-level moisture convergence over Tanzania (Figures 7.1**d** and 7.2**d**) in both experiments. The strong La Niña signal over southern Africa is observed also in the moisture flux field. However, there are noticeable differences in the cyclonic low-level moisture flux anomaly over Madagascar in Experiment 7 and 8. This anomaly is oriented in the in east-west direction in Experiment 8 and is located over northern Madagascar similar to Experiment 3, though it is weaker in Experiment 8. Here, the Benguela Niño signal appears to be

stronger than La Niña signal. This result suggests that cool SST anomalies in the central equatorial Pacific, when accompanying a Benguela Niño event, tend to weaken the influence that SST anomalies in the southeast tropical Atlantic have on the circulation southeast of Madagascar and its wider connection via modulation to the standing waves in the Southern Hemisphere (refer to earlier figure and Section here where these standing waves are first discussed).

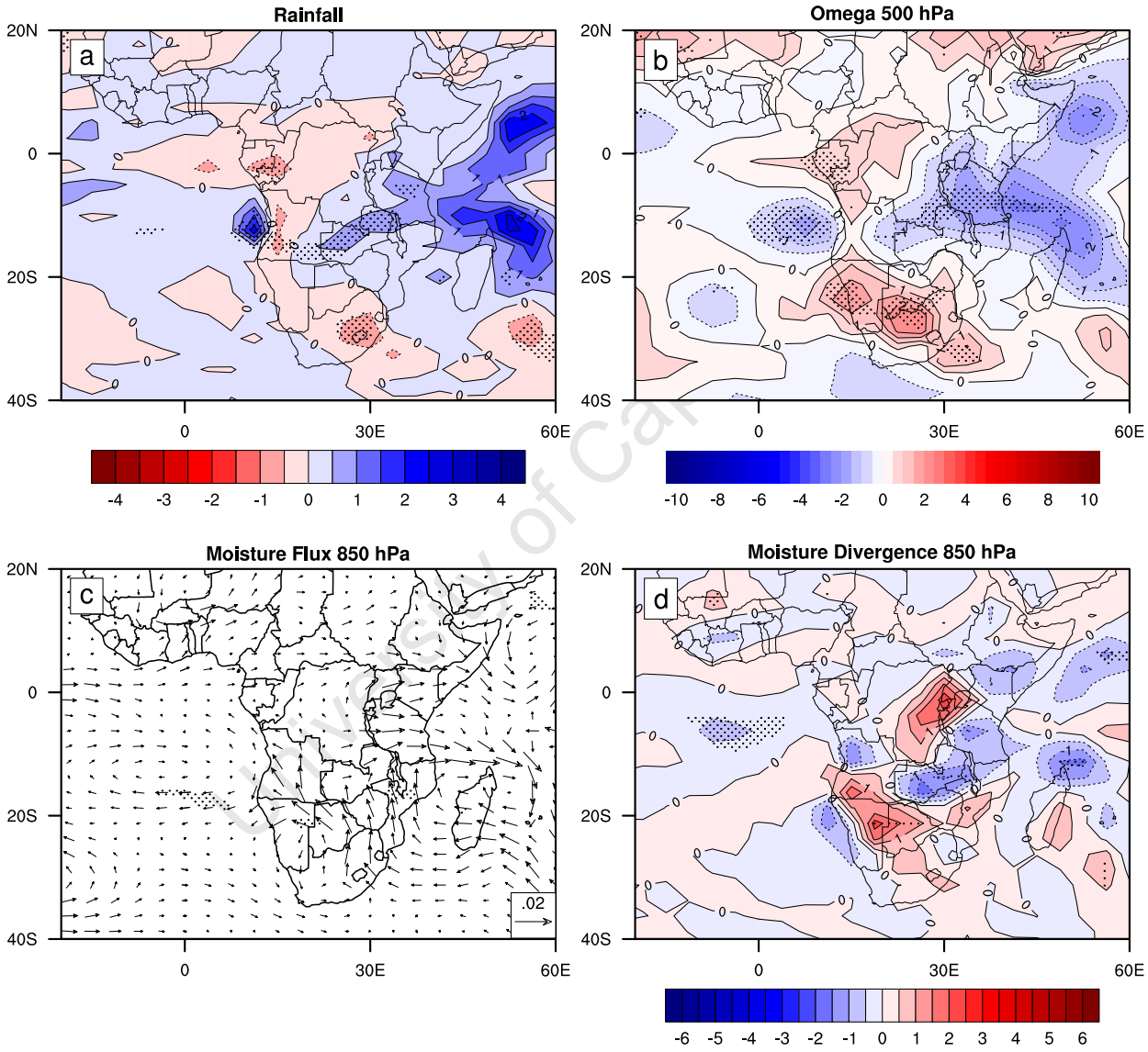

Figure 7.2: Same as Figure 7.1 but for Experiment 8.

7.3 Summary and Conclusion

This chapter set out to see how the presence of cool SST anomalies in the central equatorial Pacific Ocean that occur during a Benguela Niño event could influence the resulting rainfall and circulation over southern Africa. Results of two sets of SST anomaly experiments, Experiments 7 and 8, performed with the HadAM3 GCM have been presented. These experiments have been motivated by an observed La Niña cooling in the equatorial Pacific during the 2001 Benguela Niño event. In Experiment 7, the model was forced with an idealised pattern of negative SST anomalies in the central equatorial Pacific only and no other SST anomalies were present anywhere. The forcing has a magnitude of about -2°C and is centred over the equator around 160°W (Figure 3.1**f**). Experiment 8 involved forcing the model with idealised positive and negative SST anomalies in the southeast tropical Atlantic and the central equatorial Pacific Oceans respectively. The forcing in the central Pacific Ocean is similar to Experiment 7 while the forcing in the southeast tropical Atlantic is centred around 12°E, 17°S and has a magnitude of about 4°C (Figure 3.1**g**).

The model's response to the SST forcing in Experiment 7 consists of positive rainfall anomalies over eastern southern Africa. This result is consistent with the findings of Nicholson and Selato (2000) who found that weak positive rainfall anomalies appear in the December-February season over most parts of the eastern half of southern Africa during most La Niña events. A similar result was found by Reason *et al.* (2000) for the late summer. The model results show that the positive rainfall anomalies over eastern Africa are associated with enhanced low-level moisture convergence and uplift. The southeasterly anomalies over the southwest subtropical Indian Ocean act to strengthen the climatological westwards flux of Indian Ocean sourced moisture across subtropical southern Africa while the westerly anomalies over central southern Africa appear to weaken the mean southeasterly moisture flux away from southern Africa over the Southeast Atlantic Ocean.

Negative rainfall anomalies are generated over South Africa and the western southern Africa. These anomalies are associated with enhanced subsidence over these regions and relatively weak low-level moisture convergence.

The model's rainfall response to the SST forcing in Experiment 8 is similar to Experiment 7 except that greater anomalous rainfall is generated over the tropical Indian Ocean in Experiment 8. Also, positive rainfall anomalies of about 0.5 mm/day over Tanzania extend further southwest over Zambia in Experiment 8. These results suggest that the La Niña signal tends to dominate the Benguela Niño signal over southern Africa when these events occur simultaneously. Differences in moisture flux anomalies between Experiment 7 and 8 are noticeable over Madagascar. The cyclonic low-level moisture flux anomaly over Madagascar is slightly shifted northward similar to Experiment 3 which involved a similar SST forcing only in the southeast Atlantic. This result suggests that the Benguela Niño signal may dominate the La Niña signal in the southwest subtropical Indian Ocean. Goddard and Graham (1999) and Washington and Preston (2006) have also shown that while the SST variability of the tropical Pacific exerts some influence over the African region, it is the atmospheric response to the Indian Ocean variability that is essential for simulating the correct rainfall response over eastern, central, and southern Africa.

Chapter 8

Summary and Conclusion

Southern Africa exhibits strong variability on interannual and interdecadal time-scales which is usually linked to SST variations in the neighbouring and remote oceans. Much research on southern African climate variability has concentrated on influence from ENSO and the Indian Ocean, because it is believed that they exert more influence over southern Africa than the Atlantic Ocean. Although the ENSO phenomenon in the Pacific has profound impact on global weather patterns, not all anomalous patterns are linked to it and it has become increasingly clear that other modes of climate variation besides ENSO can have significant influence on regional climate (Chang *et al.*, 1998). Among them is a variation of SST in the tropical Atlantic Ocean. Extreme warm SSTs have been observed in the area of the Angola-Benguela Front in the southeast tropical Atlantic and Shannon *et al.* (1986) have termed these warm events 'Benguela Niños' because of their apparent similarities with El Niño events.

This thesis set out to investigate the impacts of the Benguela Niño on rainfall over southern Africa. In order to achieve the above objective, the following questions were posed.

1. What is the effect of warm SST anomaly intensity in the southeast Atlantic Ocean on southern African late summer circulation, independent of warming or cooling in the Indian Ocean?

2. What is the rainfall and circulation response over southern Africa when there are warm or cool SST anomalies in the southwest Indian Ocean in addition to a Benguela Niño event?

3. How does the location of anomalous warming of SST in the tropical southeast Atlantic Ocean influence the atmospheric response over southern Africa?

4. What is the rainfall and circulation response over southern Africa when there is a La Niña event in the Pacific occuring at the same time as a Benguela Niño?

The main tool used to address these questions is the United Kingdom Met Office (UKMO) Hadley Centre Atmospheric Model version 3 (HadAM3) general circulation model. HadAM3 is a grid-point numerical model and has been used in various African studies, for example, in investigating intraseasonal (Tennant, 2003) or interannual (Reason and Jagadheesha, 2005a,b) variability, and in sensitivity studies (Washington and Preston, 2006) as well as for operational seasonal forecasting. The ability of this model to adequately represent the climate of the southern African region was evaluated by comparing geographical maps and zonally averaged statistics of the model climatology used in Reason and Jagadheesha (2005a,b) with NCEP-NCAR reanalyses and CMAP precipitation. The emphasis was given to the February April (FMA) season since this is the main rainy season in the Angolan area of most interest to this study and previous studies have already shown that the model represents the main circulation during winter (June August) (Reason *et al.*, 2003) and summer (December February) (Reason *et al.*, 2005) adequately.

HadAM3 is able to reproduce the precipitation annual cycle and the main seasonal global climatological features of the circulation. Precipitation bands associated with the ITCZ are depicted well by the model, though the model overestimates these features over the ocean. Precipitation within the tropics is simulated reasonably well, but precipitation in the extra-tropics in both hemispheres is overestimated. The model also shows some skill in capturing regional scale feature, important for rainfall, over southern Africa, although it appears to misplace and underestimate them. The model shows less skill in simulating

lower and upper level tropospheric wind direction correctly over southern Africa, therefore this field must be interpreted with caution.

These results show that there is generally reasonable agreement of the FMA climatology between NCEP-NCAR reanalysis and HadAM3. In addition to the above results, results from Johns *et al.* (1997), Reason *et al.* (2003), Reason and Jagadheesha (2005a) and Washington and Preston (2006), there is some confidence in the ability of this model to represent the climate of southern Africa reasonably well and therefore it was used in this thesis to perform sensitivity experiments.

A set of ten experiments of various idealised SST anomalies was designed to attempt to answer the above questions. Each experiment consisted of five ensemble members (computational resources did not permit the use a larger ensemble size). Three experiments, namely, Experiments 2, 3 and 6 were designed to address the first and third questions posed in **chapter 1** and therefore consist of the forcing only in the southeast tropical Atlantic Ocean. In Experiment 2 HadAM3 was forced with positive SST anomalies, about 6°C, centred around 12°E, 17°S (Figure 3.1**a**). In Experiment 3, the forcing is similar to Experiment 2 except it is weaker, about 4°C, and less extensive (Figure 3.1**b**). Experiment 6 is similar to Experiment 2 except the forcing is slightly shifted northward (12°E, 15°S) (Figure 3.1**e**). Experiment 1 is a control run and is a base against which all other experiments were compared.

The model's response to the SST anomaly forcing in the tropical southeast Atlantic Ocean consists of positive rainfall anomalies over western Angola and near the SST forcing. These anomalies are associated with enhanced surface latent heat flux over the SST forcing and uplift near the SST forcing in the tropical southeast Atlantic Ocean. Positive anomalies in low level moisture divergence suggest that the enhanced surface latent heat flux and local uplift contribute more to the positive rainfall anomalies over western Angola and the SST forcing than do changes in moisture convergence. The enhanced uplift over this region favours stronger convective rainfall. Circulation changes over southern Africa resulting from the SST forcing in the southeast tropical suggest that Benguela Niño events tend to suppress tropical-temperate trough activities.

The model results suggest that a Benguela Niño is capable of forcing anomalous wet conditions over western Angola on its own. However, it is less clear as to how influential it is on the rainfall further inland. The resulting changes in the atmospheric circulation lead to changes in low level moisture convergence and uplift over Zambia and eastern Africa that appear to contribute to positive rainfall anomalies there. Therefore, this suggests that a Benguela Niño is capable of influencing anomalous rainfall both over western Angola and much further inland when the intensity is increased.

Widespread weak positive rainfall anomalies are generated over southern Africa when the maximum SST anomalies are located further north in the South East Atlantic. Stronger positive anomalies are produced over western Angola and near the SST forcing. Consistent with observational studies (Harangozo and Harrison, 1983, Rouault *et al.*, 2003), these model results imply that the western Angola region is susceptible to flood events during Benguela Niño. Since the onset of these events is typically around December/January, monitoring the tropical southeast Atlantic Ocean could provide an early warning system that could be beneficial to the Angolan economy.

In Experiments 4, 5, 9 and 10 the model was forced with idealised SST anomalies in the tropical southeast Atlantic and subtropical southwest Indian Oceans. These experiments were designed to address the second question. The forcing in Experiment 4 consists of a positive SST anomaly in the tropical southeast Atlantic, same as in Experiment 2, and a negative SST anomaly in the SWIO, of up to 2°C in magnitude and is centred around 50°E, 35°S. In Experiment 5, the forcing in the tropical southeast Atlantic is same as in Experiment 3 and the forcing in the SWIO is same as in Experiment 4 except it is positive. The forcing in Experiment 9 consists of a positive SST anomaly in the tropical southeast Atlantic same as in Experiment 6 and a positive anomaly in the SWIO same as in Experiment 5. In Experiment the forcing is same as in Experiment 9 except the SWIO forcing is closer to the subcontinent.

Relatively reduced positive rainfall anomalies are produced over the Mozambique/Tanzania border (Figure 6.1**a**) while negative anomalies are generated over eastern South Africa,

when the model is forced with SST anomalies in Experiment 4 (Figure 3.1**c**). The cyclonic low-level moisture flux anomaly (Figure 6.1**c**) centred over the southern Mozambique Channel advects cool and less moist air over South Africa as a result of reduced evaporation south of Madagascar due to reduced surface latent heat flux in the subtropical SWIO. Consistent with observations of Behera and Yamagata (2001), reduced rainfall may be generated over southern Africa during a Benguela Niño event when there is cooling in the SWIO.

When forced with SST anomalies of Experiments 5, 9 and 10, the model produces positive rainfall anomalies over southern Africa similar to experiment 4, except these are widespread in Experiments 9 and 10. The model generates more widespread positive rainfall anomalies over southern Africa in Experiment 10 (Figure 6.4**a**) in which the forcing in the southwest subtropical Indian Ocean is closer to the subcontinent.

Taken together, the results of Experiments 4, 5, 9 and 10 suggest that, depending on their sign and location, SST forcing in the SWIO may augment or oppose the rainfall impacts over southern Africa during a Benguela Niño event. For both the SWIO and southeast Atlantic SST anomalies, a more tropically located pattern tends to produce a larger response in the model.

Finally, Experiments 7 and 8 were designed to address the fourth question. The forcing in Experiment 7 consisted of negative SST anomalies of up to -2°C centred on the equator around 160°W in the central Pacific Ocean. In Experiment 8, the model was forced with positive SST anomalies in the tropical southeast Atlantic, same as in Experiment 3 and negative SST anomalies in the equatorial central Pacific Ocean same as in Experiment 7.

The model's response to the SST forcing in Experiment 7 consists of positive rainfall anomalies over eastern southern Africa. This result is consistent with the general observations and findings of Nicholson and Selato (2000) that weak positive rainfall anomalies appear in the December-February season over most parts of the eastern half of southern Africa during most La Niña events. When forced with SST of Experiment 8, the model generates rainfall anomalies similar to Experiment 7 except that anomalous rainfall is generated over the southwest tropical Indian in Experiment 8. These results suggest that the

La Niña signal dominates the Benguela Niño signal over southern Africa with these events occur simultaneously. Goddard and Graham (1999) and Washington and Preston (2006) have also shown that the SST variability of the tropical Pacific exerts some influence over the African region.

This study has only considered seasonal anomalies for model experiments without ocean-atmosphere interactions. The issue of whether regional SST anomalies, with ocean/atmosphere feedback, lead to changes in the frequency or intensity of dry and wet spells during the summer rainy season, or in the onset and cessation dates of this season have not been considered. Another caveat in this study is course resolution at which of the model is run. The resolution used cannot represent all small-scale features.

These factors are very important for the agriculture-driven economy of most of the countries in the region (Usman and Reason, 2004, Tadross *et al.*, 2005, Reason *et al.*, 2005, Hachigonta and Reason, 2006). Therefore, there is considerable motivation for a better understanding of the relationships between southern African rainfall variability and regional SST forcing.

References

Allan, R., Lindsay, J., and Parker, D., *El Niño Southern Oscillation and Climate Variability* (CSIRO, Australia, 1996).

Arnault, S., Chouaib, N., Diverrés, D., Jacquin, S., and Coze, O., 2004: Comparison of Topex/Posedon and Jason Altimery with ARAMIS In Situ Observations in the Tropical Atlantic Ocean. *Marine Geodesy*, **27**, 15–30.

Behera, S. K. and Yamagata, T., 2001: Subtropical SST dipole events in the southern Indian Ocean. *Geophys. Res. Lett.*, **28**, 327–330.

Biasutti, M., Battisti, D. S., and Sarachik, E. S., 2004: Mechanisms Controlling the Annul Cycle of Precipitaion in the Tropical Atlantic Sector in an Atmospheric GCM. *J. Climate*, **17**, 4708–4723.

Bitan, A. and Sa'aroni, H., 1992: The Horizontal and Vertical Extension of the Persian Gulf Pressure Trough. *Int. J. Climatol.*, **12**, 495–522.

Blake, D. W., Krishnamurti, T. N., Low-Nam, S. V., and Fein, J. S., 1983: Heat low over the Saudi Arabian desert during May 1979 (Summer MONEX). *Mon. Weather Rev.*, **111**, 1759–1775.

Blanke, B., Roy, C., Penven, P., Speich, S., McWilliams, J., and Nelson, G., 2002: Assessing Wind Contribution to the Southern Bengula Interannual Dynamics. *Globec Int. Newslett.*, **8**, 15–18.

Boyer, D., Cole, J., and Bartholomae, C., 2000: Southwestern Africa: Northern Benguela Current Region. *Marine Pollution Bull.*, **41**, 123–140.

Busalacchi, J., 1998: CLIVAR Related Research in the Tropical Atlantic. *Clivar Exchanges*, **8**.

Busuioc, A., von Storch, H., and Schnur, R., 1999a: Verification of GCM generated regional seasonal precipitation for current climate and of statistical downscaling estimates under changing climate conditions. *J. Climate*, **12**, 258–272.

Cavalcanti, I. F. A., Marengo, J. A., Satyamurty, P., Nobre, C. A., Trosnikov, I., Bonatti, J. P., Manzi, A. O., Tarasova, T., Pezzi, L. P., D'Almeida, C., Sampaio, G., Castro, C. C., Sanches, M. B., and Camargo, H., 2002: Global Climatological Features in a Simulation using the CPEC-COLA AGCM. *J. Climate*, **15**, 2965–2988.

Chang, P., Penland, C., Ji, L., Li, H., and Matrasova, L., 1998: Predicting Decadal Sea Surface Temperature Variability in the Tropical Atlantic Ocean. *Geophy. Res. Lett.*, **25**, 1193–1196.

Chervin, R. M. and Schneider, S., 1976: On determining the statistical significance of climate experiments with general circulation models. *J. Atmos. Sci.*, **33**, 405–412.

Chervin, R. M., Washington, W. H., and Schneider, S., 1976: Testing the Statistical Significance of the Response of the NCAR General Circulation Model to North Pacific Ocean Surface Temperature Anomalies. *J. Atmos. Sci.*, **33**, 413–423.

Colberg, F. and Reason, C. J. C., 2006: A Model Study of the Angola Benguela Frontal Zone: Sensitivity to Atmospheric Forcing. *Geophys. Res. Lett.*, **33**, L19608.

Colberg, F., Reason, C. J. C., and Rodgers, K., 2004: South Atlantic Response to El Niño Southern Oscillation Induced Climate Variability in an Ocean General Circulation Model. *J. Geophys. Res.*, **109**, C12015.

Cook, K. H., 2000: The South Indian Convergence Zone and Interannual Rainfall Variability over Southern Africa. *J. Climate*, **13**, 3789–3804.

Cox, P. M., Betts, R. A., Bunton, C. B., Essery, R. L. H., Rowntree, P. R., and Smith, J., 1999: The Impact of New Land Surface Physics on the GCM Simulation of Climate and Climate Sensitivity. *Climate Dynamics*, **14**, 183–203.

Crimp, S. J., Lutjeharms, J. R. E., and Mason, S. J., 1998: Sensitivity of a Tropical Temperate Trough to Sea Surface Temperature Anomalies in the Agulhas Retroflection Region. *Water SA.*, **24**, 93–100.

Crimp, S. J., van den Heever, S. C., D'Abreton, P. C., Tyson, P. D., and Mason, S. J., 1997: Mesoscale Modelling of Tropical-Temperate Troughs and Associated Systems over Southern Africa, Technical Report 595, WRC.

Cubasch, U., von Storch, H., Waskewitz, J., and Zorita, E., 1996: Estimate of climate change in Southern Europe using different downscaling techniques. *Clim. Res.*, **7**, 129–149.

Currie, B., Barthoamae, C., and Noli-Peard, K., 2002: Warm water events in the Northern Benguela: A local perspective. *Investig. Mar.*, **30**, 81–82.

De Witt, S., 1998: *Getting started*, Unified Model User Guide (sec 4.2.5), Meteorological Office, United Kingdom, met office edition.

Deardroff, J. W., 1976: Usefulness of Liquid-Water Potential Temperature in a Shallow-Cloud Model. *J. App. Meteorol.*, **15**, 98–102.

Delecluse, P. J., Servain, J., Levy, C., Arpe, K., and Bengsston, L., 1994: On the Connection between the 1984 Warm Event and the 1982-1983 ENSO. *Tellus*, **46a**, 448–464.

Dommenget, D. and Latif, M., 2000: Interannual to Decadal Variability in the Tropical Atlantic. *J. Climate*, **13**, 777–792.

Dyson, L. L. and van Heerden, J., 2002: A Model for the Identification of Tropical Weather Systems over South Africa. *Water SA.*, **28**, 249–258.

Edwards, J. M. and Slingo, A., 1996: Studies with a Flexible New Radiation Code. I: Choosing a Configuration for a Large-Scale Model. *Q. J. R. Meteorol. Soc.*, **122**, 689–719.

Enfield, D. B., 1996: Relationships of Inter-American Rainfall to Tropical Atlantic and Pacific SST Variability. *Geophys. Res. Lett.*, **23**, 3305–3308.

Enfield, D. B. and Mayer, D. A., 1997: Tropical Atlantic SST Variability and its Relation ot El Niño-Southern Oscillation. *J. Geophys. Res.*, **102**, 929–945.

Fauchereau, N., Trzaska, S., Richard, Y., Roucou, P., and Camberlin, P., 2003: Sea Surface Temperature Co-variability in the Southern Atlantic and Indian Oceans and its Connections with the Atmospheric Circulation in the Southern Hemisphere. *Int. J. Climatol.*, **23**, 663–677.

Florenchie, P., Lutjeharms, J. R. E., Reason, C. J. C., Mason, S., and Rouault, M., 2003: The Source of Benguela Niños in the South Atlantic Ocean. *Geophys. Res. Lett.*, **30**, 10.1029.

Florenchie, P., Reason, C. J. C., Lutjeharms, J. R. E., Rouault, M., Roy, C., and Masson, S., 2004: Evolution of interannual warm and cold events in the Southeast Atlantic Ocean. *J. Climate*, **17**, 2318–2334.

Folland, C. K., Palmer, T., and Parker, D., 1986: Shael rainfall and worldwide sea temperatures: 1905-85. *Nature*, **320**, 602–606.

Garzoli, S. L., Gordon, A. L., Kamenkovich, V., Pillsbury, D., and Duncombe-Rae, C., 1996: Variability and Source of the Southeastern Atlantic Circulation. *J. Marine Res.*, **54**, 1039–1071.

Gates, W. L., 1992: AMIP: The Atmospheric Model Intercomparison Project. *Bull. Amer. Meteor. Soc.*, **73**, 1962–1970.

Gates, W. L. and Coauthors, 1999: An overview of the results of the Atmospheric Model Intercomparison Project (AMIP). *Bull. Amer. Meteor. Soc.*, **80**, 29–55.

Goddard, L. and Graham, N. E., 1999: The importance of the Indian Ocean for simulating precipitation over eastern and southern Africa. *J. Geophys. Res.*, **104**, 19099–19116.

Goddard Institute for Space Studies - GISS, 1999: Global Climage Modeling, `http://www.giss.nasa.gov/research/modeling/gcm.html`, accessed 8 November, 2006.

Gregory, D., 1995: A consistent treatment of evaportation of rain and snow in large scale models. *Mon. Wea. Rev.*, **123**, 2716–2732.

Gregory, D. and Rowntree, P. R., 1990: A mass flux convection scheme with representation of cloud ensemble characteristics and stability-dependent closure. *Mon. Wea. Rev.*, **118**, 1483–1506.

Gregory, D. and Shutts, G. J., 1998: A new gravity-wave-drag scheme incorporating anisotropic orography and low-level wave breaking: impact upon the climate of the UK Meteorolgical Office Unified Model. *J. R. Meteorol.*, **124**, 463–494.

Haarsma, R. J., Campos, E. J. D., Hazeleger, W., Severijns, C., Piola, A. R., and Molteni, F., 2005: Dominant modes of variability in the south Atlantic: A study with a hierarchy of ocean-atmosphere models. *J. Climate*, **18**, 1719–1735.

Haarsma, R. J., Campos, E. J. D., and Molteni, F., 2003: Atmospheric response to South Atlantic SST dipole. *Geophys. Res. Lett.*, **30**, 1864 doi:10.11029/2003GL017829.

Hachigonta, S. and Reason, C. J. C., 2006: Interannual Variability in Dry and Wet Spell Characteristics over Zambia. *Clim. Res.*, **32**, 49–62.

Hansingo, K. and Reason, C. J. C., 2006: Sensitivity of the atmospheric response to sea-surface temperature forcing in the South West Indian Ocean: a regional climate modeling study. *S. Afri. J. Sci.*, **102**, 137–143.

Harangozo, S. and Harrison, M. S. J., 1983: On the use of synoptic data in indicating the presence of clould bands over southern Africa. *S. Afr. J. Sci.*, **79**, 413–414.

Hardman-Mountford, N. J., Richardson, A. J., Agendbag, J. J., Hagen, E., Nykjaer, L., Shillington, F., and Villacastin, C., 2003: Ocean climate of the south East Atlantic observed from satellite data and wind models. *Prog. Oceanog.*, **59**, 181–221.

Harrison, M. S. J., 1986: *A synoptic climatology of South African rainfall variations*, Ph.D. thesis, University of Witswatersrand.

Hart, T. L., 1990: Estimates of horizontal divergence and vertical velocity over northern Australia, and implications for biogeeophysical feedback. *Aus. Meteorol. Mag.*, **38**, 107–122.

Harzallah, A., Rocha De Aragao, J. O., and Sadourny, R., 1996: Interannual rainfall variability in North-East Brazil: Observation and model simulation. *Int. J. Climatol.*, **16**, 861–878.

Hermes, J. C. and Reason, C. J. C., 2005: An ocean model diagnosis of coevolving SST variability in the South Atlantic and South Indian Oceans. *J. Climate*, **18**, 2864–2882.

Hickey, H. and Weaver, A. J., 2004: The southern Ocean as a source region for tropical Atlantic variability. *J. Climate*, **17**, 3960–3972.

Hirst, A. C. and Hastenrath, S., 1983: Atmosphere-ocean mechanisms of climate anomalies in he Angol-tropical sector. *J. Phys. Oceanog.*

Hoerling, M. P., Kumar, A., and Xu, T., 2001: Robustness of the Nonlinear Climate Response to ENSO's Extreme Phases. *J. Climate*, **14**, 1277–1293.

Houghton, R. W. and Tourre, Y. M., 1992: Characteristics of low-frequency sea surface temperature fluctuations in the tropical Atlantic. *J. Climate*, **5**, 765–771.

Huang, B., 2004: Remotely forced variability in the tropical Atlantic Ocean. *Climate. Dynamics.*, **23**, 133–152.

Huang, B. and Shukla, J., 1997: Characteristics of the interannual and decadal variability in a general circulation model of the tropical Atlantic Ocean. *J. Phys. Oceanogr.*, **27**, 1693–1712.

Huang, B. and Shukla, J., 2005: Ocean-Atmosphere interactions in the tropical and subtropical Atlantic Ocean. *J. Climate*, **18**, 1652–1672.

Hulme, M., Validation of large-scale precipitation fields in General Circulation Models, *Global Precipitation and Climate Change*, (Editors) M. Desbois and F. Desalmand (Springer-Verlag, 1994), 387–405.

Hurrell, J. W., Hack, J. J., Boville, B. A., Williamson, D. L., and Kiehl, J. T., 1998: The dynamical simulation of the NCAR community climate model version 3 (CCM3). *J. Climate*, **11**, 1207–1236.

Johns, T. C., Carnell, R. E., Crossley, J. F., Gregory, J. M., Mitchell, J. B., Senior, C. A., Tett, S. B., and Wood, R. A., 1997: The second Hadley centre coupled ocean-atmosphere GCM: Model description, spin up and validation. *Clim. Dyn.*, **13**, 103–134.

Joshi, P. C. and Desai, P. S., 1985: The satellite-determined thermal structure of heat lows during Indian south-west monsoon season. *Adv. Space Res.*, **5**, 57–60.

Jury, M. R., 1996: Regional teleconnection patterns associated with summer rainfall over South Africa, Namibia and Zimbabwe. *Int. J. Climatol.*, **16**, 135–153.

Jury, M. R. and Lindesay, J. A., 1991: Atmospheric circulation controls and characteristics of a flood event in central South Africa. *J. Climatol.*, **11**, 609–627.

Kalnay, E. M., Kistler, R., Collins, W., Deaven, D., Gandin, L., Iredell, M., Saha, S., White, G., Woollen, J., Zhu, Y., Chelliah, M., Ebisuzaki, W., Higgins, W., Janowiak, J., Mo, K. C., Ropelewski, C., Wang, J., Leetmaa, A., Reynolds, R., Jenne, R., and Joseph, D., 1996: The NCEP/NCAR 40-Year Reanalysis Project. *Bull. Amer. Meteor. Soc.*, **77**, 437–471.

Kandiano, E., Bauch, H., and Muller, A., 2004: Sea Surface Temperature Variability in the North Atlantic during the last two glacial-interglacial cycles: comparison of faunal, oxygen isotopic, and Mg/Ca-derived records. *Palaeogeography Palaeoclimatology Palaeoecology*, **204**, 145–164.

Kharin, V. V., 1995: The relationship between sea surface temperature anomalies and atmospheric circulation is GCM experiments. *Clim. Dyn.*, **11**, 359–375.

Kim, J. H. and Schneider, R. R., 2003: Low-latitude control of inter-hemispheric sea surface temperature contrast in the tropical Atlantic over the past 21 kyears: the possible role of SE trade winds. *Clim. Dyn.*, **21**, 337–347.

Kim, J. H., Schneider, R. R., Müller, P. J., and Wefer, G., 2002: Interhemispheric comparison of deglacial sea-surface temperature patterns in Atlantic eastern boundary currents. *Earth Sci. Planetary Sci. Lett.*, **194**, 383–393.

Latif, M. and Barnett, T. P., 1995: Interactions of the tropical oceans. *J. Climate*, **8**, 952–964.

Latif, M. and Grötzner, A., 2000: The equatorial Atlantic oscillation and its response to ENSO. *Clim. Dyn.*, **16**, 213–218.

Lean, J. and Rowntree, P. R., 1997: Understanding the sensitivity of a GCM simulation of Amazonian Deforestation to the specification of vegetation and soil characteristics. *J. Climate*, **10**, 1216–1235.

Leighton, R. and Deslandes, R., 1991: Monthly anticyclonicity and cyclonicity in the Australian region: 23-year averages., Technical report, Bureau of Meteorology, Bureau of Meteorology P.O Box 1289K, Melbourne, Australia, 3001.

Li, D. and Shine, K. P., 1995: A 4-dimensional ozone climatology for UGAMP models, Technical Report 35, UGAMP.

Lindesay, J. A., 1988: South African rainfall, the Southern Oscillation and Southern Hemisphere semi-annual cycle. *Int. J. Climatol.*, **8**, 17–30.

Lindesay, J. A., Harrison, M. S. J., and Haffner, M. P., 1986: The Southern Oscillation and South African rainfall. *S. Afr. J. Sci.*, **82**, 196–198.

Livezey, R. E., 1985: Statistical Analysis of General Circulation Model Climate Simulation, Sensitivity and Prediction Experiments. *J. Atmos. Sci.*, **42**, 1139–1149.

Lough, J. M., 1986: Tropical Atlantic sea surface temperatures and rainfall variatios in sub-saharan Africa. *Mon. Wea. Rev.*, **114**, 561–570.

Makarau, A., 1995: *Intra-seasonal oscillatory modes of Southern Africa summer circulation*, Ph.D. thesis, University of Cape Town.

Marlow, J., Lange, C., Wefer, G., and Rosell-Mele, A., 2000: Upwelling intensification as part of the Pliocene-Pleistocene climate transition. *Science*, **290**, 2288–2291.

Mason, S. J., 1995: Sea surface temperature-South African rainfall associations, 1910-1989. *Int. J. Climatol.*, **15**, 119–135.

Mason, S. J. and Jury, M. R., 1997: Climatic Change and Variability over Southern Africa: A reflection on Underlying Processes. *Prog. Phys. Geog*, **21**, 23–50.

Meeuwis, J. M. and Lutjeharms, J. R. E., 1990: Surface thermal characteristics of the Angola-Benguela Front. *S. Afr. J. Mar. Res.*, **9**, 261–279.

Moura, A. D. and Shukla, J., 1981: On the dynamics of the droughts in northeast Brazil: Observations, theory and numerical experiments with a general circulation model. *J. Atmos. Sci.*, **38**, 2653–2675.

Mulenga, H., 1998: *Southern African climatic anomalies, summer rainfall and the Angola low*, Ph.D. thesis, University of Cape Town.

Murphy, J. M., Sexton, D. M. H., Barnett, D. N., Jones, G. S., Webb, M. J., Collins, M., and Stainforth, D. A., 2004: Quantification of modeling uncertainties in a large ensemble of climate change simulations. *Nature*, **430**, 768–772.

Nicholson, S. E., 2003: Comments on "The South Indian Convergence Zone and Interannual Rainfall Variability over Southern Africa" and the Question of ENSO's Influence on Southern Africa. *J. Climate*, **16**, 555–562.

Nicholson, S. E. and Entekhabi, D., 1986: The quasi-periodic behavior of rainfall variability in Africa and its relationship to the Southern Oscillation. *J. Clim. Appl. Meteorol.*, **34**, 331–348.

Nicholson, S. E. and Entekhabi, D., 1987: Rainfall Variability in Equatorial and Southern Africa: Relationships with Sea Surface Temperatures along the Southwestern Coast of Africa. *J. App. Meteo.*, **26**, 561–578.

Nicholson, S. E. and Kim, J., 1997: The relationship of the El Niño-Southern Oscillation to African rainfall. *Int. J. Climatol.*, **17**, 117–135.

Nicholson, S. E. and Selato, J. C., 2000: The influence of La Niña on African Rainfall. *Int. J. Climatol.*, **20**, 1761–1776.

Palastanga, V., Vera, S. C. S., and Picola, A. R., 2002: On the leading modes of sea surface temperature variability on the South Atlantic Ocean. *Exchanges*, **25**.

Penland, C. and Matrosova, L., 1998: Prediction of tropical Atlantic Sea surface temperatures using linear inverse modeling. *J. Climate*, **11**, 483–496.

Ponater, M., Köning, W., Sausen, R., and Sielmann, F., 1994: Circulation Regime Fluctuation and their Effect on Intraseasonal Variability in the ECHAM Climate Model. *Tellus*, **46A**, 265–285.

Pope, V. D., Gallani, M. L., Rowntree, P. R., and Stratton, R. A., 2000: The impact of new parameterizations in the Hadley Centre climate model:HadAM3. *Climate. Dynamics.*, **16**, 123–146.

Portela, A. and Castro, M., 1996: Summer thermal lows in the Iberian peninsula: A three dimensional simulation. *Q. J. R. Meteorol. Soc.*, **122**, 1–22.

Rácz, Z. and Smith, R. K., 1999: The dyanamics of heat lows. *Q. J. R. Meteorol. Soc.*, **125**, 225–252.

Ramage, C. S., *Monsoon Meteorology* (Academic Press, 1971).

Rautenbach, C. J. and Jury, M. R., 1997: Atlantic Ocean perturbation run with the CSIRO-9 GCM, Technical Report 34, University of Pretoria.

Reason, C. J. C., 2001: Subtropical Indian Ocean SST dipole events and southern African rainfall. *Geophys. Res. Lett.*, **28**, 2225–2227.

Reason, C. J. C., 2002: Sensitivity of the southern African circulation to dipole sea surface temperature patterns in the south Indian Ocean. *Int. J. Climatol.*, **22**, 377–393.

Reason, C. J. C., Allan, R. J., Lindesay, J. A., and Ansell, T. J., 2000: ENSO and Climatic Signals across the Indian Ocean Basin in the Global Context: Part I, Interannual Composite Patterns. *Int. J. Climatol.*, **20**, 1285–1327.

Reason, C. J. C., Hachigonta, S., and Phaladi, R. F., 2005: Interannual Varibility n rainy Season Characteristics over the Limpopo region of Southern Africa. *Int. J. Climatol.*, **25**, 1835–1853.

Reason, C. J. C. and Jagadheesha, D., 2005a: Relationships between South Atlantic SST Variability and Atmospheric Circulation over the South African Region during Austral Winter. *J. Climate*, **18**, 3339–3355.

Reason, C. J. C. and Jagadheesha, D., 2005b: A model investigation of recent ENSO impacts over southern Africa. *Meteorol. Atmos. Phys.*, **89**, 181–205.

Reason, C. J. C., Jagadheesha, D., and Tadross, M., 2003: A Model Investigation of Interannual Winter Rainfall Variability over Southwestern South Africa and Associated Ocean-Atmosphere Interaction. *S.Afr. J. Sci.*, **99**, 75–80.

Reason, C. J. C., Landman, W., and Tennant, W., 2006: Seasonal to decadal prediction of southern African climate and its links with variability of Atlantic Ocean. *Bull. Amer. Meteor. Soc.*, **87**, 941–955.

Reason, C. J. C. and Mulenga, H., 1999: Relationships between South African rainfall and SST anomalies in the south west Indian Ocean. *Int. J. Climatol.*, **19**, 1651–1673.

Reason, C. J. C. and Rouault, M., 2006: Sea surface temperature variability in the tropical southeast Atlantic Ocean and West African rainfall. *Geophys. Res. Lett.*, **33**, L21705 doi:10.1029/2006GL027145.

Reason, C. J. C., Rouault, M., Melice, J., and Jagadheesha, D., 2002: Interannual Winter Rainfall Variability over Southwestern South Africa and Associated Ocean-Atmosphere Interactions. *Meteor. Atmos. Phys.*, **80**, 19–29.

Reichmann, Z. and Smith, R. K., 2003: Terrain influence on the dyanmics of heat lows. *Q. J. R. Meteorol. Soc.*, **129**, 1779–1793.

Reynolds, W. R., Rayner, N. A., Smith, T. M., Stocks, D. C., and Wang, W., 2002: An Improved In Situ and Satellite SST analysis for Climate. *J. Climate*.

Reynolds, W. R. and Smith, T. M., 1994: Improved Global Sea Surface Temperature Analyses using Optimum Interpolation. *J. Climate*, **7**, 929–948.

Robertson, A. W., Farrara, J. D., and Mechoso, C. R., 2003: Simulation of the Atmospheric Response to South Atlantic Sea Surface Temperature Anomalies. *J. Climate*, **16**, 2540–2551.

Robinson, D. and Clark, P. A., 1998: *Atmospheric Tracers*, Unified Model User Guide, Meteorological Office, United Kingdom, met office edition.

Rocha, A. and Simmonds, I. H., 1997a: Interannual variability of southern African summer rainfall. Part I: Relationships with air-sea interactions proccesses. *Int. J. Climatol.*, **17**, 235–265.

Rocha, A. and Simmonds, I. H. (Editors), 1997b: *Distinct modes of SST-forced rainfall variability over southern hemisphere continents* (1997b).

Ropelewski, C. F. and Halpert, M. S., 1987: Global and regional scale precipitation patterns associated with the El Niño/Southern Oscillation. *Mon. Wea. Rev.*, **115**, 1606–1626.

Ropelewski, C. F. and Halpert, M. S., 1989: Precipitation patterns associated with the high index phase of the Southern Oscillation. *J. Climate*, **2**, 268–284.

Rouault, M., Florenchie, P., Fauchereau, N., and Reason, C. J. C., 2003: South east tropical Atlantic warm events and southern African rainfall. *Geophys. Res. Lett.*, **30**, 8009.

Rouault, M., Illig, S., Bartholomae, C., Reason, C. J. C., and Bentamy, A., 2007: Propagation and Origin of Warm Anomalies in the Angola Benguela Upwelling System in 2001. *J. Marine System*, **68**, 473–488.

Rowson, D. R. and Colucci, S. J., 1992: Synoptic climatology of thermal low-pressure systems over south-western Northern America. *Int. J. Climatol.*, **12**, 529–545.

Senior, C. A. and Mitchell, J. F. B., 1993: Carbon dioxide and Climate: The impact of Cloud parameterization. *J. Climate*, **6**, 393–418.

Servain, J., 1991: Simple climatic indices for the tropical Atlantic Ocean and some applications. *J. Geophys. Res.*, **96**, 137–146.

Servain, J., Busalacch, A. J., McPhaden, M. J., Moura, A. D., Reverdin, G., Vianna, M., and Zebiak, S. E., 1998: A Pilot Research Moored Array in the Tropical Atlantic (PIRATA). *Bull. Amer. Meteo. Soc.*, **79**, 2019–2031.

Shannon, L. V., Boyd, A. J., Brundrit, G. B., and Taunton-Clark, J., 1986: On the existence of an El Niño-type phenomenon in the Benguela system. *J. Marine Res.*, **44**, 495–520.

Shannon, L. V. and Nelson, G., *The South Atlantic: Present and Past Circulation.* (Springer-Verlag, Berlin, 1996).

Smith, R. N. B., 1990: A scheme for predicting layer clouds and their water content in a general circulation model. *Q. J. R. Meteorol.*, **116**, 435–460.

Smith, R. N. B., 1998: *Boundary Layer*, Unified Model User Guide (sec 2.1.3) Meteorological Office, United Kingdom, met office edition.

Smith, T. M., Karl, T. R., and Reynolds, R. W., 2002: How acculate are climate simulations. *Science*, **296**, 483–484.

Sutton, R. T., Jewson, S. P., and Rowell, D. P., 2000: The elements of climate variability on the tropical Atlantic Region. *J. Climate*, **13**, 3261–3284.

Tadross, M. A., Hewitson, B. C., and Usman, M. T., 2005: The Interannual Variability of the Onset of the Maize Growing Seaon over South Africa and Zimbabwe. *J. Climate*, **18**, 3356–3372.

Tennant, W., 2003: An assessment of intraseasonal variability from 13-yr GCM simulations. *Mon. Weather Rev.*, **13**, 1975–1991.

Todd, M. and Washington, R., 1999: Circulation anomalies associated with tropical-temperate troughs in southern Africa and the south west Indian Ocean. *Climate Dynamics*, **15**, 937–951.

Todd, M., Washington, R., and Palmer, P. I., 2004: Water vapour transport associated with tropical-temperate trough systems over southern Africa and the southwest Indian Ocean. *Int. J. Climatol.*, **24**, 555–568.

Tourre, Y. M., Rajagopalan, B., and Kushnir, Y., 1999: Dominant patterns of climate variability in the Atlantic Ocean during the last 136 years. *J. Climate.*, **12**, 2285–2299.

University Corporation for Atmospheric Research - UCAR, 1999: Impacts of model structure and dynamics, `http://mete.ucar.edu/nwp/pcu1/ic2/frameset.htm?openTopic(1)`, accessed 8 November, 2006.

Usman, M. T. and Reason, C. J. C., 2004: Dry spell frequencies and their variability over southern Africa. *Clim. Res.*, **26**, 199–211.

von Storch, H. and Navarra, A. (Editors), *Analysis of Climate Variability: Applications of Statistical Techniques* (Springer Verlag, 1999).

von Storch, H. and Roeckner, E., 1983: Methods for the verification of general circulation models applied to the Hamburg University GCM. Part I: Test of individual climate states. *Mon. Wea. Rev.*, **111**, 1965–1976.

von Storch, H., Zorita, E., and Cubasch, U., 1993: Downscaling of global climate change estimates to regional scales: An application to Iberian rainfall in wintertime. *J. Climate*, **6**, 1161–1171.

von Storch, H. and Zwiers, F. W., *Statistical Analysis in Climate Research* (Cambridge University Press, 1999).

Wagner, R. G. and da Silva, A. M., 1994: Surface conditions associated with anomalous rainfall in the Guinea coastal region. *Int. J. Climatol.*, **14**, 179–199.

Walker, N. D., 1990: Links between South African summer rainfall and temperature variability of the Agulhas and Benguela Current systems. *J. Geophys. Res*, **95**, 3297–3319.

Washington, R. and Preston, A., 2006: Extreme wet year over southern Africa: role of Indian Ocean sea surface temperature. *J. Geophys. Res.*, **111**, D15104, doi:10.1029/2005JD006724.

Washington, R. and Todd, M., 1999: Tropical-temperate links in southern African and southwest Indian Ocean satellite-derived dailly rainfall. *Int. J. Climatol.*, **19**, 1601–1616.

Webster, S., 1998: *Gravity-wave Drag*, Unified Model User Guide (sec 2.1.8), Meteorological Office, United Kingdom, Met office edition.

Williams, C. J. R., Kniveton, D. R., and Layberry, R., 2008: Influence of South Atlantic Sea Surface Temperatures On Rainfall Variability And Extremes Over Southern Africa. *J. Climate*.

Wu, R. and Kirtman, B. P., 2005: Near-Annual SST Variability in the Equatorial Pacific in a coupled general circulation model. *J. Climate*, **18**, 4454–4473.

Xie, P. and Arkin, P. A., 1996: Analysis of Global Monthly Precipitation using Gauge Observations, Satellite Estimates and Numerical Model Predictions. *J. Climate*, **9**, 840–858.

Xie, P. and Arkin, P. A., 1997: Global precipitation: A 17-year monthly analysis based on guage observations, satellite estimates, and numerical model outputs. *Bull. Amer. Meteor. Soc.*, **78**, 2539–2558.

Xie, S. and Carton, J. A., *Tropical Atlantic Variability: Patterns, Mechanisms and Impacts. Earth Climate: The Ocean-Atmosphere Interaction* (Geophsical Monograph, AGU, 147 Wahsington D.C., 2004).

Zebiak, S. E., 1993: Air-sea interactions in the Equatorial Atlantic region. *J. Climate*, **6**, 1567–1586.

Zhang, G. J. and McPhaden, M. J., 1995: The relationship between sea surface temperature and latent heat flux in the equatorial Pacific. *J. Climate*, **8**, 589–605.

Appendix A

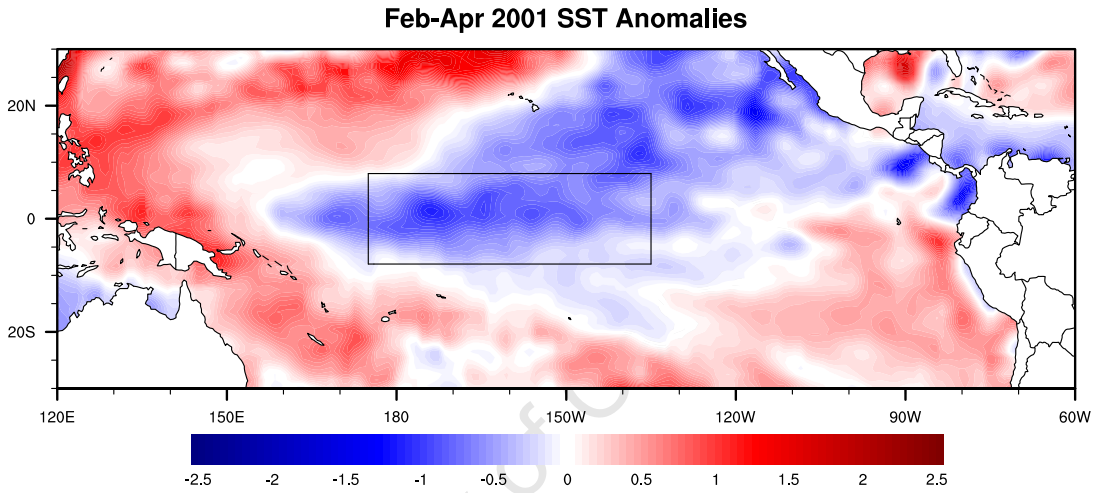

Figure A.1: SST anomalies in the central equatorial Pacific Ocean. The box represents the region of cool SST anomalies used to force HadAM3 (8°S-8°N, 175°E-135°W)

Appendix B

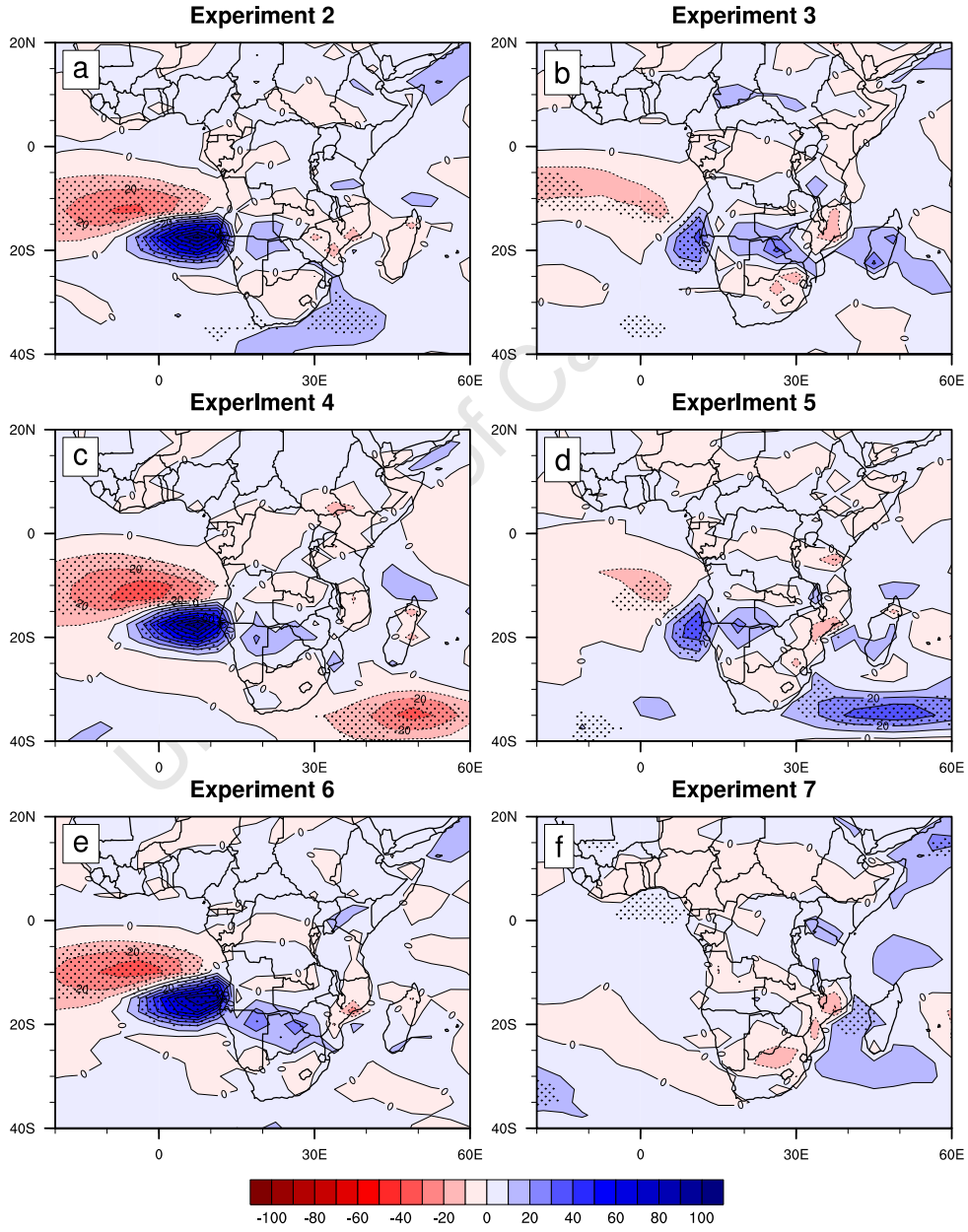

Figure B.1: Surface Latent heat flux anomalies for Experiments 2 - 10. Stippled regions indicate statistically significant anomalies at 90% confidence level.

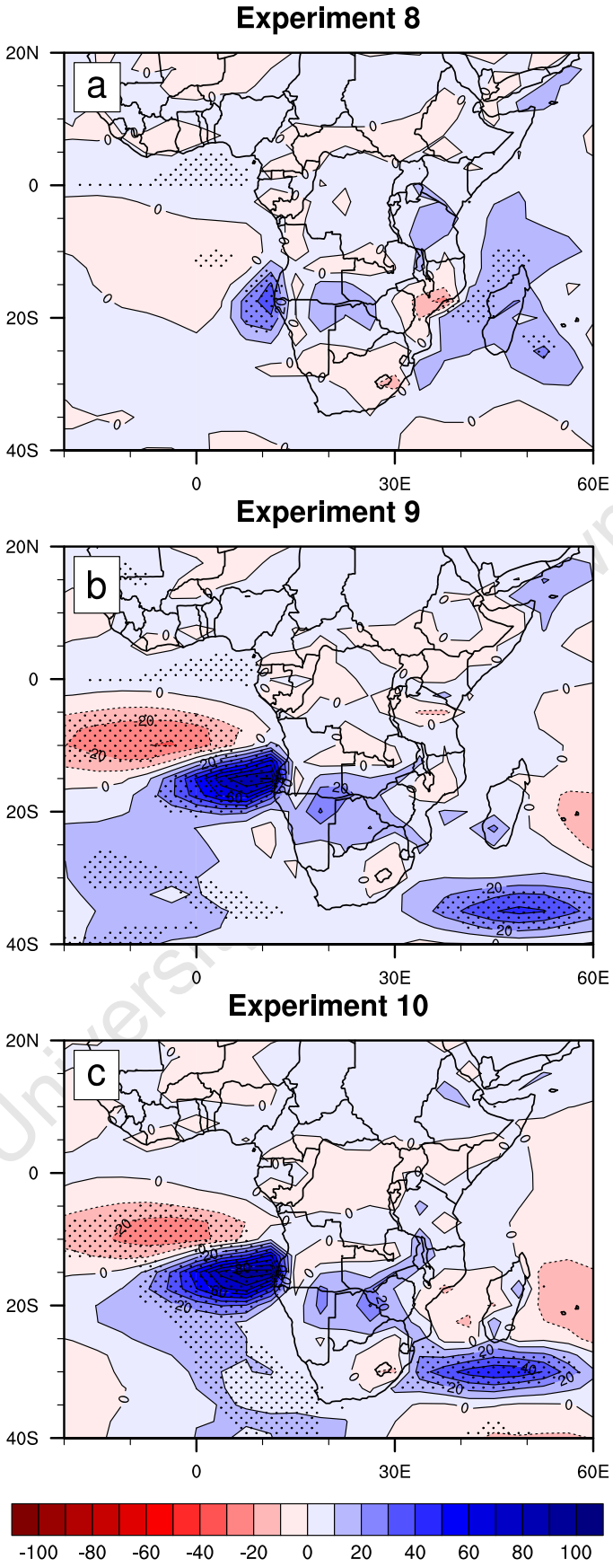

Figure B.1: continued

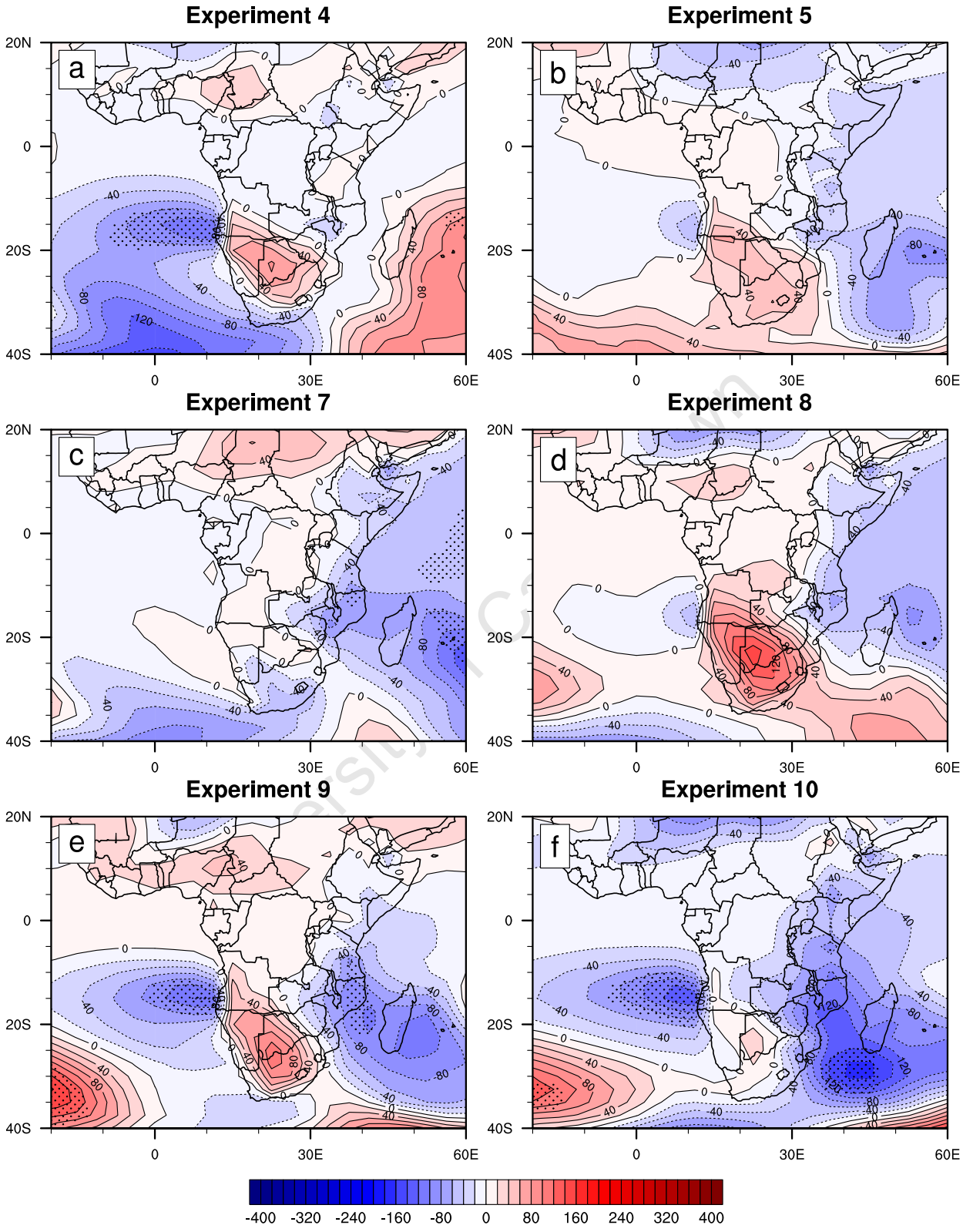

Figure B.2: Sea Level Pressure anomalies for Experiment2 4,5,7-10

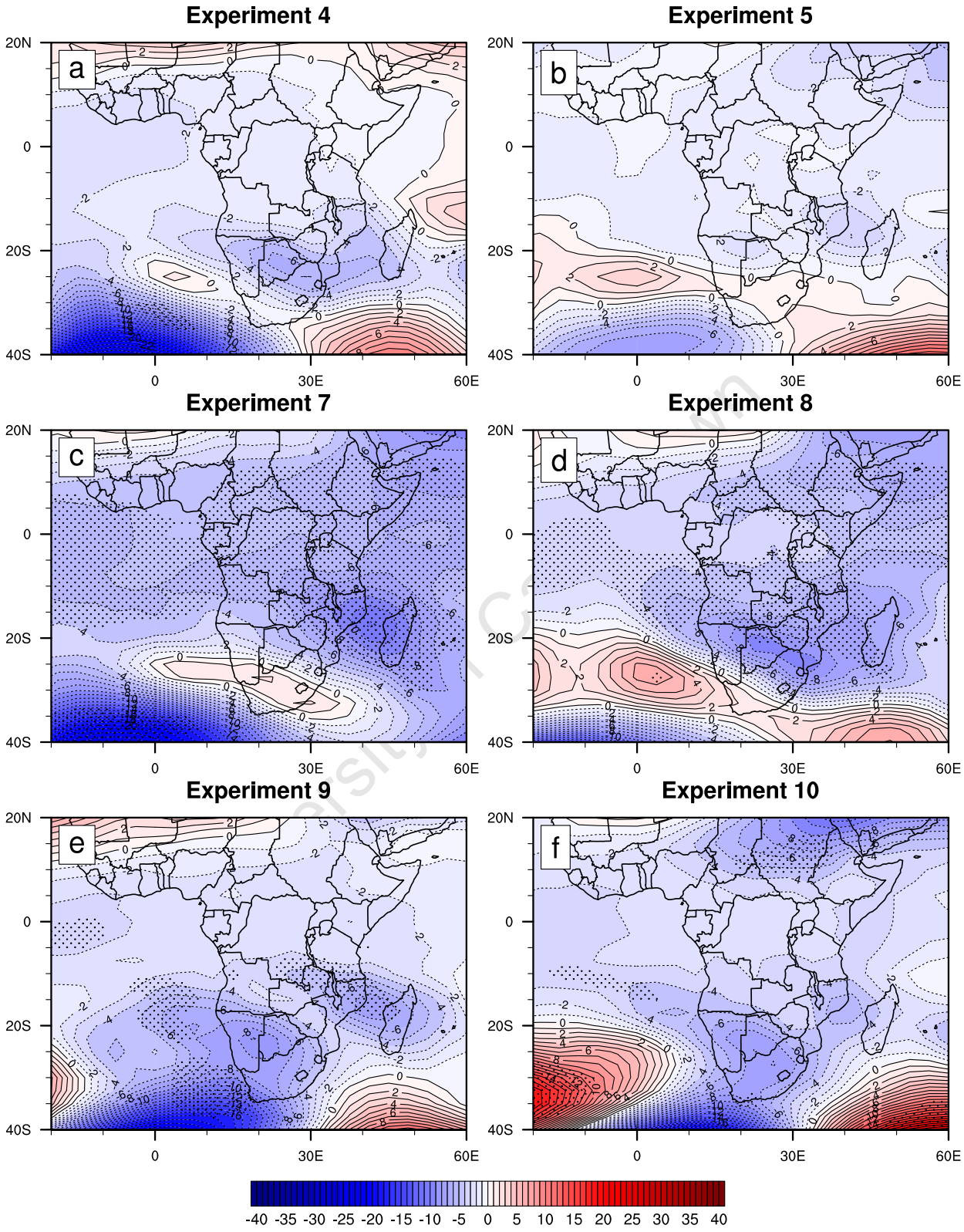

Figure B.3: Same as Figure B.2, but for geopotential height